LA-UR-19-20814
Approved for public release; distribution is unlimited.

Title: Introduction to High Explosives

Author(s): Menikoff, Ralph

Intended for: LANL seminar series

Issued: 2019-04-29 (rev.1)

Introduction to High Explosives

Ralph Menikoff, T-1

HE seminar series
April, 2019

Managed by Triad National Security, LLC for the U.S. Department of Energy's NNSA

Table of Contents

Outline

1. Introduction / Overview
   - What is a detonation wave
   - Detonation wave vs Shock wave
   - Detonation properties and applications
   - Plastic-bonded explosive (PBX)
   - PBX manufacture
   - Example meso-scale structure
   - Energetic materials
2. Reactive flow equations
   - Model PDEs
   - Single irreversible reaction
   - EOS for partly burned HE
   - Constraints on EOS
   - P-T equilibrium
   - Example: Ideal HE

Chemical heat release
Conservation form of PDEs
Wave structure
Characteristic equations
Shock acceleration
Shock state & characteristics
Summary

3. Detonation locus
Shock jump conditions
Hugoniot equation
Shock relations
Unsupported detonation wave
CJ state relations
Overdriven detonation wave
Shock and detonation loci
Detonation speed dependence on initial state
EOS uncertainty

Deflagration locus

4. Planar detonation wave
   - Unsupported detonation wave
   - Wave profiles
   - Reaction zone width
   - Derivation of ZND profile
   - Detonation locus and Rayleigh line
   - Taylor wave
   - Experimental PBX 9501 profile
   - Simulated PBX 9502 profile
   - Chemical energy released
   - Measurement of energy released

5. Shock-to-detonation transition
   - Initiation mechanism
   - Shock initiation experiments
   - Pop plot data (ambient PBX 9502)
   - Pressure range for Pop plot

Chemical rate
Temperature variation
Lot dependence
Density variation
Homogeneous vs Heterogeneous initiation
Super-detonation
Shock desensitization
Other shock initiation
Quench propagating detonation wave
HE initiation for simulation

6. Ignition and growth concept of Hot Spots
Hot spot burning
Hot spot requirements
Perspective on hot spot burn rate
Hot spot burn rate
Properties of hot spot burn rate
Pore collapse as hot spot mechanism for shock initiation

Heuristic burn rate
Model calibration

7. Diameter effect and curvature effect
   - Unconfined rate stick
   - Diameter effect
   - Modified jump conditions
   - Duct flow equations
   - Characteristic equation
   - Curvature effect
   - Detonation Shock Dynamics (DSD)
   - Comment on converging wave front
   - Experimental measurement of Dn(k)
   - Example PBX 9502
   - Breakdown of DSD assumptions
   - Rate stick simulation

8. CJ state and release isentrope
   - Products EOS data

CJ detonation speed
CJ pressure — conventional HE
CJ pressure — insensitive HE
Overdriven detonation locus
Cylinder test experiment
Cylinder test uncertainties
Cylinder test and curvature effect
Cylinder test and wall velocity

9. Failure diameter, corner turning and dead zones
   - Failure diameter
   - Simulation above failure diameter
   - Weak confinement
   - Simulation below failure diameter
   - Additional comments on failure
   - Corner turning – experiment
   - Corner turning – simulation

10. EOS models and calibration data

Mei-Gruneisen EOS
Reactants EOS
Products EOS
Example EOS model loci
Does VN spike pressure matter ?
Example EOS model isotherms
Thermo-chemical codes
References
Zoomed figures

Outline of HE seminar series

1. Introduction / Overview
   Part I: Mathematical Description
2. Reactive flow equations
3. Detonation locus
4. Planar detonation wave
   Part II: Detonation Phenomena and Experiments
5. Shock-to-detonation transition
6. Ignition and growth concept of Hot Spots
7. Diameter effect and curvature effect
8. CJ state and release isentrope
9. Failure diameter, corner turning and dead zones
   Part III: Reactants and Products EOS
10. EOS models and calibration data

Topics Not Covered

- Thermal ignition
- Deflagration-to-Detonation Transition
- Low velocity impact ignition
- Specific reactive burn models
- Numerical simulations

1. Introduction / Overview

What is a detonation wave

Explosive: Reactants $\rightarrow$ Products

Meta-stable reactants $\Rightarrow$ Irreversible reaction

Detonation wave (unsupported)

1. Lead shock triggers fast reaction
2. Reaction releases chemical energy
   Large increase in pressure
3. Energy release drives shock

Once initiated detonation wave is self-sustaining

Releases large amount of energy ($\sim$ 4 MJ/kg)
in short time ($\sim$ 10 μs)

KE of 2 ton car at 100 mph = 1.8 MJ, about $(6\,\text{cm})^3$ of HE

NIF, 2 MJ of laser energy (few ns)

Detonation wave vs Shock wave

- Shock and detonation wave supersonic wrt flow ahead and subsonic wrt flow behind except
  underdriven detonation wave is sonic wrt flow behind
- Weak shock speed $\rightarrow$ sound speed
  Detonation wave has minimum speed $>$ sound speed
- Shock decays if not supported
  Overdriven detonation wave similar to shock wave
  Underdriven detonation is self-sustaining
- Pressure increases across both shock and detonation waves
  Shock is discontinuity (numerical width for shock capturing)
  Detonation wave, physical width due to finite reaction rate ($\sim$ 0.1 mm)
- EOS determines shock locus and planar detonation locus
  Detonation wave speed depends on local front curvature

Detonation properties and applications

Example solid explosives

	TNT	HMX based PBX 9501	TATB based PBX 9502	
P	19.	35.	28.	GPa
D	6.9	8.8	7.8	km/s
ρ	1.64	1.84	1.89	g/cc

Applications of explosives

1. Mining
2. Construction and demolition
3. Push metals to high velocity (several km/s)
   High pressure EOS data (up to tens of MB)
   LASL Shock Hugoniot Data (Ed. S. Marsh, 1980)
4. Explosive driven flux compression generator (30 MA at 10 kV)
5. Weapons

Plastic-bonded explosive (PBX)

Heterogeneous materials

- Explosive grains + small amount of impurities
- Polymeric binder
- pores

Fuel and oxidizer within explosive molecule

analog of premixed combustion rather than laminar combustion

Ex: HMX, C_4 H_8 N_8 O_8 cyclo-tetramethylene-tetranitramine

TATB, C_6 H_6 N_6 O_6 triamino-trinitro-benzene

PBX grain size distribution: 10 to 200 microns (loose specification)

Heterogeneities affect burn rate

- Shock-to-detonation transition
- Rate dominated by hot spots

  Rather than chemical rate at shock temperature

PBX manufacture

- Batch of molding powder
  Combine coarse and fine HE grains
  Coat grains with binder to form granules (conglomerate of grains)
- Blend batches into a lot
  Adjust to specifications (*e.g.*, mass fraction of HE and binder)
- Heat and press molding powder to form PBX
  Compress out porosity to achieve specified density
    Can get partial alignment of HE crystal orientation
    Grains can fracture and change size distribution
- PBX heterogeneities
  Statistically more similar within a lot than between lots
- Experiment should record relevant PBX information
  Lot, density and firing temperature
  Allows for corrects when comparing experiments

Example meso-scale structure

PBX 9501

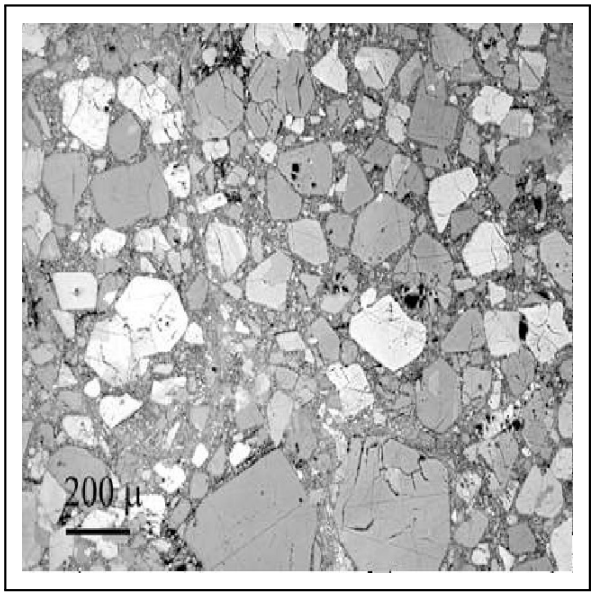

polarized light micrograph

2 % porosity

Skidmore *et al.*, 1998

PBX 9502 (dry aminated)

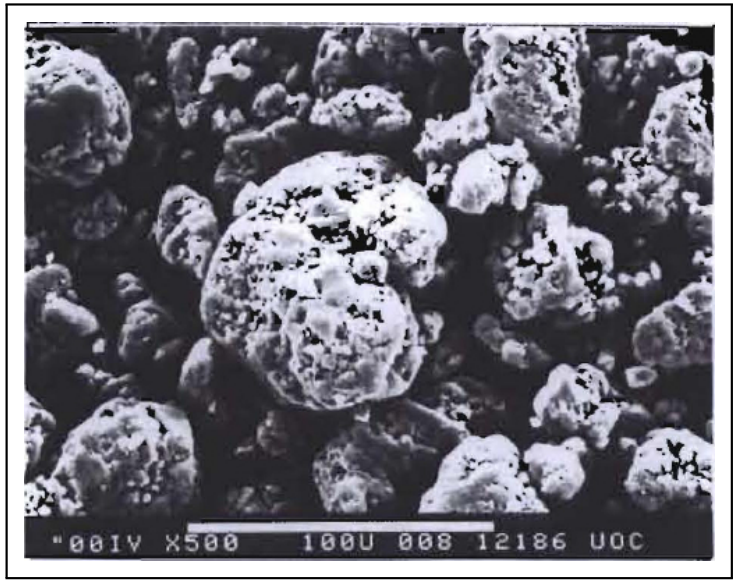

scanning electron micrograph

2.5 % porosity

Pantex

Newer techniques

- X-ray computer micro-tomography
- Ultra-small angle neutron scattering

Energetic materials

Detonation wave for explosive (fast burn mode)
Deflagration wave for propellant (slow burn mode)

Differences in wave properties

- Detonation wave is compressive and pressure increasing
  Deflagration wave is expansive and pressure decreasing
- Detonation driven by shock wave (wave width $\sim$ 100 μm)
  Deflagration driven by heat conduction (wave width $\sim$ 0.1 μm)
- Detonation wave speed up to 9 km/s
  Deflagration wave speed typically mm/s to cm/s
- Detonation wave supersonic ahead and subsonic behind
  Deflagration wave are subsonic both ahead and behind front

Energetic materials

Detonation wave for explosive (fast burn mode)
Deflagration wave for propellant (slow burn mode)

Differences in wave properties

- Detonation wave is compressive and pressure increasing
  Deflagration wave is expansive and pressure decreasing
- Detonation driven by shock wave (wave width $\sim$ 100 μm)
  Deflagration driven by heat conduction (wave width $\sim$ 0.1 μm)
- Detonation wave speed up to 9 km/s
  Deflagration wave speed typically mm/s to cm/s
- Detonation wave supersonic ahead and subsonic behind
  Deflagration wave are subsonic both ahead and behind front

Energetic materials

Detonation wave for explosive (fast burn mode)
Deflagration wave for propellant (slow burn mode)

Differences in wave properties

- Detonation wave is compressive and pressure increasing
  Deflagration wave is expansive and pressure decreasing
- Detonation driven by shock wave (wave width $\sim 100\ \mu$m)
  Deflagration driven by heat conduction (wave width $\sim 0.1\ \mu$m)
- Detonation wave speed up to 9 km/s
  Deflagration wave speed typically mm/s to cm/s
- Detonation wave supersonic ahead and subsonic behind
  Deflagration wave are subsonic both ahead and behind front

Energetic materials

Detonation wave for explosive (fast burn mode)
Deflagration wave for propellant (slow burn mode)

Differences in wave properties

- Detonation wave is compressive and pressure increasing
  Deflagration wave is expansive and pressure decreasing
- Detonation driven by shock wave (wave width $\sim 100\ \mu$m)
  Deflagration driven by heat conduction (wave width $\sim 0.1\ \mu$m)
- Detonation wave speed up to 9 km/s
  Deflagration wave speed typically mm/s to cm/s
- Detonation wave supersonic ahead and subsonic behind
  Deflagration wave are subsonic both ahead and behind front

Energetic materials

Detonation wave for explosive (fast burn mode)
Deflagration wave for propellant (slow burn mode)

Differences in wave properties

- Detonation wave is compressive and pressure increasing
  Deflagration wave is expansive and pressure decreasing
- Detonation driven by shock wave (wave width $\sim$ 100 μm)
  Deflagration driven by heat conduction (wave width $\sim$ 0.1 μm)
- Detonation wave speed up to 9 km/s
  Deflagration wave speed typically mm/s to cm/s
- Detonation wave supersonic ahead and subsonic behind
  Deflagration wave are subsonic both ahead and behind front

Reaction zone for detonation wave in heterogeneous solid
Deflagration wavelets from hot spots

2. Reactive flow equations

Model PDEs

Euler equations + rate equation for reaction progress variable

For single irreversible reaction with reaction progress variable λ

$$\partial_t \begin{pmatrix} \rho \\ \rho u \\ \rho(e + \frac{1}{2}u^2) \\ \rho\lambda \end{pmatrix} + \partial_x \begin{pmatrix} \rho u \\ \rho u^2 + \underline{P} \\ \rho u(e + \frac{1}{2}u^2 + \underline{P}V) \\ \rho u\lambda \end{pmatrix} = \begin{pmatrix} 0 \\ 0 \\ \rho Q\underline{\mathcal{R}} \\ \rho\underline{\mathcal{R}} \end{pmatrix}$$

ρ, u, e are density, particle velocity and specific internal energy

Q is specific energy release and $\mathcal{R}$ is reaction rate

Last component reduces to rate equation (ODE along particle path)

$$(\mathrm{d}/\mathrm{d}t)\lambda = (\partial_t + u\partial_x)\lambda = \mathcal{R}$$

Fluid flow and reaction coupled through pressure $P(V, e, \lambda)$ and reaction rate $\mathcal{R}(V, e, \lambda)$

Single irreversible reaction

Chemical reaction: Reactants $\rightarrow$ Products

as reaction progress variable goes from $\lambda = 0$ to $\lambda = 1$

Typically, λ is mass fraction of products

Irreversible reaction implies $\mathcal{R} \geq 0$

Reactants are meta-stable

Not chemical equilibrium but large potential barrier

Lowers accuracy requirement for simulations

Require $\mathcal{R} \rightarrow 0$ as $\lambda \rightarrow 1$, rate vanishes when reactants depleted

- PDE generalize to multi-step reactions

  Needed for thermal ignition
- Multi-step reactions not used for detonation waves

  For Arrhenius chemical rates

  Rate limiting reaction (smallest T_a) at high temperatures

  Burn rate dominated by hot spots and not chemical rate at average T
- Exception is second reaction for slow carbon clustering (TATB)

EOS for partly burned HE

For partly burned HE need $P(V, e, \lambda)$, $T(V, e, \lambda)$

1. Reactants EOS for $\lambda = 0$, unreacted
2. Products EOS for $\lambda = 1$, completely burned
3. Mixture rule to interpolate for $0 < \lambda < 1$, partly burned

Example: Ideal HE

$P(V, e, \lambda) = (\gamma - 1)(e + \lambda Q)/V$

$T(V, e, \lambda) = (e + \lambda Q)/Cv$

Q is chemical energy release and Cv is specific heat

Tacitly assume partly burned HE is homogeneous

i.e., completely characterized by V, e, λ

Heterogeneity of PBX accounted for only in reaction rate

Constraints on EOS

- Thermodynamic consistency
  EOS derived from thermodynamic potential
  e.g., Helmholtz free energy or Gibbs free energy
- Thermodynamic stability
  $K_s \geq K_T \geq 0$ and $C_P \geq C_V \geq 0$ for fixed λ
  where K is bulk modulus and C is specific heat
- EOS models have limited domains
  K_T breaks down for solid EOS models in expansion
  $C_V \to 0$ as $T \to 0$ does not hold for products EOS
    Unphysical van der Waal loops at low temperature
- Detonation phenomena requires thermicity is positive

$$\frac{(\partial_\lambda P)_{V,e}}{\rho c^2} = \frac{\Delta V}{V} - \Gamma \frac{\Delta H}{c^2} > 0$$

Contributions from heat release ΔH and change in volume ΔV
Can have endothermic reaction if ΔV sufficiently large

P-T equilibrium

Frequently used mixture rule is P-T equilibrium

$$P(V, e, \lambda) = P_p(V_p, e_p) = P_r(V_r, e_r)$$
$$T(V, e, \lambda) = T_p(V_p, e_p) = T_r(V_r, e_r)$$
$$V = \lambda V_p + (1 - \lambda) V_r$$
$$e = \lambda e_p + (1 - \lambda) e_r$$

Subscripts ‘p’ and ‘r’ denote products and reactants, respectively

Corresponds to phase separation between reactants and products

Unique solution provided that reactants and products EOS are both thermodynamically consistent and stable

Thermodynamic consistent mixture rule

$G(P, T, \lambda) = \lambda G_p(P, T) + (1 - \lambda) G_r(P, T)$

Thermodynamic stability of mixture rule

G is jointly concave in P and T

Example: Ideal HE

Reactants (ideal gas)

$$P_r(V,e) = (\gamma - 1)e/V$$
$$T_r(V,e) = e/C_V$$
$$\widetilde{P}_r(V,T) = (\gamma - 1)C_V\, T/V\ ,$$

Products (ideal gas with energy offset)

$$P_p(V,e) = (\gamma - 1)(e+Q)/V$$
$$T_p(V,e) = (e+Q)/C_V$$
$$\widetilde{P}_p(V,T) = (\gamma - 1)C_V\, T/V$$

PT equilibrium

$$V_r = V_p = V$$
$$e_p = e - (1-\lambda)\, Q$$
$$e_r = e + \lambda\, Q$$

Equivalent to

$$P(V,e,\lambda) = (\gamma - 1)(e+\lambda Q)/V$$
$$T(V,e,\lambda) = (e+\lambda Q)/C_V$$

Chemical heat release

Degree of freedom for the relative energy origins of products and reactants from the transformation

$$P'_p(V, e) = P_p(V, e + q)$$
$$(\mathrm{d}/\mathrm{d}t)e' = -P'(\mathrm{d}/\mathrm{d}t)V + (Q - q)(\mathrm{d}/\mathrm{d}t)\lambda$$

Solution to PDEs invariant if for mixture rule $e = \lambda e_p + (1 - \lambda)e_r$

Heat release can be

- explicit, Q in energy equation
- or offset in energy origin between reactants and products q
- or both

Convention (for ambient reactants):

- Chose $e_0 = 0$ for reactants and energy origin of products such that $P_{cj} = P_p(V_{cj}, e_{cj})$ where $e_{cj} = \frac{1}{2}P_{cj} \cdot (V_0 - V_{cj})$ and subscript 'cj' denotes the CJ detonation state
- Then $Q = 0$.

Conservation form of PDEs

Form of PDEs

$$\partial_t \vec{w} + \nabla_{\vec{x}} \cdot \overleftrightarrow{F}(\vec{w}) = \vec{s}$$

Integrate over volume element Ω

$$\begin{aligned}\partial_t \int_\Omega \mathrm{d}\mathcal{V}\, \vec{w} &= -\int_\Omega \mathrm{d}\mathcal{V}\, \nabla \cdot \overleftrightarrow{F} + \int_\Omega \mathrm{d}\mathcal{V}\, \vec{s} \\ &= -\int_{\partial\Omega} \mathrm{d}\mathcal{S}\, \hat{n} \cdot \overleftrightarrow{F} + \int_\Omega \mathrm{d}\mathcal{V}\, \vec{s}\end{aligned}$$

$\vec{w}$ is vector of conserved quantities
$\overleftrightarrow{F}$ is flux (advection and force terms)
$\vec{s}$ is source function with no derivatives

In 1-D, surface integral reduces to jump across volume element
For discontinuity in $\vec{w}$, in rest frame of wave front
conservation requires flux is continuous $\Rightarrow$ shock jump conditions

Wave structure

Linearize PDEs, $\partial_t \vec{w} + \left[\nabla_{\vec{w}} \vec{F}\right] \cdot \partial_x \vec{w} = \vec{s}$

2 acoustic waves with characteristic velocities $u \pm c$

Entropy and λ can be discontinuous across a contact

P and u continuous and advects with the particle velocity

Reactive flow PDEs are hyperbolic

$\nabla_{\vec{w}} \vec{F}$ has real eigenvalues (characteristic speeds)

Shock jump conditions

- Finite source terms do not affect jump conditions
- Fluid variable ρ, u, e

  Same jump conditions as for Euler equations
- Fourth jump condition

  $\Delta[\rho(u_s - u)\lambda] = 0$

  From mass jump condition, $\rho(u_s - u) =$ mass flux is constant

  Hence $\Delta[\lambda] = 0$ if mass flux $\neq 0$ (shock)

λ is continuous across shock wave

Characteristic equations

acoustic wave families

$$[(\mathrm{d}/\mathrm{d}t) + c\partial_x]P + \rho c[(\mathrm{d}/\mathrm{d}t) + c\partial_x]u = s\mathcal{R}, \qquad \text{along } \mathrm{d}x/\mathrm{d}t = u + c$$
$$[(\mathrm{d}/\mathrm{d}t) - c\partial_x]P - \rho c[(\mathrm{d}/\mathrm{d}t) - c\partial_x]u = s\mathcal{R}, \qquad \mathrm{d}x/\mathrm{d}t = u - c$$

contact wave families

$$(\mathrm{d}/\mathrm{d}t)P - c^2(\mathrm{d}/\mathrm{d}t)\rho = s\mathcal{R}, \qquad \text{along } \mathrm{d}x/\mathrm{d}t = u$$
$$(\mathrm{d}/\mathrm{d}t)\lambda = \mathcal{R}, \qquad \mathrm{d}x/\mathrm{d}t = u$$

where

- $\mathrm{d}/\mathrm{d}t = \partial_t + u\partial_x$ is convective time derivative
- $s = \Gamma\rho\lambda Q + (\partial_\lambda P)_{V,e}$
- $\Gamma = (V\partial_e P)_{V,\lambda}$ is Grüniesen coefficient

Characteristic velocities (wave speeds) are $u + c$, $u - c$ and u
Thermicity enters as source term

Shock acceleration

Pressure profiles at sequence of times

shock decay

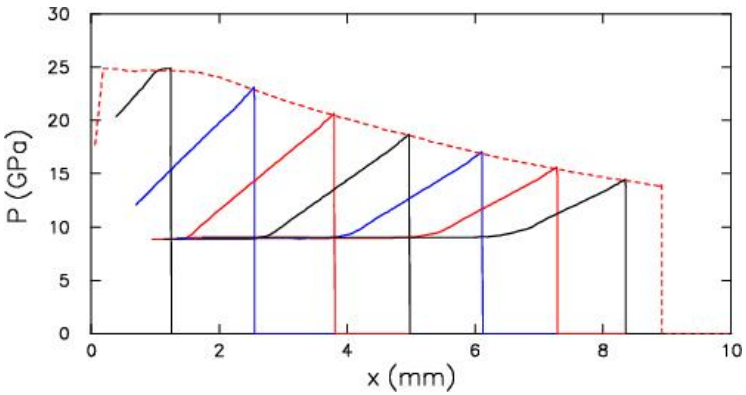

shock growth

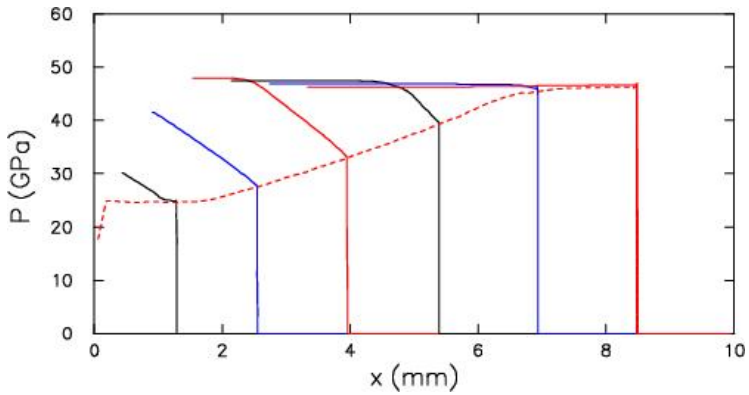

shock-to-detonation transition

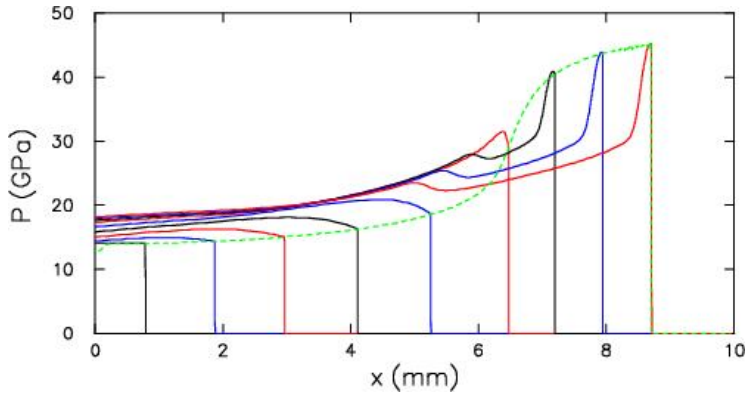

Shock state & characteristics

Characteristics in rest frame of shock front

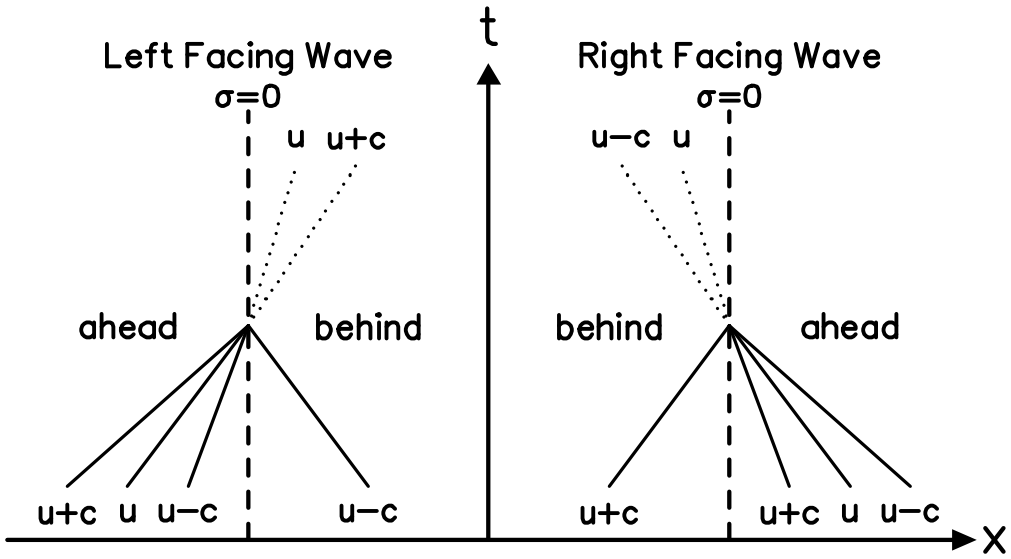

- Ahead state

  Determined by characteristics ahead of shock front
- Behind state

  Shock locus from ahead state

  Incoming characteristic behind front

  Source terms affect behind state

Summary

Reactive burn model (solid explosives)

1. EOS for reactants
2. EOS for products
3. Mixture rule for partly burn HE
4. Reaction rate (accounts for heterogeneities)

Typically, heuristic to motivate fitting form for rate
Calibrate rate to fit subset of experimental data
  Highly non-linear minimization of metric for difference between experimental and simulated data
Calibration of rate depends on EOS
Aim is an engineering model for
  shock initiation, propagating detonation waves and other detonation phenomena

3. Detonation locus

Shock jump conditions

- Local conservation across shock discontinuity
  or quasi-steady detonation wave profile
- All variable are function of $\xi = x - Dt$ where D is wave speed
  $\partial_x = \mathrm{d}/\mathrm{d}\xi$ and $\partial_t = -D(\mathrm{d}/\mathrm{d}\xi)$
  From PDEs in conservation form ▸ PDEs

$$\Delta[\rho(u-D)] = 0 \qquad \text{mass}$$

$$\Delta[\rho u(u-D) + P] = 0 \qquad \text{momentum}$$

$$\Delta\left[\rho\left(\tfrac{1}{2}u^2 + e\right)(u-D) + Pu\right] = \rho(u-D)Q\Delta[\lambda] \qquad \text{energy}$$

- Combine mass and momentum equation
  $\rho(u-D)\Delta[u-D] + \Delta[P] = 0$
- Combine with energy equation
  $\rho(u-D)\Delta\left[\tfrac{1}{2}(u-D)^2 + e + PV\right] = \rho(u-D)Q\Delta[\lambda]$

Hugoniot equation

Summary of shock jump conditions

- Depend only on velocity differences
  $D - u$ ahead and behind wave
  Galilean invariance of Euler equations
- Symmetry for left and right facing waves
  If $D - u$ is solution then $-(D - u)$ is solution with same V and e
  Parity invariance ($x \to -x$ and $u \to -u$) of Euler equations
- Reduce 3 jump conditions by eliminating velocity
  Results in 1 equation for only thermodynamic variables

Hugoniot equation

$$e = \lambda Q + e_0 + \frac{1}{2}\left[P(V, e, \lambda) + P_0\right] \cdot (V_0 - V)$$

For fixed λ: 1 equation for 2 variables V and e
Shock or partly burned detonation locus is curve in (V, P)–plane

Shock relations

$$e = \lambda Q + e_0 + \frac{1}{2}\left[P(V, e, \lambda) + P_0\right] \cdot (V_0 - V)$$

$\lambda = 0$ gives reactants shock locus
$\lambda = 1$ gives the products detonation locus

- When ahead state is at rest $u_0 = 0$
  $P = P_0 + \rho_0 u D$ and $V/V_0 = 1 - u/D$
  Measurement of particle and wave speeds u and D determines point on shock/detonation locus
- $\frac{P - P_0}{V_0 - V} = (\rho_0 D)^2$
  Slope of Rayleigh line in (V, P)–plane
- $(\Delta u)^2 = (P - P_0)(V_0 - V)$
  Change in particle velocity from thermodynamic variables

Straight forward to transform from (V, P)–plane to (u_p, u_s)–plane

Unsupported detonation wave

Example shock/detonation locus for PBX 9502

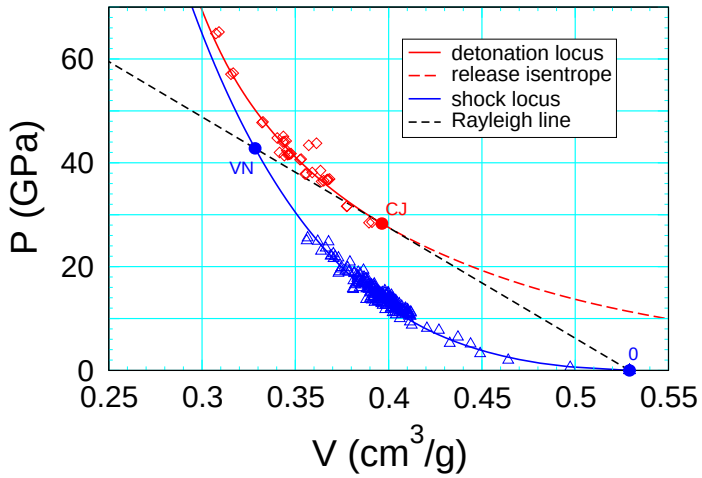

Rayleigh line with $D = D_{CJ}$

Chapman, 1899
Jouguet, 1905 & 1906
von Neumann, WW II $\sim$ 1945

- Chapman-Jouguet (CJ) state
  Hugoniot locus tangent to Rayleigh line
  Sonic point ($D = u + c$) on detonation locus
  D_{CJ} is minimum detonation speed
  Unsupported (self-sustaining) detonation wave
- von Neumann (VN) spike
  Lead shock in reactants

CJ state relations

Explicit formula for CJ state ($P_0 = 0$)

$$D_{CJ}^2 = 2(\gamma^2 - 1)Q \qquad \text{Ideal HE only}$$

$$P_{CJ} = \frac{\rho_0 D_{CJ}^2}{\gamma+1}$$

$$V_{CJ} = \frac{\gamma}{\gamma+1} V_0$$

$$u_{CJ} = \frac{D_{CJ}}{\gamma+1}$$

$$c_{CJ} = \frac{\gamma}{\gamma+1} D_{CJ}$$

where $\gamma = c^2/(PV)$ is adiabatic exponent at CJ state

Detonation pressure proportional to energy release Q

Detonation speed proportional to square root of Q

$c_{CJ} = \gamma u_{CJ} > u_{CJ}$ (sonic with respect to front, $u_{CJ} + c_{CJ} = D_{CJ}$)

Typically, for solid explosive $\gamma_{CJ} \approx 3$

Overdriven detonation wave

Example shock/detonation locus for PBX 9502

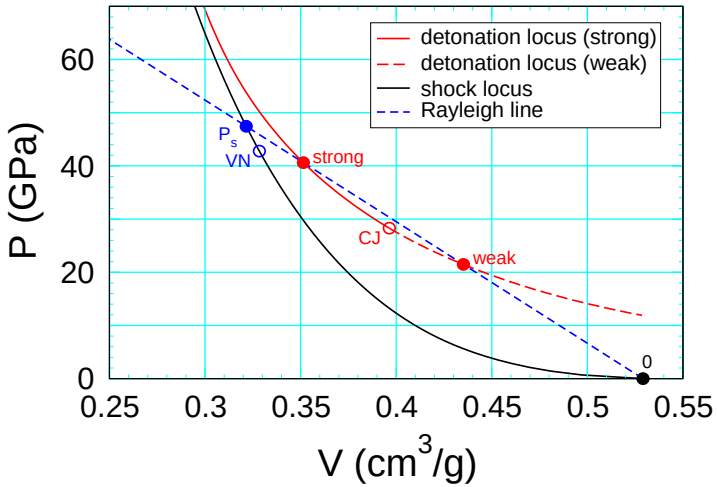

Rayleigh line with $D > D_{CJ}$

2 branches for $D > D_{CJ}$

- Subsonic ($D < u + c$) strong detonation ($P > P_{CJ}$)
  Profile for reaction zone
  Overdriven detonation wave
- Supersonic ($D > u + c$) weak detonation ($P < P_{CJ}$)
  no profile (unphysical)

Shock and detonation loci

Example shock/detonation locus for PBX 9502

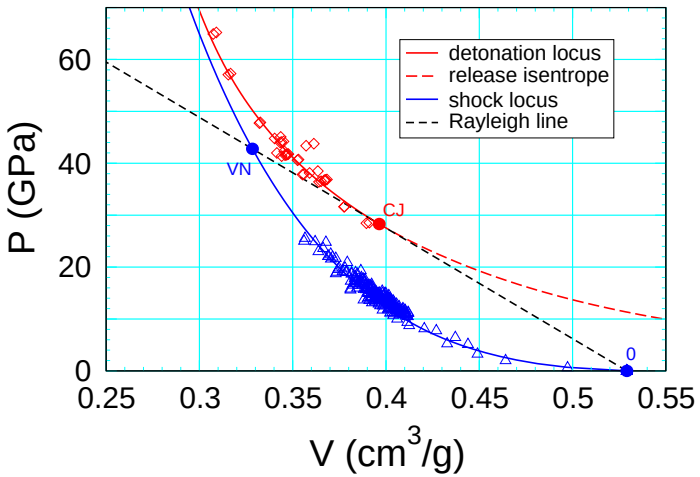

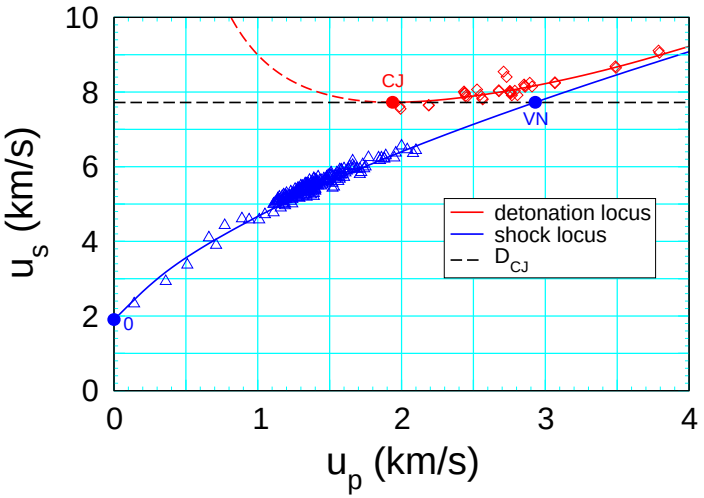

Data

- Overdriven detonation waves

  Experiments with flyer plate to support detonation
- Reactants shock Hugoniot

  $u_s(u_p)$ concave down for weak shocks

  Extrapolation for strong shocks

Detonation speed dependence on initial state

- PBX density can vary with pressing conditions
  Detonation speed depends on energy release per volume
- Range of temperatures, $-55 < T < 75C$, for applications
  Thermal expansion affects initial density
  EOS models may be inaccurate due to change in porosity
  Also issue with thermal cycling

Linearize Hugoniot equation and sonic condition

$$\frac{\Delta D_{cj}}{D_{cj}} = A\frac{\Delta \rho_0}{\rho_0} + B\frac{\Delta e_0}{D_{cj}^2}$$

where

$$A = \frac{\gamma(\gamma - \Gamma - 1)}{2\gamma - \Gamma} \qquad B = \frac{\Gamma}{2\gamma - \Gamma}(\gamma + 1)^2$$

γ is adiabatic exponent, $\gamma \approx 3$ at CJ state
Γ is Grüniesen coefficient, $\Gamma \approx 0.5$ at CJ state

EOS uncertainty

- Density is measured at room temperature
  $\rho_0 = \mathrm{mass}/\mathrm{volume}$ with volume from water immersion measurement
- Density at temperature from thermal expansion
  Uncertainty in coefficient of thermal expansion
  For PBX 9502, HE crystals anisotropic and partly align (texture)
  Ratchet growth (thermal cycling) affects density
- Uncertainty in initial energy from reactant EOS
  EOS models typically calibrated to shock Hugoniot
  Γ, C_V and thermal expansion coefficient not accurate
  2^{nd} order effect for purpose of calculating D_{CJ}
- Equilibrium products EOS
  Independent of initial reactants state
  Provided composition and impurities are the same

Deflagration locus

Solutions to Hugoniot equation for $\lambda = 1$

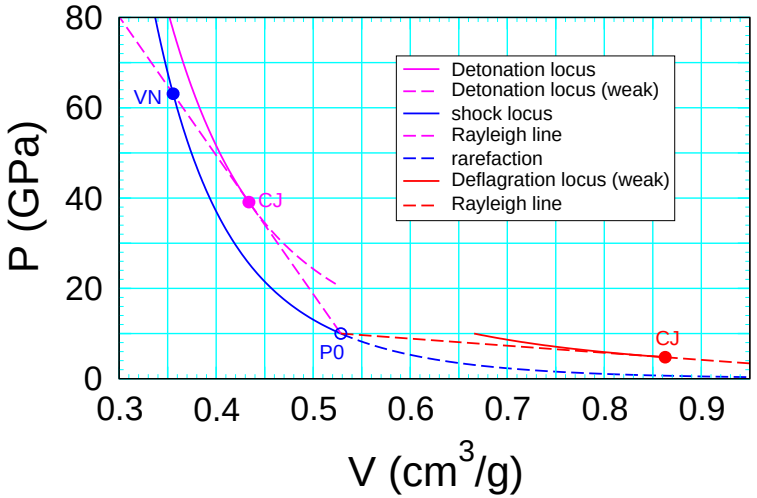

- $V < V_0$ (compression)
  D_{CJ} is minimum detonation speed
  Strong branch ($P \geq P_{CJ}$) allowed
  Supersonic ahead and subsonic behind
  Weak branch, no profile
- $V > V_0$ (expansion)
  Unlike shock, entropy increasing due to reaction
  $\widetilde{D}_{CJ}$ is maximum deflagration speed
  Weak branch ($V < \widetilde{V}_{CJ}$ possible)
  Flow subsonic ahead and subsonic behind
  Profile for point on locus determined by heat conduction
- Between detonation and deflagration loci
  Unphysical, $P > P_0$ and $V > V_0$ implies $D^2 < 0$

4. Planar detonation wave

Unsupported detonation wave

- Chapman-Jouguet detonation wave is shock like discontinuity propagating at the CJ detonation speed
  "Programmed burn" model for propagating detonation waves
- Zeldovich (1940), von Neumann (1942), Doering (1943)
  Modeled reaction zone due to finite rate (reactive fluid equations)
- Unsupported 1-D detonation
  Steady ZND reaction zone
  + Taylor wave (rarefaction) which spreads out in time
    End of reaction zone and head of rarefaction coincide

Wave diagram

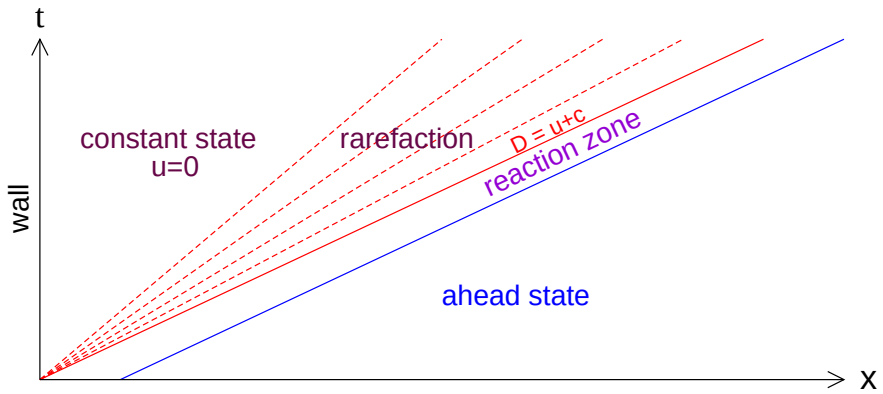

Wave profiles

Pressure profiles at sequence of times

Lab frame

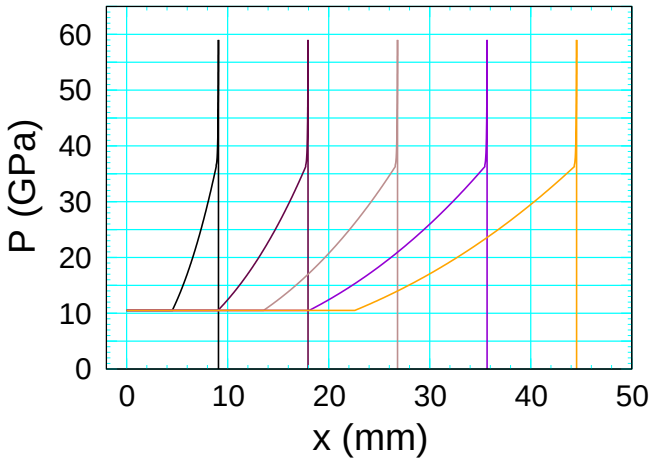

Relative to detonation front

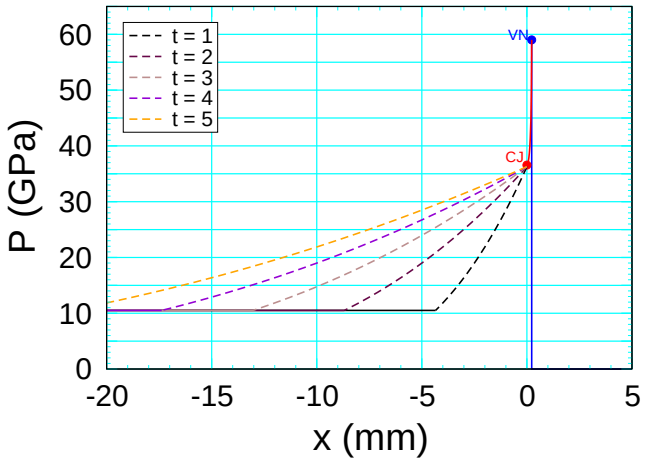

V-P trajectory

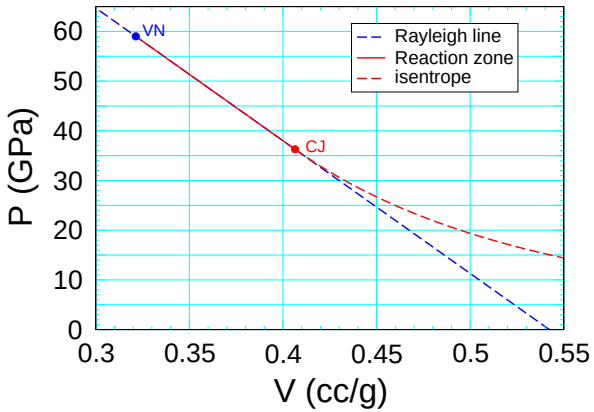

zoom on reaction zone

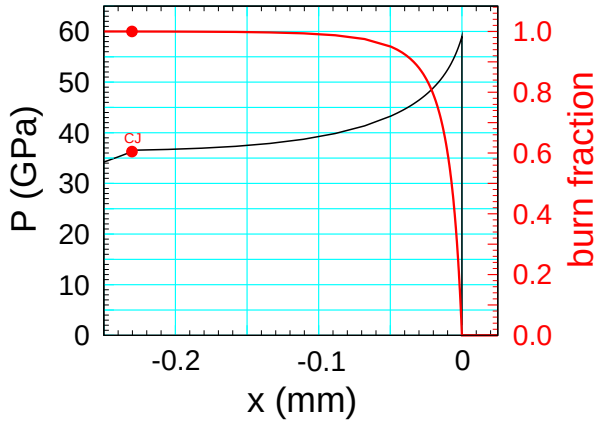

Reaction zone width

Depletion factor: $\mathcal{R} \to 0$ as reactants burned up

$\mathcal{R} \propto (1-\lambda)^n$ as $\lambda \to 1$

Tail of wave profile

$(\mathrm{d}/\mathrm{d}t)\lambda = \mathcal{R}(\lambda)$

- $n < 1$

  Hot spot burn rate

  Finite burn time and reaction zone width

  $1 - \lambda(t) \propto (t_* - t)^{1/(1-n)}$ as $t \to t_*$

  Important for curvature effect

- $n = 1$

  First order reaction

  exponential tail, $1 - \lambda(t) \propto \exp(-t)$ as $t \to \infty$

- $n > 1$

  Reaction order for chemical reaction

  Algebraic tail, $1 - \lambda(t) \propto t^{-1/(n-1)}$ as $t \to \infty$

Derivation of ZND profile

Partly burned detonation loci

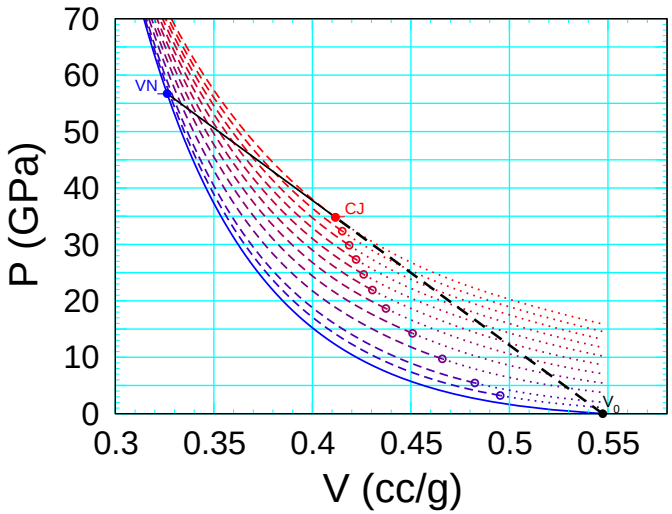

- For steady wave, $\xi = x - D\,t$ mass, momentum and energy fluxes are constant in rest frame of front

  ▸ jump conditions

- In (V, P)–plane flow on intersection of Rayleigh line, slope $= -(\rho_0 D_{CJ})^2$ and partly burned detonation loci Parameterized points by λ

Rate equation reduces to ODE

$$(\mathrm{d}/\mathrm{d}\xi)\lambda = -\mathcal{R}\big(V(\lambda), e(\lambda), \lambda\big)/[D - u(\lambda)]$$

where $V(\lambda)$, $e(\lambda)$, $u(\lambda)$ are point on partly detonation locus with detonation speed D, reduces to algebraic equation in 1 variable

Profile for strong branch of detonation locus, $D \geq D_{CJ}$

Detonation locus and Rayleigh line

Point of partly burned detonation locus with detonation speed D

Use jump condition to reduce to 1 equation for $V(\lambda)$

Newton iteration to find solution $f(V) = 0$

$$e_h(V) = \lambda Q + e_0 + \tfrac{1}{2} m^2 (V_0 - V)^2 + P_0 (V_0 - V)$$

$$P_h(V) = P(V, e_h(V), \lambda)$$

$$f(V) = P_h - P_0 - m^2 (V_0 - V)$$

$$f'(V) = -(c/V)^2 + \Gamma \left[P_h - P_0 - m^2 (V_0 - V) \right] / V + m^2$$

$$V \to V - f(V)/f'(V) \quad \text{Newton iteration}$$

where $m = \rho_0 D$ is mass flux for detonation speed
which defines Rayleigh line

For ODE for $\lambda(\xi)$ use last V to start iteration.

Algorithm very robust for any model EOS.

Taylor wave

1. ODEs for CJ isentrope of products EOS and velocity for rarefaction wave (right facing) ▸ characteristic equations

$$\frac{\mathrm{d}}{\mathrm{d}V}\begin{pmatrix} e \\ u \end{pmatrix} = -\begin{pmatrix} P(V,e) \\ c(V,e)/V \end{pmatrix}$$

Integrate trajectory starting at CJ state $(V_{CJ},\ e_{CJ},\ u_{CJ})$
til the back boundary condition is met (such as piston velocity)

2. Rarefaction wave (right facing)
   All variable (V, e, u) are constant on characteristics, $\mathrm{d}x/\mathrm{d}t = u + c$
   Characteristics are straight line in (t, x) ▸ wave diagram
   Characteristic speed is monotonic function V
   for convex isentropes, $(\partial^2 P/\partial V^2)_S > 0$
   Almost all materials have convex isentropes
   Exceptions for anomalous cases, such as near critical point

Experimental PBX 9501 profile

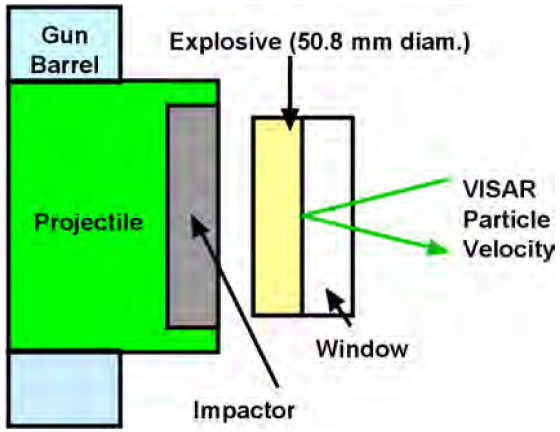

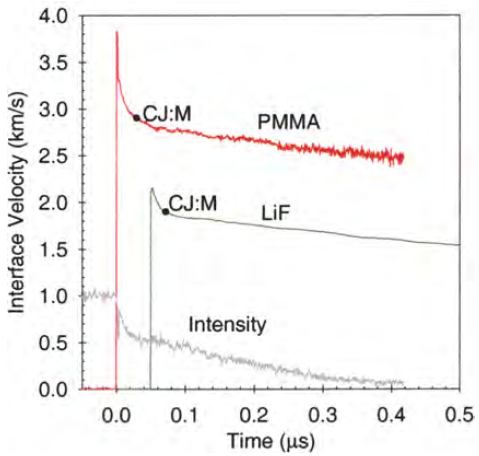

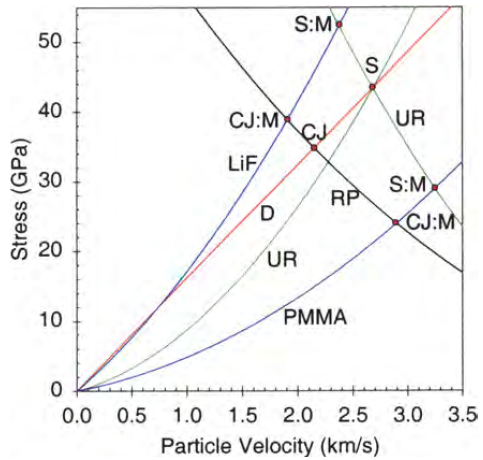

Gustavsen, Sheffield & Alcon

11th Detonation Symposium (1998)

6 experiments (4 PMMA + 2 LiF)

- Initiation pressure 3.9 to 6 GPa
  Detonation runs for 8 to 17 mm
- Peak gets clipped
  $\sim$ 2 ns temporal resolution
  VISAR spot size (0.5 mm)
  PBX/window interface
  8 μm kapton + 0.4 μm Al + glue
- VN spike pressure
  38.7 to 53.4 GPa
- reaction time 19 to 60 ns
  Does not account for profile $u(t)$

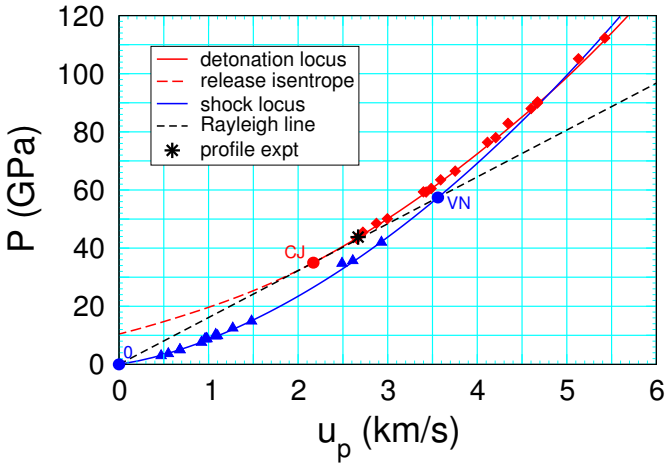

Simulated PBX 9502 profile

- Numerical shock profile
  Rather than discontinuous shock
- Head of rarefaction/end of reaction zone
  Rapid but smooth transition
  rather than kink
- With low resolution
  Burning in shock rise
  clip VN spike

Planar propagating detonation wave

Used as verification test

Semi-analytic solution to compare with

For any EOS and any burn rate

High resolution simulation

V-P trajectory

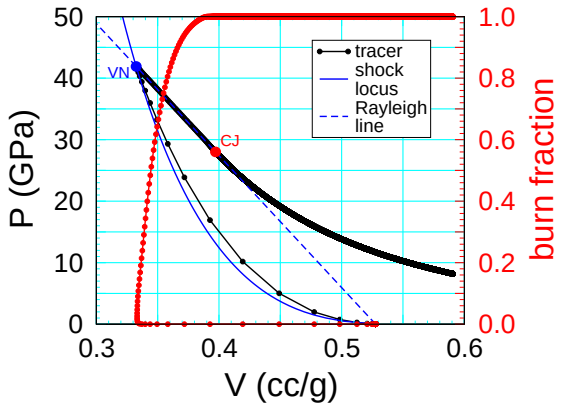

Reaction zone profile

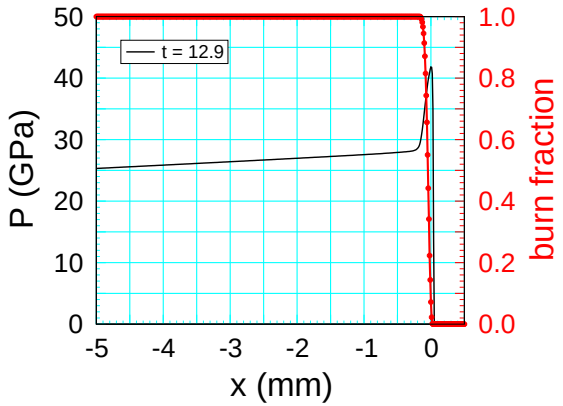

Chemical energy released

Heat of detonation is change in enthalpy ($H = e + PV$)
between products expanded out to $P = 0$ and reactants state

Heat release
$-\Delta$ enthalpy is area shown in red

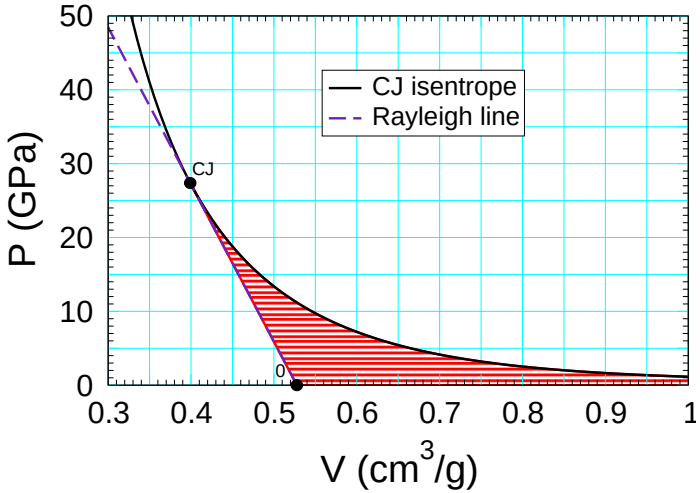

cylinder test

Cylinder test wall velocity

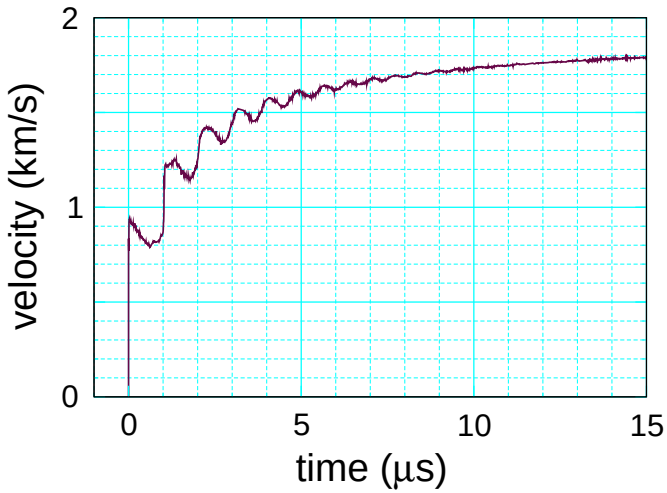

convert HE energy to KE of wall

Useful energy limited by expansion

At expansion of $V_0/V = 7$, $P \approx 0.1$ GPa
and recover above 80 % of chemical energy

Measurement of energy released

- Bomb calorimeter
  Large volume implies small change in pressure when HE reacts
  1. Inert gas in calorimeter gives heat of detonation
  2. Air in calorimeter gives heat of combustion
     Additional reactions with oxygen in air
     For oxygen poor explosives, such as for TNT
- Heat of formation
  If products species are known
  reactants $\rightarrow \sum_i \nu_i \, \mathrm{prod}_i$
  where ν_i are stoichiometry coefficients
  $\Delta H_{\mathrm{reaction}} = \sum_i \nu_i H_{\mathrm{prod}_i} - H_{\mathrm{reactants}}$

Convention for heat release

$$Q = -\Delta H_{\mathrm{reaction}} \begin{cases} > 0 & \text{for exothermic reaction} \\ < 0 & \text{for endothermic reaction} \end{cases}$$

5. Shock-to-detonation transition

Initiation mechanism

Positive feedback mechanism for shock initiation

- Shock initiates reaction

  Hot spot burning for heterogeneous HE
- Reaction increase shock strength

  Source term in characteristic equation and pressure gradient

  Pressure gradient from competition

  reaction starting earlier vs later with higher rate
- Increased shock pressure increase reaction rate

  More hot spots and increased burning around each hot spot

Lead shock pressure vs distance of run

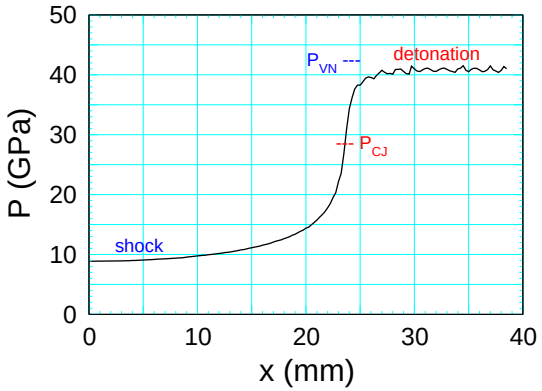

Similar to thermal runaway

$T(t)$ for constant volume burn

Shock initiation experiments

1-D shock initiation with sustained shock

- Wedge experiment (1960)

  Lead shock trajectory
  Shock breakout on wedge
  outruns side rarefaction
  Booster/Attenuator minimizes
  pressure gradient

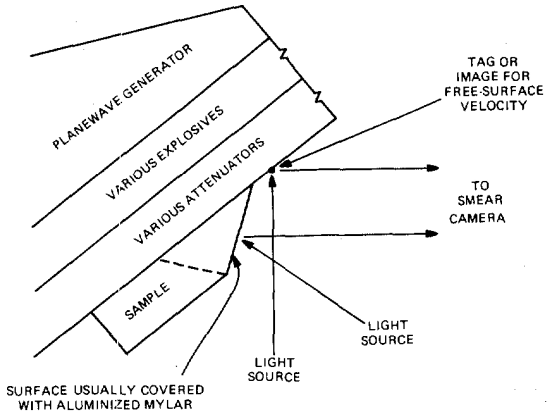

- Gas gun experiment

  Embedded magnetic velocity gauges
  25 μm Teflon + 5 μm Al + 25 μm Teflon

  Tracker gauge for shock trajectory
  Lagrangian velocity time histories
  Vary shock loading with
  material layers on projectile

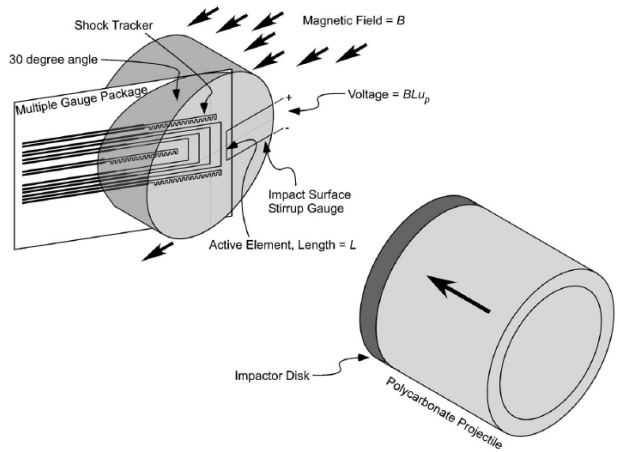

Gustavsen *et al.*, late 1990

Pop plot data (ambient PBX 9502)

Shock trajectory

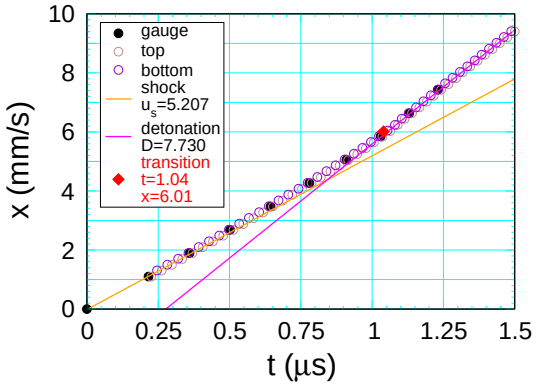

Velocity profiles

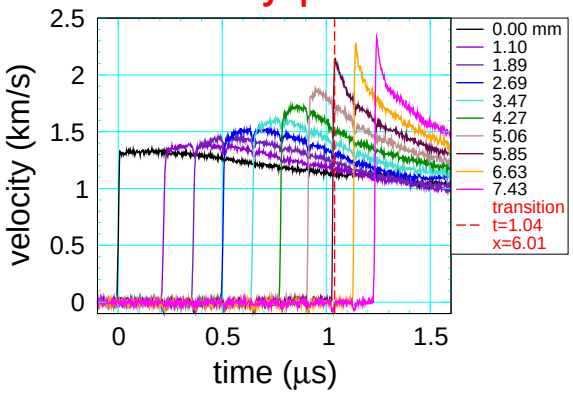

distance-of-run

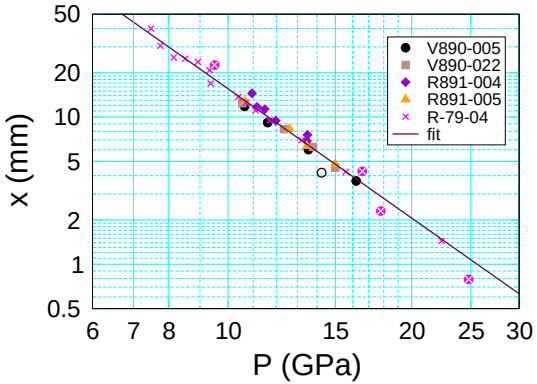

time to detonation

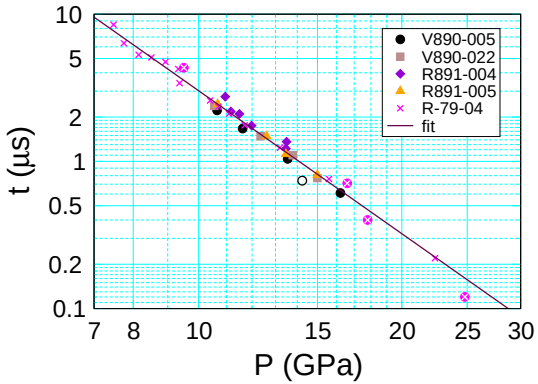

$x(t)$

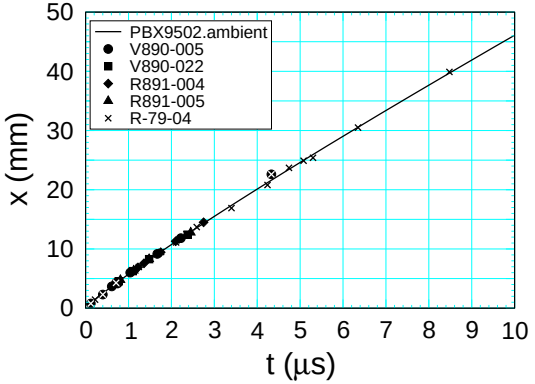

- Linear on log-log plot
  Both run distance and run time, and $x(t)$

Pressure range for Pop plot

Limitations on Pop plot data

- Low pressure
  Large run distance
  Sustained drive pressure limited by side rarefactions
  Pore collapse not effective at low pressures
    PBX shock width due to visco-elastic and elastic-plastic effects
    Run distance greater than linear fit on log-log plot
  Data for HMX based PBXs (projectile from 6 inch howitzer) show
    Run distance and run time bend upward at low pressures
- High pressure
  Short run distance
  Large uncertainties in shock trajectory and initial shock pressure
  Transients if run distance $\gtrsim$ steady reaction zone width

Chemical rate

Reactants shock temperature

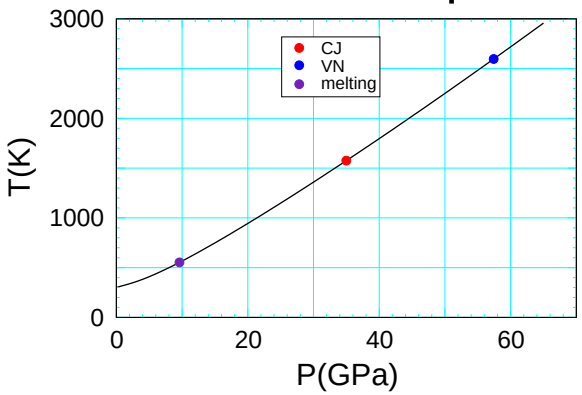

- 3 GPa on Pop plot for PBX 9501
  Time to detonation 3 to 4.5 μs
- Shock temperature 358 K
- Melt temperature, 550 K
  Thermal initiation time, $\sim$ 5000 s
- Chemical rate at shock temperature
  Orders of magnitude too low

Hot Spots reconcile discrepancy

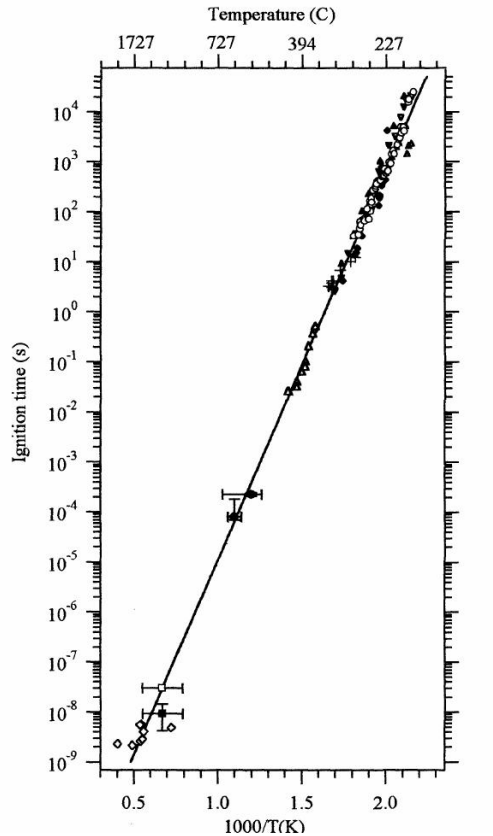

Henson-Smilowitz global rate

Temperature variation

PBX 9502

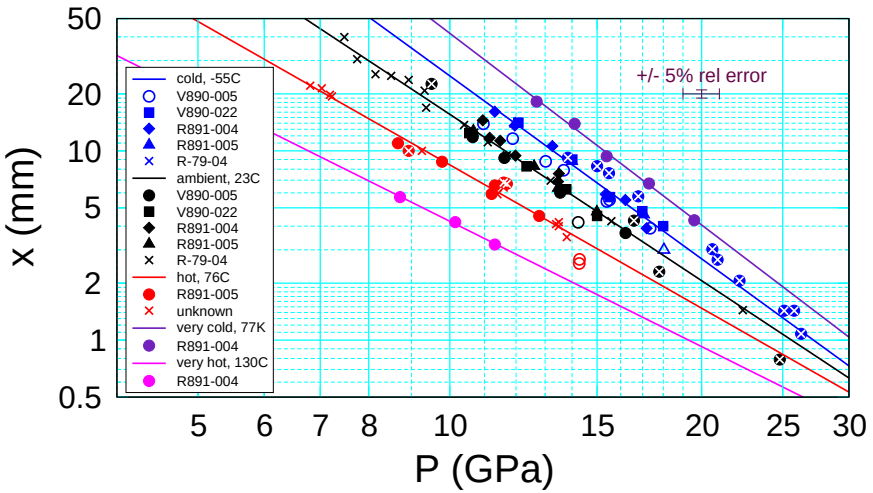

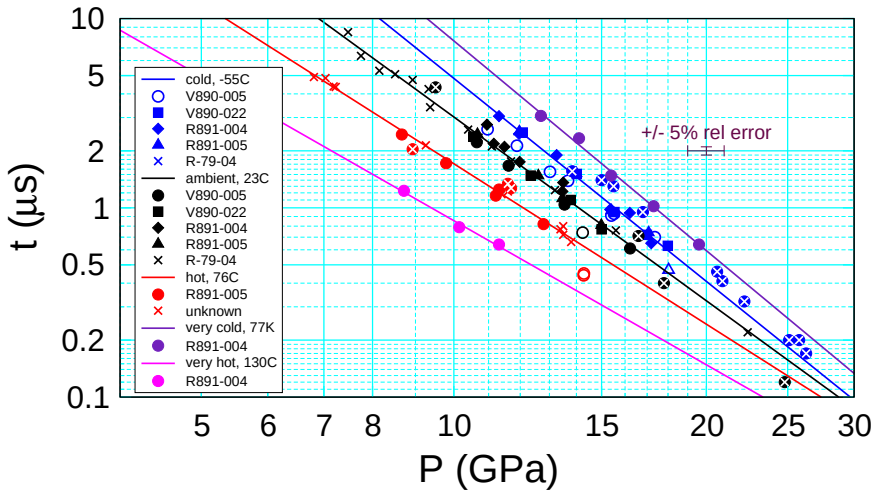

- Shock sensitivity
  More sensitive explosive has shorter run distance
- As temperature increases
  More sensitive
- Scatter in data ($\pm 7\,\%$ & outliers up to $30\,\%$)
  Uncertainties from experiment
  Sample variation from heterogeneities

Lot dependence

cold (-55 C) PBX 9502

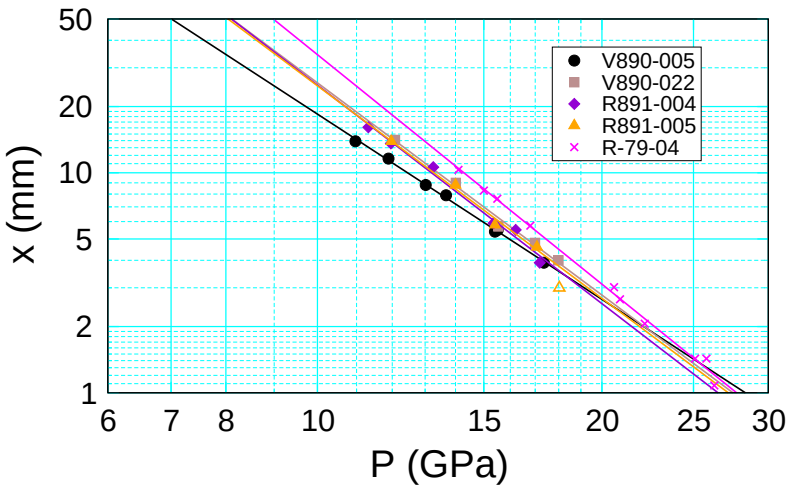

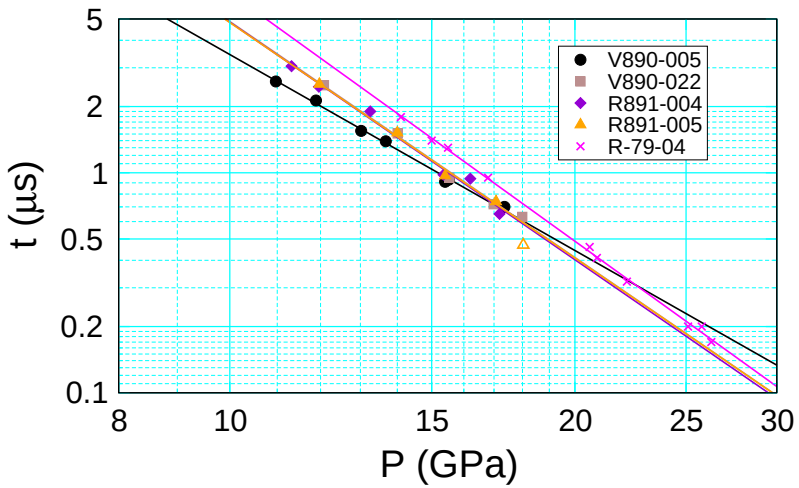

- Large lot dependence
  Greater than uncertainty in data
  Correlated variation in run time and run distance
- Burn rate affected by variation in heterogeneities
  Model parameters need to be fit for each lot
  or loss accuracy and potentially predictivity
- Issue for detonator/booster systems

Density variation

run distance

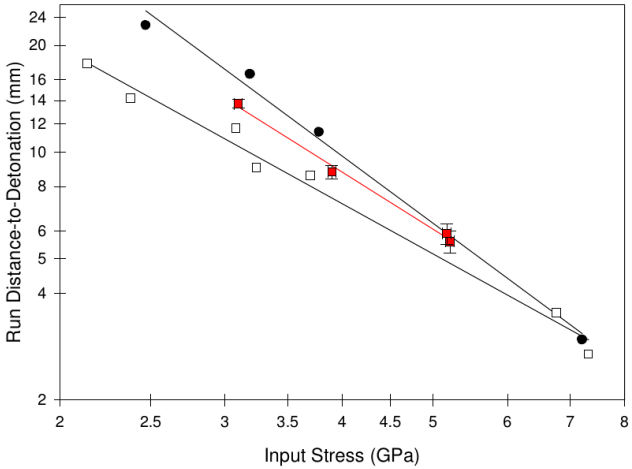

run time

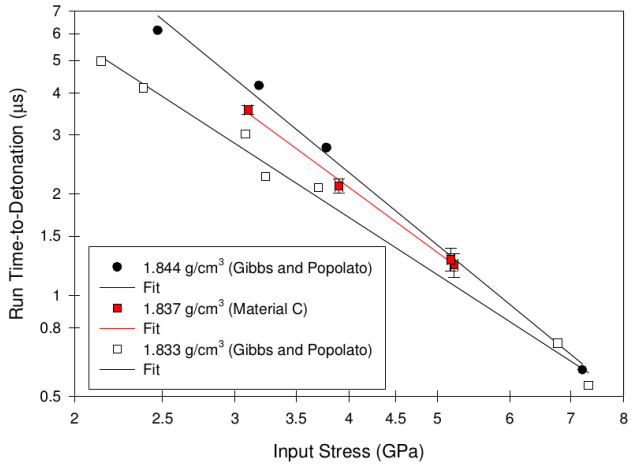

Gustavsen *et al.*, 1999

- PBX 9501 pressing density
  1.833, 1.837 and 1.844 g/cc
  small density variation ± 5 mg/cc or ± 0.3 %
  large change in porosity ± 20 %
- run distance at 3 GPa, 11 to 19 mm or ± 25 %
- run time at 3 GPa, 3 to 4.5 μs or ± 20 %

Homogeneous vs Heterogeneous initiation

Chemical rate at bulk temperature vs hot spot rate
(Two papers by Campbell, Davis, Ramsay & Travis 1961)

- Homogeneous shock initiation
  Thermal runaway near HE interface
  Leading to super-detonation wave
  in shock compressed HE Detonation overtakes lead shock
- Heterogeneous shock initiation
  Reaction behind lead shock
  Shock strengthens to detonation
- Adding glass beads to nitromethane
  Velocity profiles change character from homogeneous to heterogeneous
  Also bubbles in liquid nitroglycerin

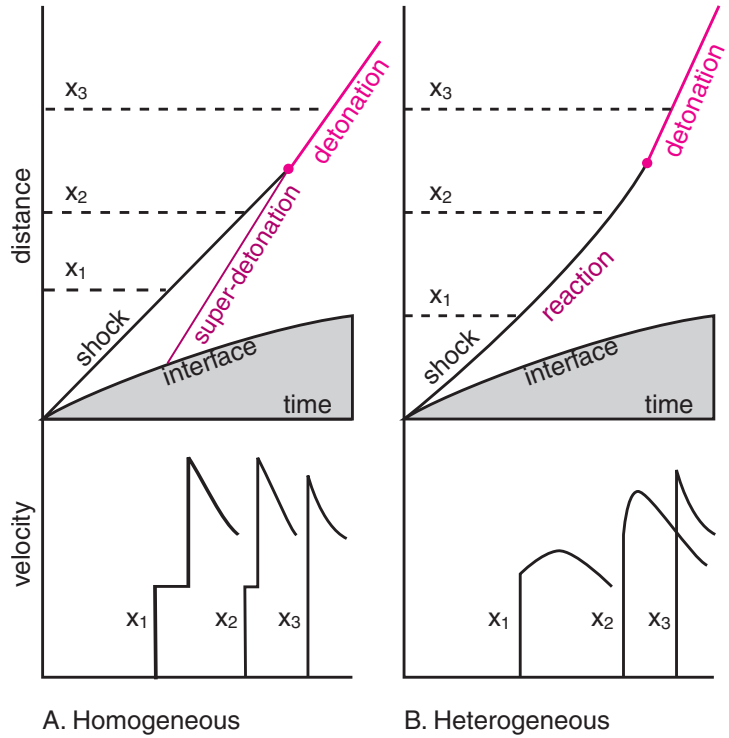

Super-detonation

- Wave loci (shock or detonation)
  Depends on state ahead of wave
  Not unique for material
- Shocked compressed state
  Higher energy per volume
  Detonation wave has
  higher D_{CJ} and P_{CJ}
  then for ambient state
  Called super-detonation
- Vary initial temperature
  Changes ahead state and CJ state varies
  Smaller effect than super-detonation

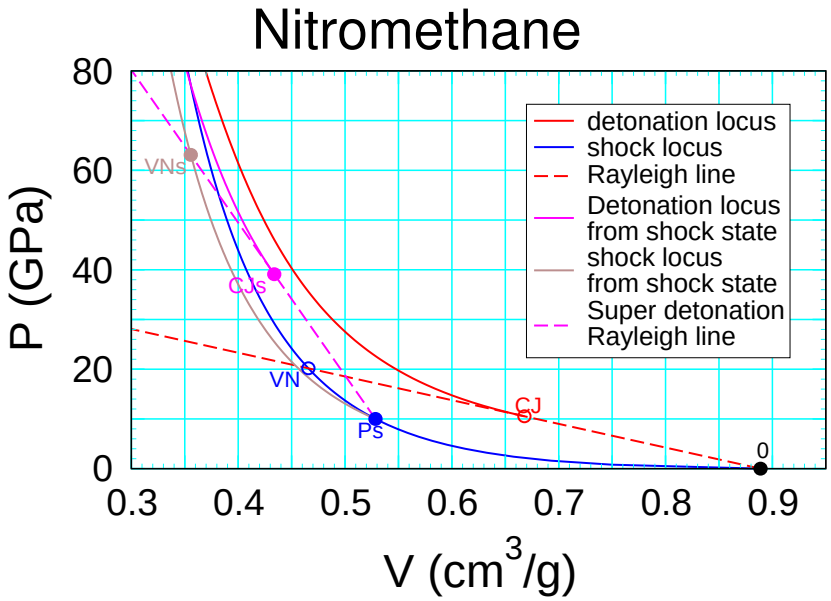

Shock desensitization

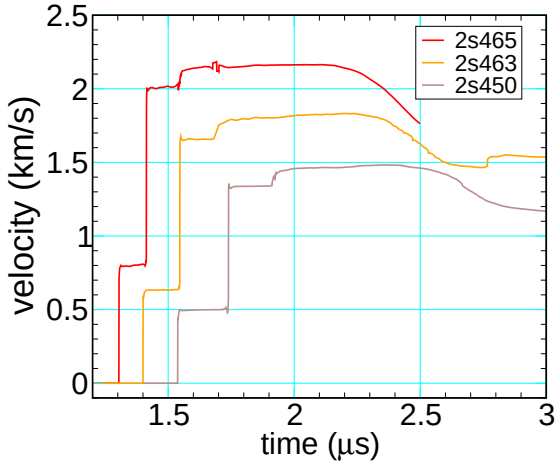

Double shock PBX 9502

shot	P1 GPa	P2 GPa
2s450	5.3	19
2s463	7.0	25
2s465	9.0	33

- Double shock
  Rate set by first shock
- Single crystal HMX very insensitive compared to PBX 9051
  Failed to detonate in 7 mm at shock pressure of 34 GPa
- Interpretation
  First shock closes pores and sets hot spot density
- Shock/rarefaction/shock
  Rate between first and second shock

Other shock initiation

Complex shock loading

- **Short shock**
  Time duration of shock less than time to detonation
  1-D version of fragment impact
- **Multiple shocks**
  Shock desensitization
  Weak transverse shock can quench propagating detonation wave
  Dead zones for corner turning
- **Shock followed by rarefaction**
  Gap test
  Detonation wave in donor HE $\rightarrow$ inert $\rightarrow$ acceptor HE
- **Shock initiation with divergence**
  Detonator / booster

Quench propagating detonation wave

Detonation wave in PBX 9502

Transverse shock from steel flyer plate

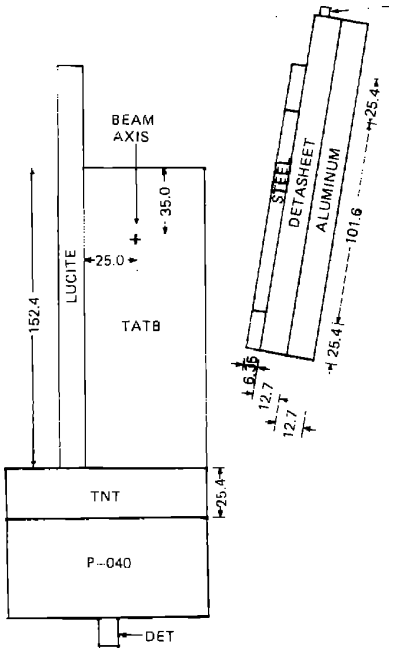

Phermex shot # 1697

static

dynamic

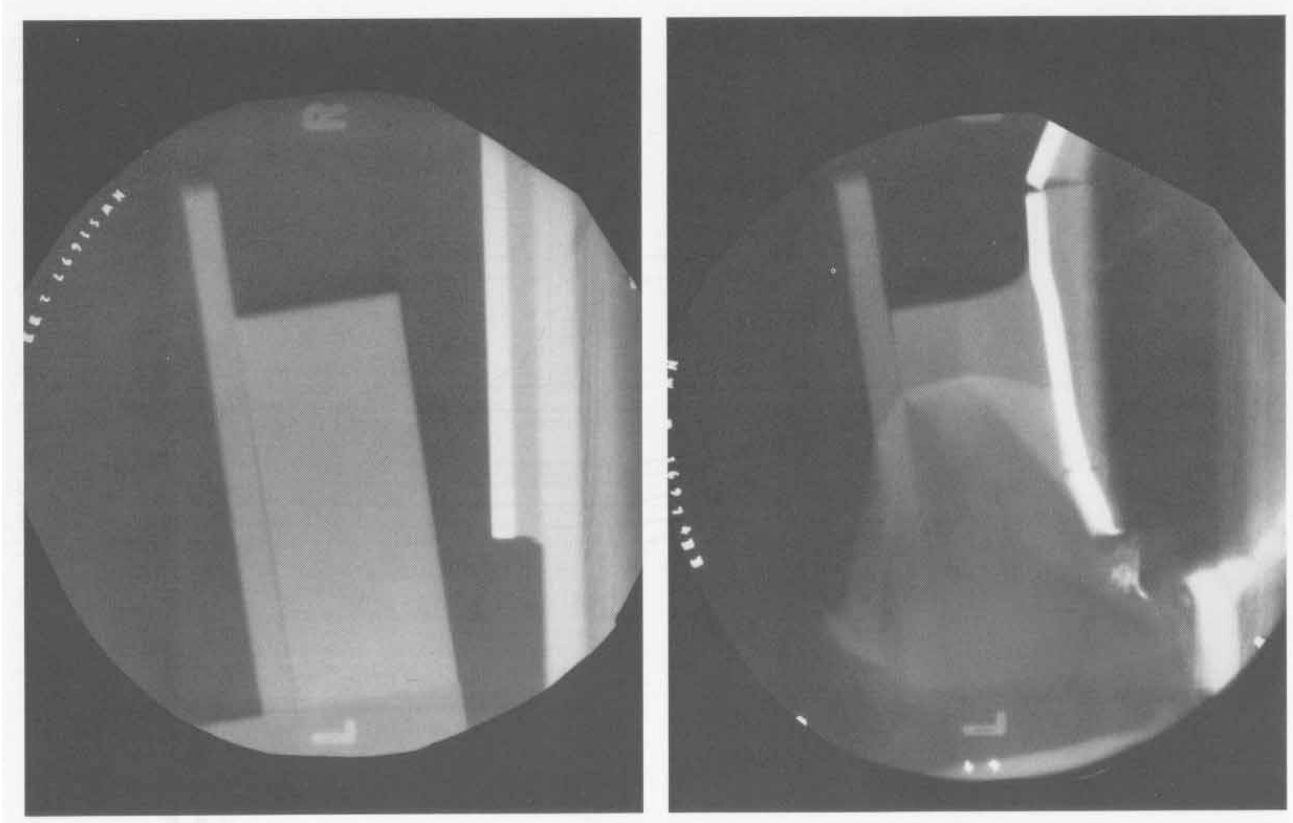

HE initiation for simulation

Initiate detonation wave in simulation

- ‘Hot spot’
  Small region of high pressure
  Products at CJ state
- Drive shock into reactants
  Riemann problem determines shock pressure in reactants
  Rarefaction into hot spot
- Prompt shock-to-detonation transition
  Hot spot needs to be large enough to maintain pressure
  over time to detonation from Pop plot
  at reactants shock pressure
  Similar to short shock initiation

Hot spot plays role of a detonator

Or programmed burn HE to generate hot spot

6. Ignition and growth concept of Hot Spots

Hot spot burning

Hot spots for initiation by friction and impact (Bowden & Yoffe, 1952)
Hot spots for shock initiation in heterogeneous HE (Campbell *et al.*, 1961)
Ignition & Growth concept (Lee & Tarver, 1980)

- Shock front triggers hot spots
  Void collapse on fast time scale
- Burn centers
  Competition: heat conduction & reaction
    Small hot spots quench
    Large hot spots become burn centers
- Reactive wavelets
  Deflagration wave from burn centers
  Burn rate = (front area) · (deflagration speed)
- Depletion of reactants
  Overlap of reactive wavelets
  Geometric effect on front area

Potential hot spot sites

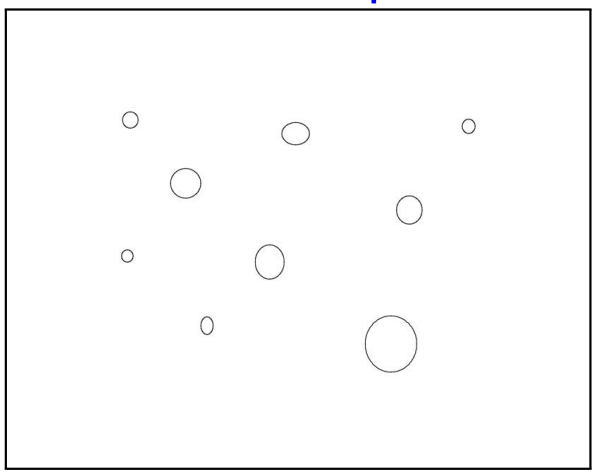

Pores or cracks
inter- or intra-granular

Hot spot burning

Ignition & Growth concept (Lee & Tarver, 1980)

- Shock front triggers hot spots
  Void collapse on fast time scale
- Burn centers
  Competition: heat conduction & reaction
  - Small hot spots quench
  - Large hot spots become burn centers
- Reactive wavelets
  Deflagration wave from burn centers
  Burn rate = (front area) · (deflagration speed)
- Depletion of reactants
  Overlap of reactive wavelets
  Geometric effect on front area

Shock sweeps over pores

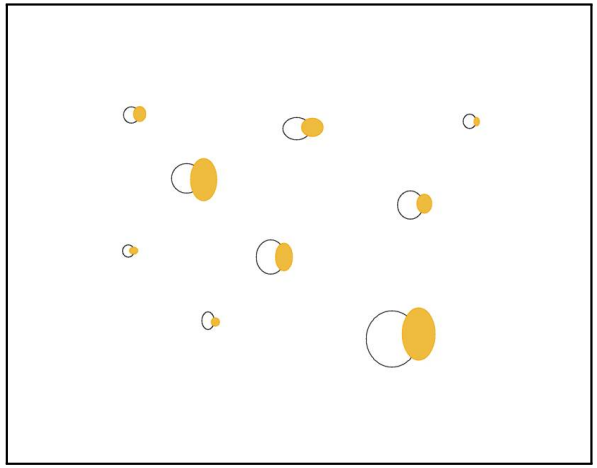

Hot spots form

Localized spatial regions
of high temperature

Hot spot burning

Ignition & Growth concept (Lee & Tarver, 1980)

- Shock front triggers hot spots
  Void collapse on fast time scale
- Burn centers
  Competition: heat conduction & reaction
    Small hot spots quench
    Large hot spots become burn centers
- Reactive wavelets
  Deflagration wave from burn centers
  Burn rate = (front area) · (deflagration speed)
- Depletion of reactants
  Overlap of reactive wavelets
  Geometric effect on front area

Ignition phase

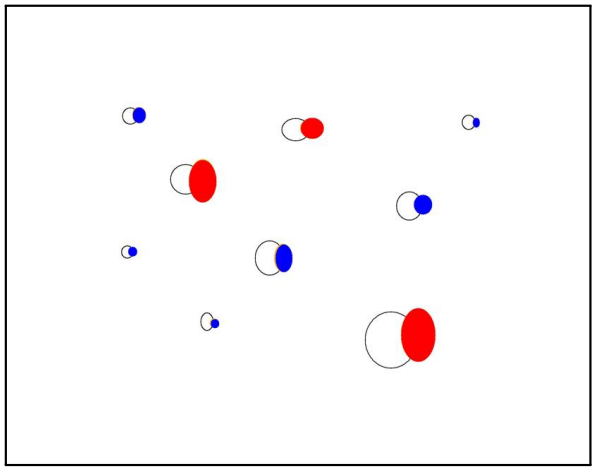

Hot spots react
some form burn centers

average $\mathcal{R}(T) \gg \mathcal{R}(\text{average } T)$

Burning dominated by
tail of temperature distribution

Hot spot burning

Ignition & Growth concept (Lee & Tarver, 1980)

- Shock front triggers hot spots
  Void collapse on fast time scale
- Burn centers
  Competition: heat conduction & reaction
    Small hot spots quench
    Large hot spots become burn centers
- Reactive wavelets
  Deflagration wave from burn centers
  Burn rate = (front area) · (deflagration speed)
- Depletion of reactants
  Overlap of reactive wavelets
  Geometric effect on front area

Early growth phase

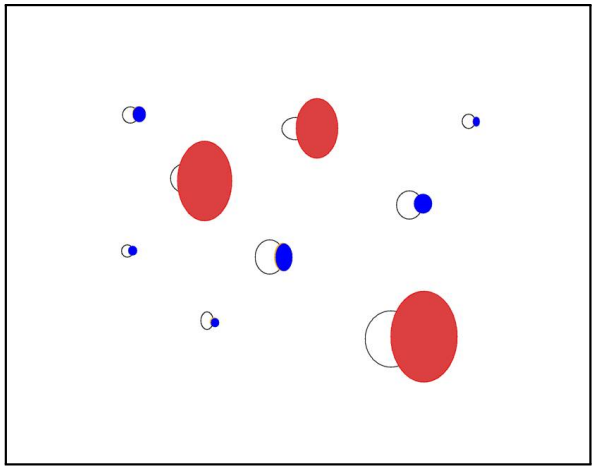

Burn front area increases

Reactants & products
are phase separated

Hot spot burning

Ignition & Growth concept (Lee & Tarver, 1980)

- Shock front triggers hot spots
  Void collapse on fast time scale
- Burn centers
  Competition: heat conduction & reaction
    Small hot spots quench
    Large hot spots become burn centers
- Reactive wavelets
  Deflagration wave from burn centers
  Burn rate = (front area) · (deflagration speed)
- Depletion of reactants
  Overlap of reactive wavelets
  Geometric effect on front area

Late growth phase

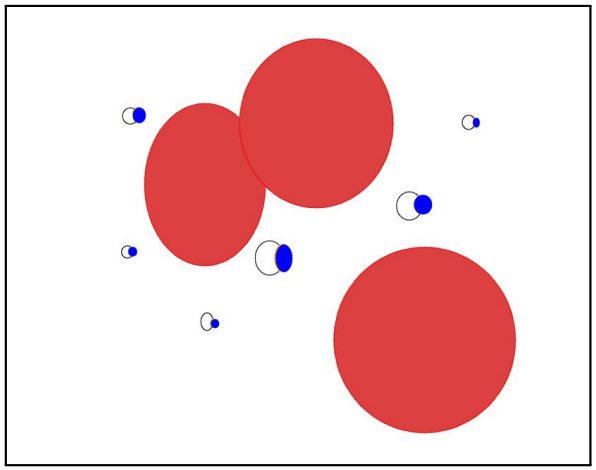

Depletion limited

Burn front area decreases

Hot spot requirements

- Minimum hot spot temperature
  Pop plot run time for PBX 9501: 4 μs at 3 GPa
  Hot-spot thermal ignition time likely 10 times faster ▸ gauge
  (little reaction in ignition phase, volume of hot spots is small)
  Estimate based on Henson-Smilowitz global rate for HMX (PBX 9501)
  Temperature greater than 1100 K at 3 GPa ▸ rate
  Need dissipative mechanism to localize energy in hot spot
- Hot spot size range
  (deflagration wave width) $<$ (hot spot size) $<$ (detonation wave width)
  Estimated hot spot size between 0.1 μm and 5 μm
  USANS data goes to smaller sizes
  Manufacturing defect if pores on the order of small grain size
  Single hot spot can trigger deflagration but not detonation
- Number density of pores
  For fixed porosity, number density scales as (pore size)$^{-3}$

Perspective on hot spot burn rate

- Subgrid model for effective burn rate
  Accounts for effect of small unresolved length scales
  Hot spot burning implies rate is dominated by
    Tail of temperature distribution
    Not mean field theory homogenization
- Rate depends on nature of PBX heterogeneities
  PBX not completely characterized by thermodynamic variables
  Lot dependence on Pop plot data as seen for cold PBX 9502
  Variation of thermal expansion of PBX 9502
    Partial orientation of TATB grain (texture) & crystal anisotropy
- History dependent response
  Shock desensitization (rate set by lead shock)
  Ratchet grow (thermal cycling decreases density)
    Stress relaxation at grain contacts
- Need to calibrate engineering models
  Most burn models, calibration needed for each ρ_0 and T_0
  Effectively treats each initial condition as distinct explosive

Hot spot burn rate

Hot spot concept suggests (heuristic) form of rate

$$\mathcal{R} = \mathrm{g}(\lambda) \cdot (\text{deflagration speed}) \cdot (\text{burn center number density})^{1/3}$$

where $g(\lambda)$ is scaling of wavelet front area
and depends on heterogeneities

- (burn center number density) depends on lead shock strength
  Naturally accounts for shock desensitization
  Rate increases with shock strength
- (deflagration speed) depends on reactants state
  Deflagration speed proportional to P^n with $n \lesssim 1$
  Experiments on propellants up to about 0.1 GPa
  Diamond Anvil Cell with HMX up to 35 GPa
  room temperature rather than shock temperature

Properties of hot spot burn rate

Require a 'large number' of small hot spots

- Statistical behavior
  Small fluctuations for reproducible detonation phenomenon
- Deflagration speed much smaller than detonation speed
  Compensate with large number of burn centers

  (reaction time) $\propto$ (av distance between burn centers) / (deflagration speed)

  (av distance between burn centers) $\propto$ (burn center number density)$^{1/3}$
- Burn center density increases with initial temperature
  Shifts hot spot distribution to higher temperatures
  More hot spots can trigger deflagration wavelets
- Number density of hot spots increases with shock pressure
  Transit time to detonation decreases with shock pressure
- Number density of pores increases with porosity
  Number of potential hot spot sites increase

Pore collapse as hot spot mechanism for shock initiation

Energy localization requires dissipative mechanism

- Pore collapse produces sufficiently high temperatures
  Either micro-jetting or viscous heating
- Hot-spot temperature increases with shock strength
  More burn centers and faster rate at higher shock pressure
- Pore collapse consistent with shock sensitivity
  More pores at higher porosity and faster rate
- Pore collapse consistent with shock desensitization
  First shock crushes pores and eliminates potential hot spot sites
- Pore collapse consistent with low pressure Pop plot data
  Linear Pop plot (log-log scale) breaks down at low pressure

In the pressure range of Pop plot data
other mechanism don't produce sufficient heating

Below pressure of Pop plot data other mechanism needed
Such as shear heating for low velocity impact

Heuristic burn rate

Growth rate for Lee & Tarver's Ignition and Growth model of form

$$\mathcal{R}(\lambda, P) \propto \lambda^{n_1}(1-\lambda)^{n_2} P^n$$

- $\lambda^{n_1}(1-\lambda)^{n_2}$ factor
  Represents to scaling of reactive wavelet area
  Needed to fit embedded velocity gauge time histories
- P^n factor where P is local pressure
  Fits Pop plot data
- Diamond anvil cell or isentropic compression experiments
  Model predicts fast reaction at CJ pressure
  Experiments show negligible reaction
  Hot spots require dissipation for localized energy
- Rate too large for multiple shocks
  Doesn't account for shock desensitization

Fitting form (15 parameters) can be calibrated to subset of data
Does not provide flexibility needed for wide range of phenomena

Model calibration

- Select data to fit (subjective)
  Experiments aimed at single detonation phenomena
- Metric to compare model with data (subjective)
  Simulated data for model (2-D simulation computationally expensive)
  Resolution for accurate simulation and uncertainty in data
- Calibration
  Iterative algorithm to vary parameters to minimize metric
- Issues
  Minimization is highly non-linear (local or global minimum)
  Metric may be insensitive to correlated changes in parameters
  or insufficient data may lead to underdetermined model
- Domain of applicability
  Tacit assumption: hot spot distribution same as calibration experiments
  Model accurate for applications similar to calibration experiments
  May loss accuracy for other applications

7. Diameter effect and curvature effect

Unconfined rate stick

- Cylinder of HE surrounded by air
  Initiate at one end and run long enough to reach steady state
  rule of thumb, length 4 times the diameter
- Measurements
  Timing pins for axial detonation speed
  Curvature effect: Wave breakout along diameter with streak camera

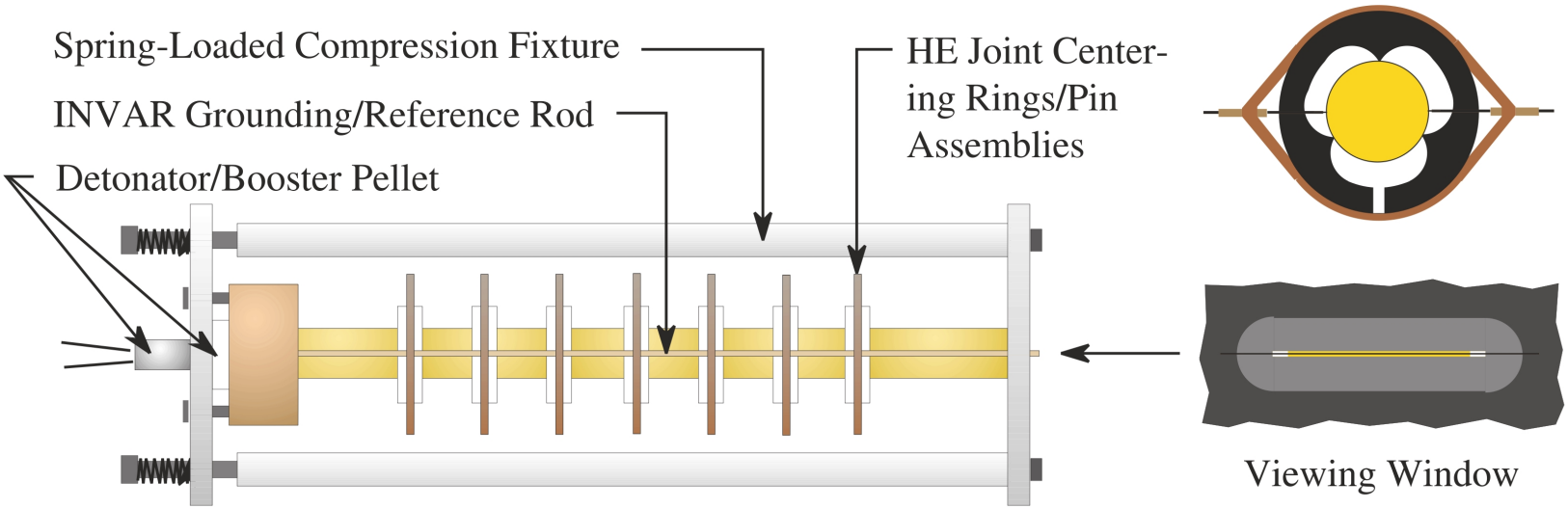

Hill *et al.*, 11th Detonation Symposium (1998)

Diameter effect

- Axial detonation speed as function of rate stick diameter
  Detonation speed decreases as diameter decreases
  Less than D_{CJ}, minimum based on shock jump conditions
- Minimum diameter to propagate detonation wave
- Limit of large diameter, $D(R)/D_{CJ} \rightarrow 1 - a/R$ as $R \rightarrow \infty$

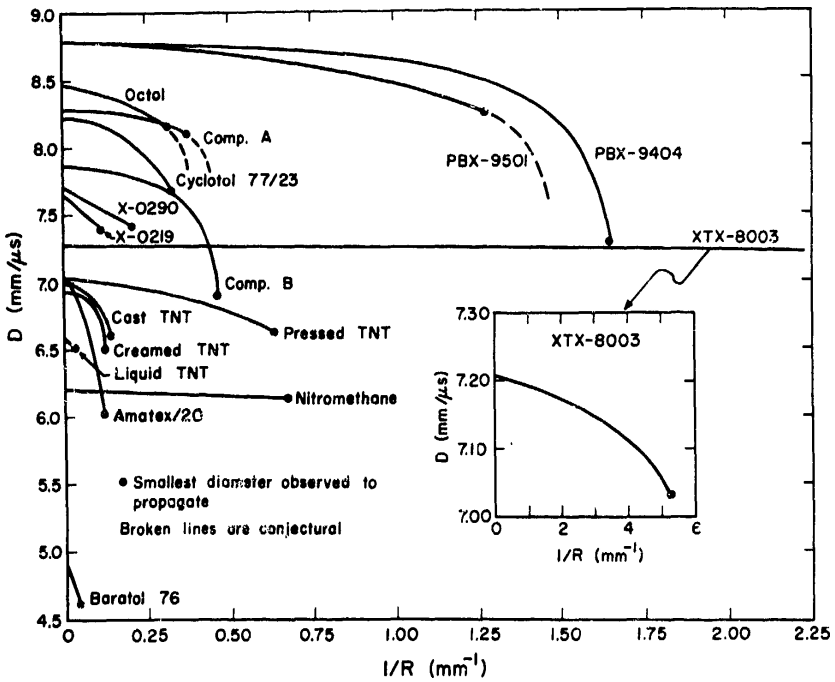

Detonation speed vs 1/R
Campbell & Engelke (1976)
6^{th} Detonation Symposium

Modified jump conditions

- Stream tube in rest frame of detonation front

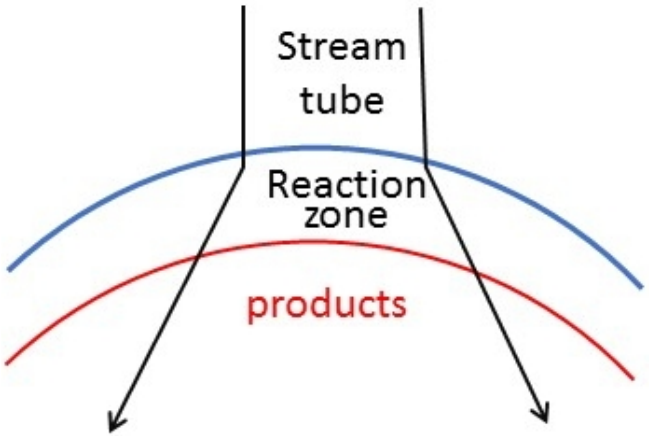

Blue is lead shock front
Red is end of reaction zone
subscripts 'a' and 'b' denote states ahead and behind reaction zone
A is cross sectional area
Diverging wave front if $A_b > A_a$

Duct flow equations

Flux is proportion to cross sectional area

At shock front $\mathrm{d}\ln(\mathit{area})/\mathrm{d}x = \kappa$ is mean front curvature

- Partly burned detonation loci

Correction to jump conditions from reaction zone width + front curvature

Diverging detonation wave, $\kappa > 0$

Sonic point lies within reaction zone

Detonation speed decreases with mean front curvature κ

1-D duct flow equations & jump conditions

$$\partial_t \begin{pmatrix} \rho A \\ \rho A u \\ \rho A(e + \frac{1}{2}u^2) \\ \rho A \lambda \end{pmatrix} + \partial_x \begin{pmatrix} \rho A u \\ \rho A u^2 + AP \\ \rho A u(e + \frac{1}{2}u^2 + PV) \\ \rho A u \lambda \end{pmatrix} = \begin{pmatrix} 0 \\ P\partial_x A \\ -P\partial_t A + \rho A Q \mathcal{R} \\ \rho A \mathcal{R} \end{pmatrix}$$

For quasi-steady detonation A is fixed and $\partial_t A = 0$
Re-express PDEs in conservation form with additional geometric source term

$$\partial_t \begin{pmatrix} \rho \\ \rho u \\ \rho(e + \frac{1}{2}u^2) \end{pmatrix} + \partial_x \begin{pmatrix} \rho u \\ \rho u^2 + P \\ \rho u(e + \frac{1}{2}u^2 + PV) \end{pmatrix} = -\kappa \begin{pmatrix} \rho u \\ \rho u^2 \\ \rho u(e + \frac{1}{2}u^2 + PV) \end{pmatrix} + \begin{pmatrix} 0 \\ 0 \\ \rho Q \mathcal{R} \end{pmatrix}$$

and $(\mathrm{d}/\mathrm{d}t)\lambda = \mathcal{R}$

For partly burned detonation loci, steady wave variables function of $\xi = x - Dt$
Integrating across reaction zone, no longer perfect differential
Jump conditions no longer algebraic expressions depend on rate as well as EOS

$$\kappa = \begin{cases} 1/x & \text{PDEs corresponds to cylindrical-symmetric flow} \\ 2/x & \text{PDEs corresponds to spherically-symmetric flow} \end{cases}$$

Characteristic equation

Extra geometric source term for diverging wave

For right facing characteristic, $\mathrm{d}x/\mathrm{d}t = u + c$

$$(\mathrm{d}/\mathrm{d}t)P + \rho c(\mathrm{d}/\mathrm{d}t)u = \left[\Gamma\rho\lambda Q + (\partial_\lambda P)_{V,e}\right]\mathcal{R} - \kappa\rho c^2 u$$

Shock acceleration needed for shock-to-detonation transition is competition among

1. Pressure gradient behind shock front
2. Chemical reaction
3. Geometric source term for divergent flow

Curvature effect

- Theory, Bdzil, Stewart, Aslam (circa 1990)
  1-D quasi-steady reaction zone profile along streamlines
  e.g., cylindrically diverging detonation is quasi-steady
  Neglect transverse flow and curvature of streamlines
  Steady duct flow ODEs for stream tube assuming
  Unsupported diverging wave front
  Reaction zone profile determines unique detonation speed, $D_n(\kappa)$
  ▸ profile ODEs
- Reaction zone width is important length scale
  Slope of $D_n(\kappa)$ depends on reaction zone width
  Resolution requirement for simulations
- Diameter effect vs Curvature effect
  Diameter effect is global for unconfined rate stick
  Curvature effect is local
  With DSD theory can predict diameter effect

Detonation Shock Dynamics (DSD)

DSD theory developed by Bdzil, Stewart, Aslam (circa 1990)

Reaction zone to sonic point decouples from flow behind

- Boundary condition
  Front angle with inert determined by shock polar analysis ▸ shock polar
  Several cases depending on relative acoustic impedance
    weak confinement and strong confinement most important
- Time evolution of detonation front
  $D_n(\kappa)$ + boundary angle determines evolution of front
  using level set algorithm
  Precompute burn time table, $t_{bt}(\vec{x})$, before hydro simulation
- Model for propagating diverging detonation wave
  Generalization of programmed burn model
    Huygen's construction from geometric optics
    with constant wave speed D_{cj}
  Pseudo-burn rate
    Analogous to artificial viscosity for shock capturing

Comment on converging wave front

- Cylindrical or spherically converging shock wave
  Guderley similarity solution for polytropic EOS
  Shock velocity hence shock pressure increases as shock propagates
- Converging detonation wave
  Detonation speed increases as detonation propagates
  or collision of diverging fronts ▸ example
  Interaction portion of front is overdriven
  - Reaction zone is subsonic wrt front
    Analog of planar overdriven detonation wave
    Supported by flow behind reaction zone
  - DSD assumption breaks down
    Detonation wave does not decouple from flow behind

Experimental measurement of $D_n(\kappa)$

- Unconfined rate stick
  Initiate at one end and allow to run to steady state
  Measure axial detonation speed with timing pins
- Measure front shape
  Record wave breakout along diameter with streak camera
- Front curvature
  Calculate mean front curvature κ from front shape $z(r)$
  Sum of principal components in radial and azimuthal directions
  Formula involves first and second derivatives of z wrt r
  Smooth shape utilizing fitting form for $z(r)$
  Calculate derivatives analytically
- Normal detonation speed
  $D_n = D_{axial}/cos(\theta)$
  and $\tan(\theta) = dz/dr$

Example PBX 9502

ref: Hill & Aslam, 14th Detonation Symposium (2010)

- Temperature and lot dependence
  Heterogeneities affect burn rate which affects reaction zone width and slope of $D_n(\kappa)$
- Fast and slow TATB rate
  $D_n(\kappa)$, large slope for small κ then rapidly changes to moderate slope
  Sonic point moves from end of slow reaction to near end of fast reaction
  Large change in reaction zone width to sonic point

Curvature effect with lot

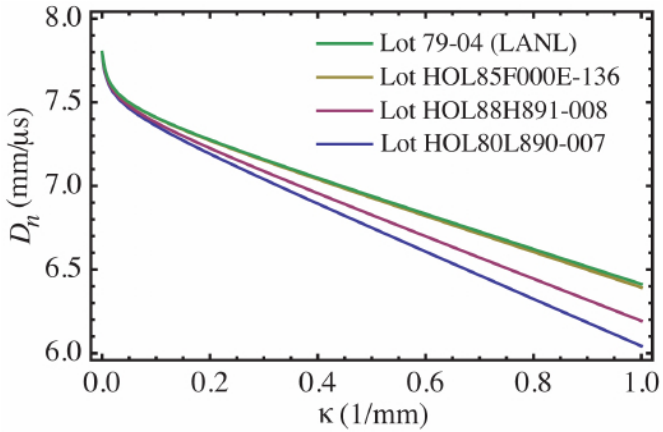

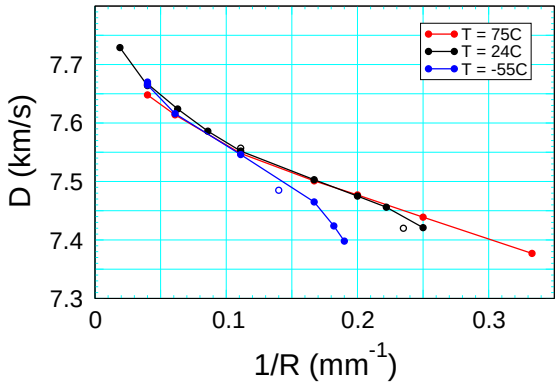

Campbell 1984

Diameter effect with T

Breakdown of DSD assumptions

- Dependence of $D_n(\kappa)$ on rate stick diameter
  Lead shock pressure changes rapidly in boundary layer
  Leads to transverse gradients not accounted for in duct flow ODEs
  Model ODEs do not have solution for large κ
  but simulations fit shape of detonation front
  Discussed further in lecture 9 on failure diameter

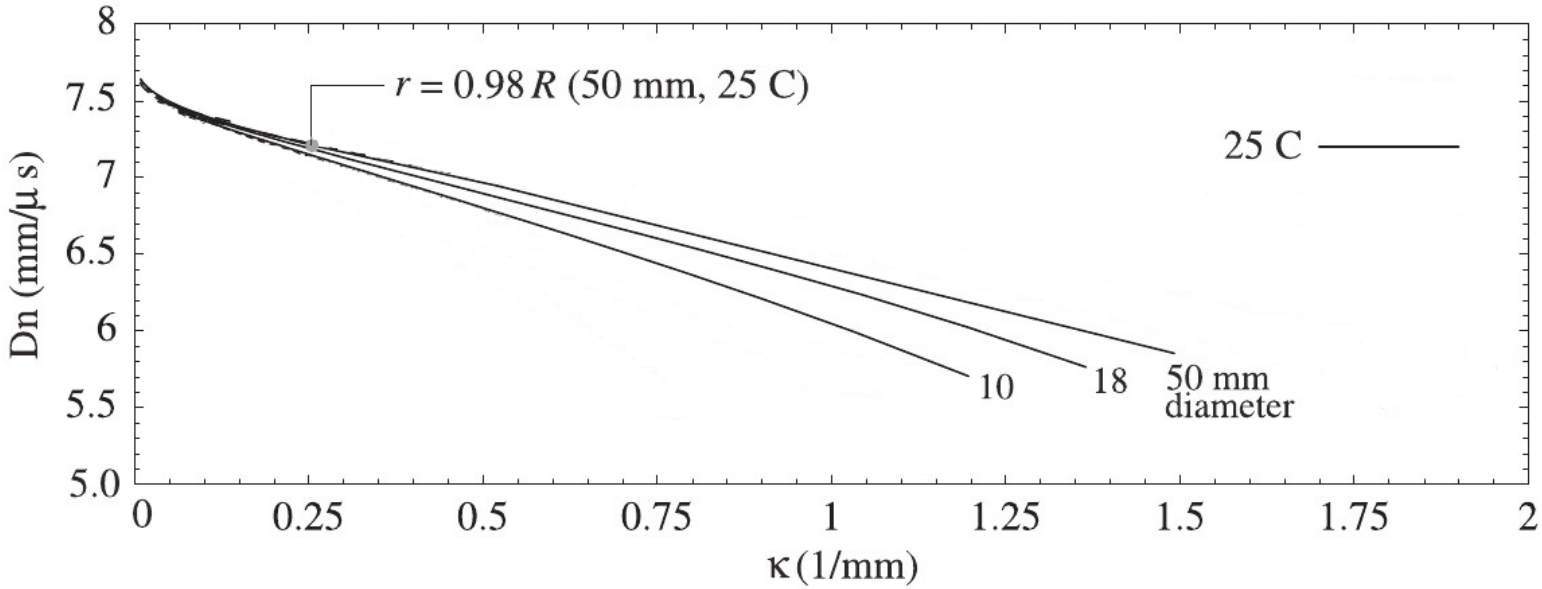

Hill, Bdzil & Aslam, 11th Detonation Symposium (1998)

Rate stick simulation

5 mm radius PBX 9502 rate stick

Fit front shape with fine zoning

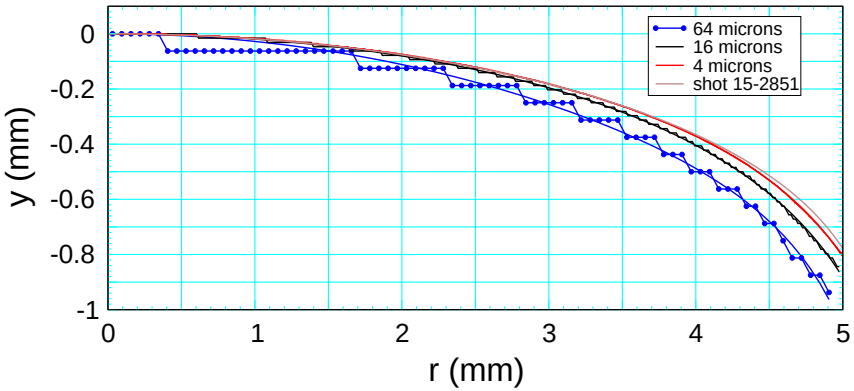

$\kappa \approx 1$ mm^{-1} at boundary

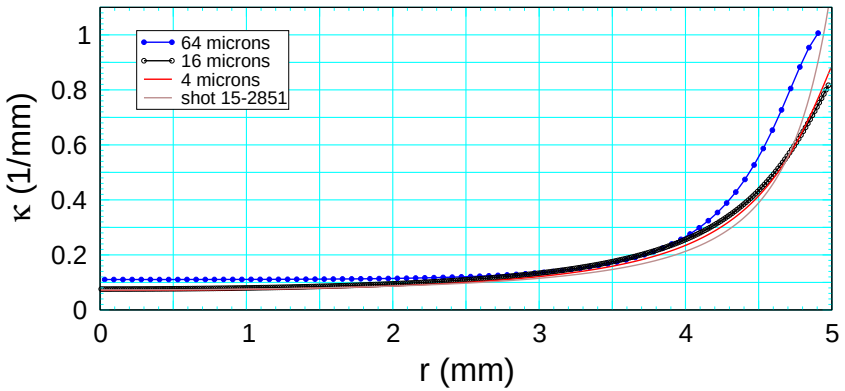

Profile ODEs have solution only up to 0.4 mm^{-1}

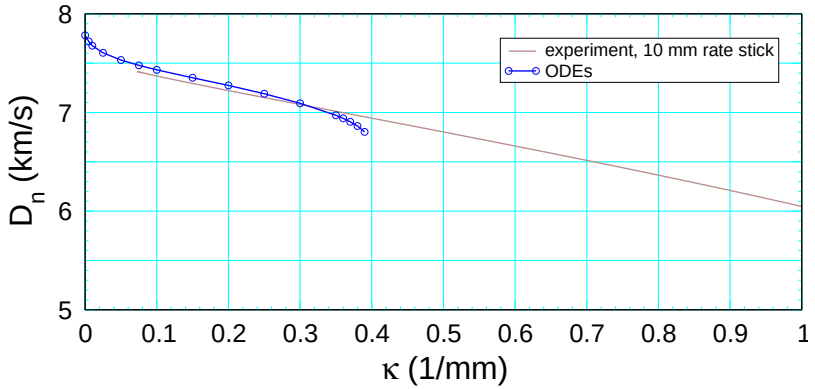

8. CJ state and release isentrope

Products EOS data

Minimum data needed for good model

- CJ state
  - Detonation speed & pressure
  - Issues
    - Approach to steady state (final percent slow due to sonic point)
    - Length of run for planar wave
- Overdriven detonation locus
  - Requires supported planar wave
- CJ release isentrope
  - 1-D release isentrope from overdriven detonation
    - Grüneisen coefficient from pair of overdriven isentropes
    - Γ allows extrapolating in e off the release isentrope
  - 2-D Cylinder test or Sandwich test or Disc Accelerate Experiment (DAX)
    - Unlike shock Hugoniot, infer isentrope with simulations

Requires many experiments, hence time consuming and expensive

Limited data for many PBXs

CJ detonation speed

Experiments

- Planar detonation wave
  Thin flyer plate (short shock)
  Overdrive for prompt initiation
  Long enough run to decay to steady underdriven detonation
  Timing pins to measure detonation speed
- Extrapolate diameter effect
  $D(R) = D_{CJ}(1 - a/R)$ for large R
  Large diameter needed for PBX 9502

0.5 and 1 inch $\Rightarrow$ 7.70 km/s

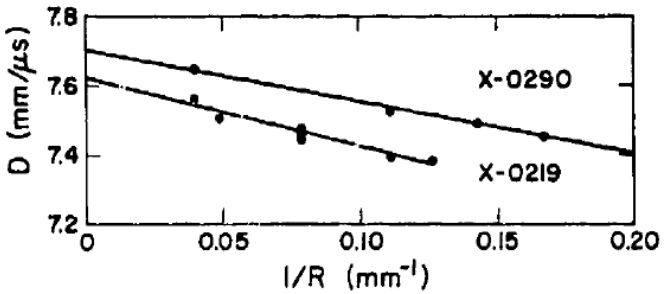

Campbell & Engelke 1976

2 and 4 inch $\Rightarrow$ 7.78 km/s

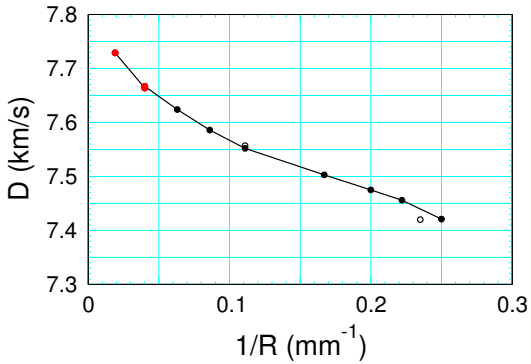

Campbell 1984

CJ pressure — conventional HE I

Jump equation for steady planar wave, $P_{cj} = \rho_0 u_{CJ} D_{CJ}$
Problem is to determine u_{cj} for underdriven detonation

- Conventional HE
  Thin reaction zone width < 0.1 mm ▸ CHE
  Kink (discontinuous derivative) at CJ state
- Assume CJ detonation (discontinuity to CJ state)
  Steep reaction zone pressure gradient decays in thin foil or window
- VISAR/PDV probe
  Need to account for impedance mismatch between HE and window
  Standard wave analysis in (u_p, P) plane is inexact
    Clipping of von Neumann spike
    Reaction zone profile affect reflected wave in HE
      $P(u)$ not same as rarefaction nor shock locus

▸ 9501 profile experiment

CJ pressure — conventional HE II

Historic method for P_{CJ}, 1960 – 1980

1. Plane wave lens + HE sample + thin metal plate
   Measure free surface jump-off velocity of plate
   Repeat for series of plate thicknesses
2. Extrapolate jump-off velocity to 0 thickness, u_{fs}
   From plate EOS determine pressure corresponding u_{fs}
   P_{CJ} = shock pressure $\approx$ at particle velocity $u_p = \frac{1}{2} u_{fs}$

Approximations

- Plate thick enough for pressure to decay to P_{cj}
  Shock transit time greater than reaction time in HE
- Plate thin enough to be at same particle velocity as end of HE
  Flow in plate is shock match from CJ state followed by rarefaction
  Reverberation time small compare to velocity change from rarefaction
- In limit of zero plate thickness, lead shock at CJ pressure

CJ pressure — conventional HE III

PBX 9501 planar detonation → steel

Simulated pressure and velocity profiles at sequence of times

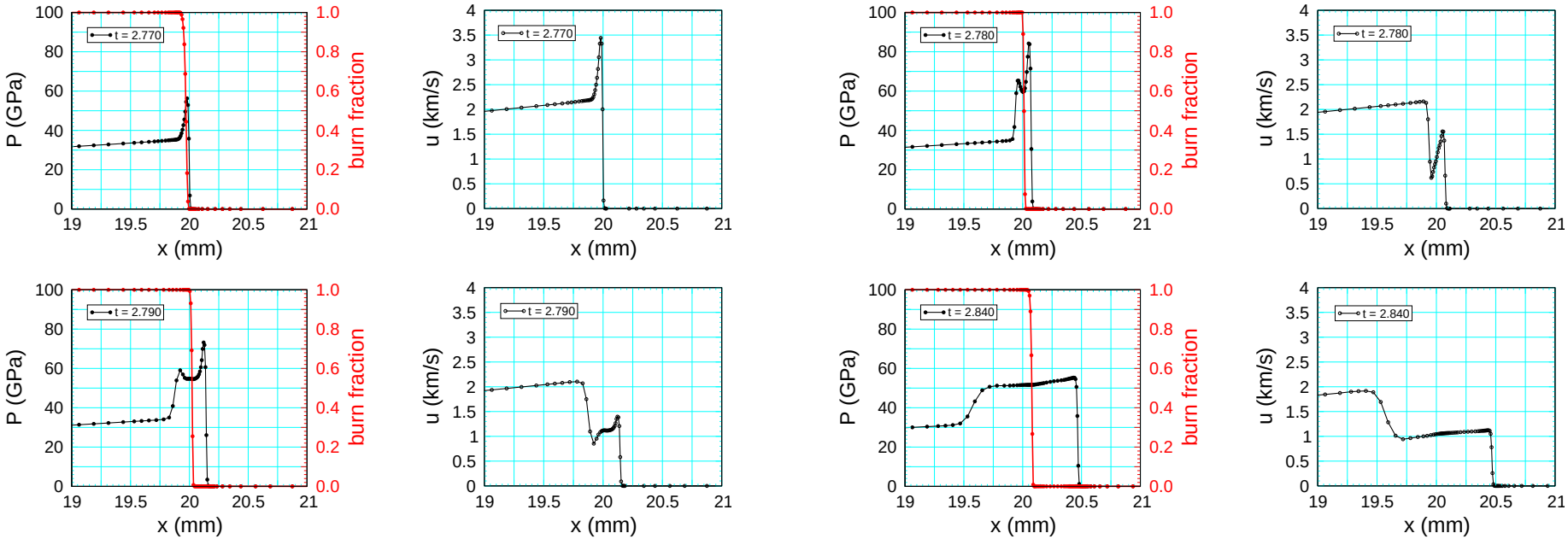

Initial 9501/steel interface at 20 mm

Burn fraction shows interface

Reaction zone gradient decays rapidly in inert

CJ pressure — conventional HE IV

Lagrangian tracer particles

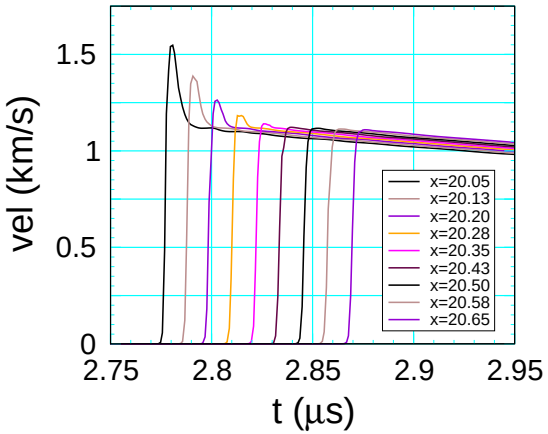

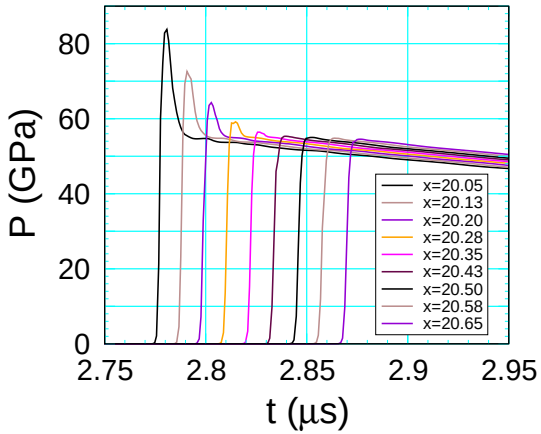

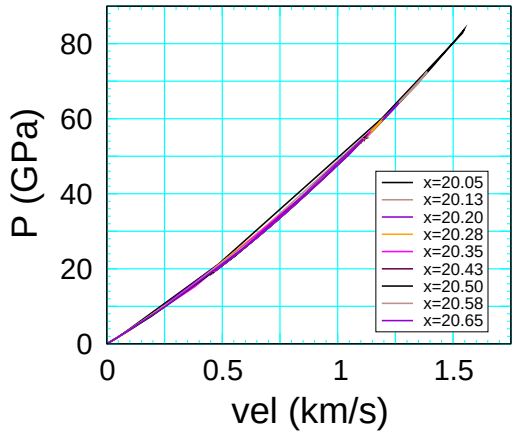

Inexact wave analysis

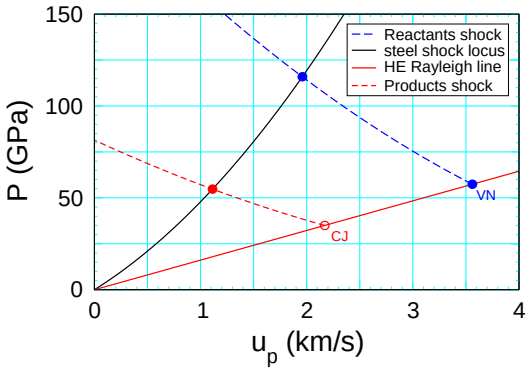

- VN spike gets clipped
  Depends on distance from HE surface
  Need slope of reactants reflected shock locus
- CJ state in steel (window)
  Depends on velocity profile
  More accurate if inert to clip reaction zone
  Slope of products reflected shock ($\rho_{CJ} D_{CJ}$)
  Determined by sonic condition

CJ pressure — insensitive HE I

- Insensitive HE
  Large reaction zone width $>$ 1 mm

  Where does reaction zone end
  and rarefaction begin ?

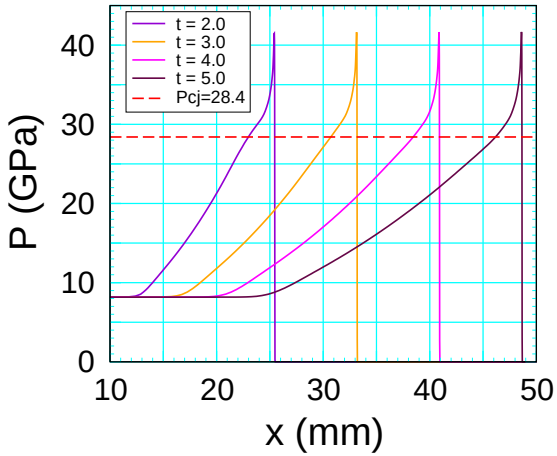

- Series of unsupported experiments
  Initiation with varying run distance
  Align front then CJ state
  at end of steady profile

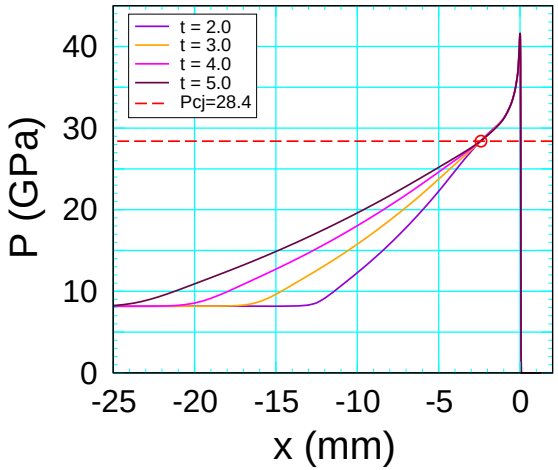

CJ pressure — insensitive HE II

- Data for unsupported experiments

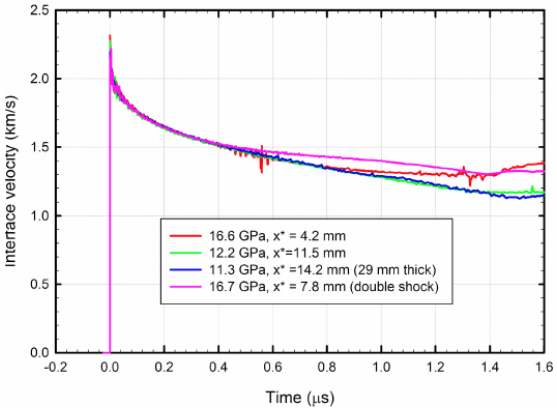

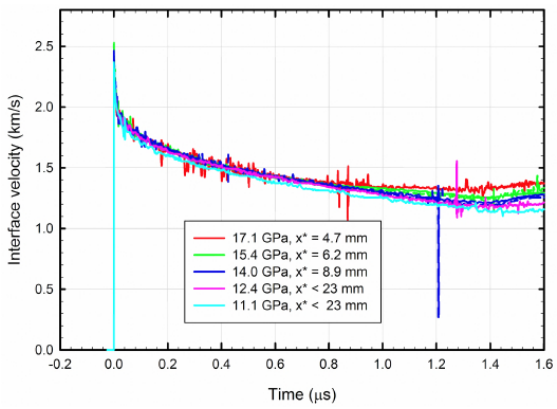

EDC 35 at 23C PBX 9502 at -55C

Gustavsen, Bartram, Sanchez, SCCM 2009, p253-256

Better with longer distances of run and same initiation pressure

Need to correct for window impedance mismatch

model reaction zone (see Davis & Ramsay 7^{th} Det Symp, 1982)

- Limit of overdriven detonation wave

Series of experiments varying support (Gustavsen *et al.*, 2014)

Flow behind detonation

Constant state for $D > D_{CJ}$

Rarefaction for $D < D_{CJ}$

Overdriven detonation locus

- Supported planar detonation wave
  Explosively driven flyer plate or projectile from gas gun
- Constant state behind detonation
  VISAR or PDV probe at end of HE to measure velocity time history
  u behind wave is well defined, in contrast to unsupported detonation
  Correct for impedance match with window
- Detonation locus
  Series of experiments varying flyer plate velocity
- Additional data
  Pick width of flyer for Detonation + Constant State + Rarefaction
  Determines sound speed behind detonation wave
  $\gamma = c^2/(PV)$ on detonation locus
  and release isentrope from overdriven detonation state
  $\Gamma = V(\partial P/\partial e)_V$ from pair of release isentropes
  uncertainty from round-off and low precision data

Cylinder test experiment

- Standard test
  1 inch diameter HE
  0.1 inch thick copper tube
  2 inch long HE pellets slip fit
    wall tolerance 1 mil
    gives 1 % uncertainty in wall mass
- Scaled tests (consistency check)
  0.5 and 2 inch diameter HE
- Steady state flow
  Curved detonation front
    Approximately isentropic behind front
  Ringing in the wall (copper material strength)
  Radial variation of pressure
- Data
  Axial detonation speed
  Wall velocity from multiple probes

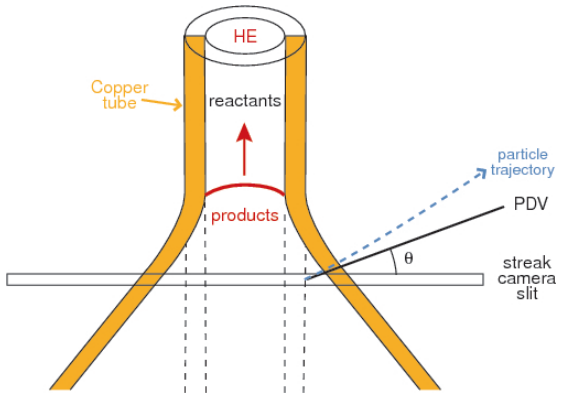

Log pressure

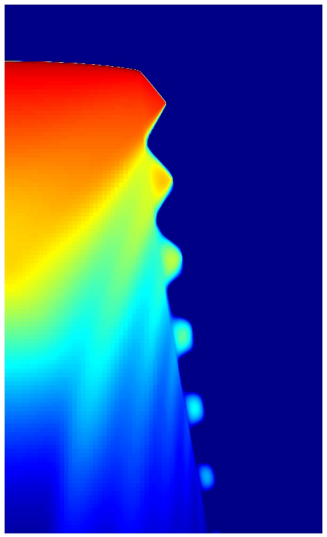

Cylinder test uncertainties

- Wall velocity variation
  With azimuthal angle
  wall thickness tolerance
- Detonation speed variation
  With lot and initial temperature
- Wall expansion
  $R/R_0 \approx 3$ ($V/V_0 \approx 9$) at 15 μs
  $P \sim 0.1$ GPa
  Wall acceleration > 0 but decreasing
- Wall thins with expansion
  Thickness $\propto$ 1/Radius
  Spall at larger radii
- Fit products isentrope
  Match data with simulations

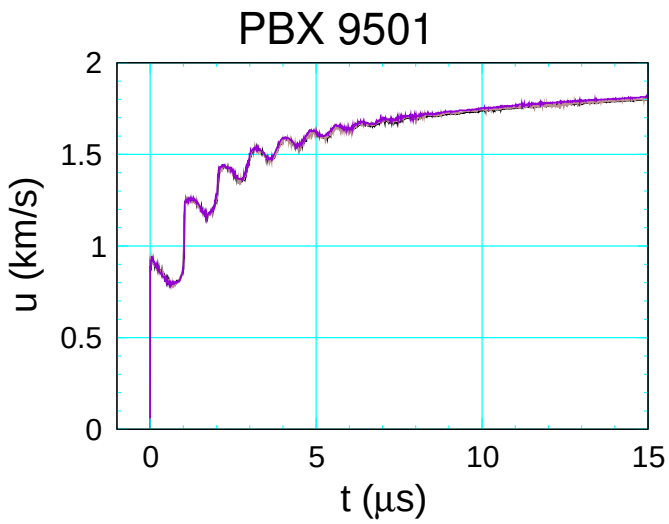

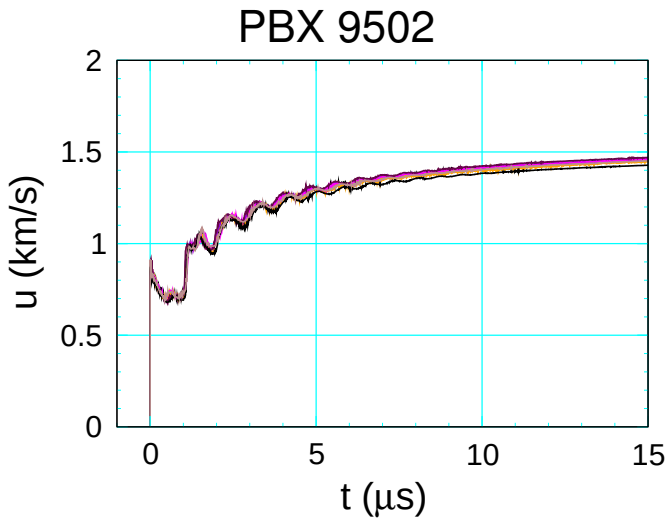

Pemberton *et al.*, 2011

Cylinder test and curvature effect

PBX 9502 fast rate (narrow reaction zone)

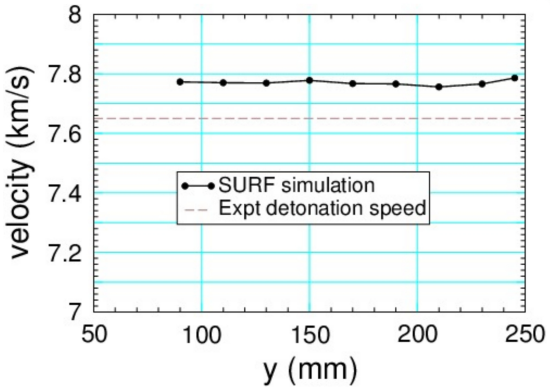

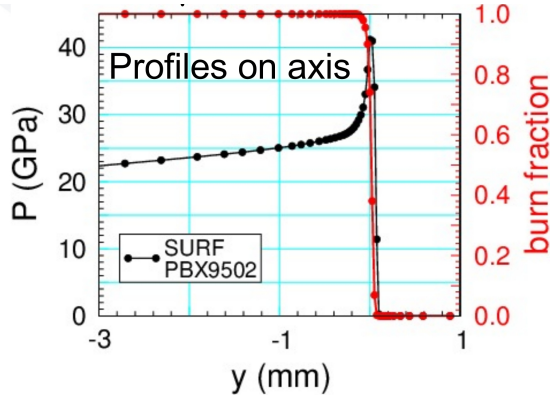

PBX 9502 fast/slow rate (wide reaction zone)

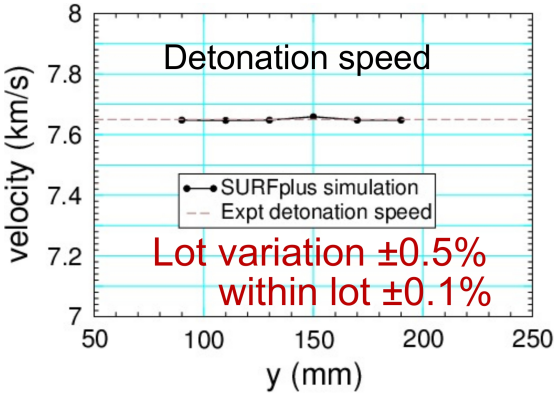

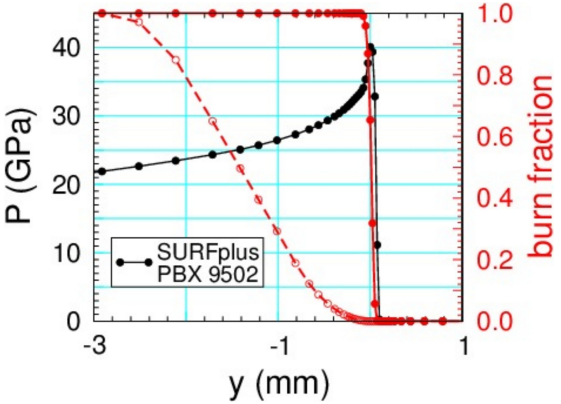

Curvature effect

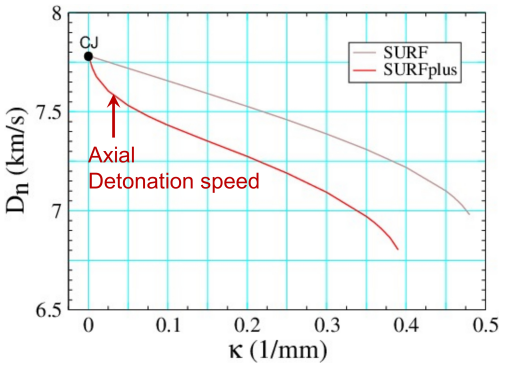

Cylinder test and wall velocity

- Common practice
  Fit to JWL EOS using programmed burn
  with D_{CJ} = axial detonation speed
  Issues:
  1. Curvature effect depends on HE diameter
  2. EOS fitting parameters depend on diameter
- Sensitive of wall velocity to rate
  After first wall shock, velocity insensitive to rate
  Energy release after sonic point
  Does not contribute to detonation wave speed
  But does contribute to wall velocity

PBX 9502 fast rate

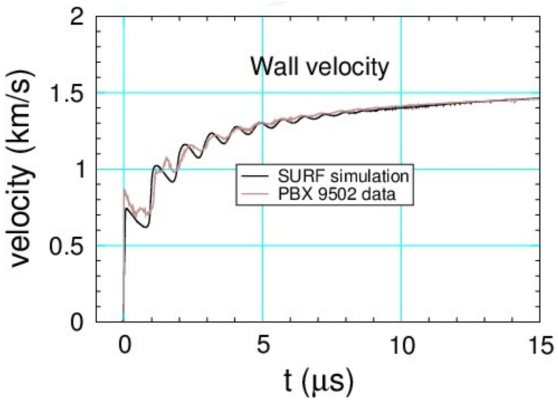

PBX 9502 fast/slow rate

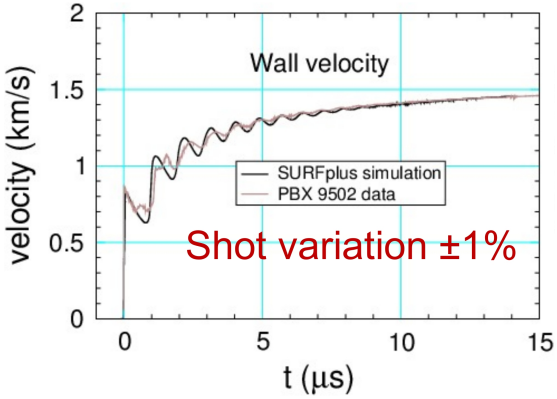

9. Failure diameter, corner turning and dead zones

Failure diameter

- Diameter effect experiments ▸ diameter effect
  Series of unconfined rate sticks with decreasing diameter
  Detonation wave does not propagate below failure diameter
- Trends
  Fast rate and narrow reaction zone have smaller failure diameter
    Also better for corner turning
  Failure diameter decreases with increasing temperature (larger rate)
  Failure diameter can depend on lot (grain distribution affects burn rate)
- Failure cone
  Replace HE cylinder with cone
    Aims to get failure diameter with 1 experiment
  Detonation slightly overdriven due to decreasing diameter
    Fails at small diameter than standard ‘failure diameter’
    Requires model and simulation to correct for affect of tapper

Simulation above failure diameter

PBX 9502 at 10 mm diameter

- Detonation wave
  Initiated at bottom
- Small test cylinder (5 mm radius)
  Slightly overdriven
  length/diameter = 4
- Sonic shock at boundary ▸ shock polar
  Boundary layer with large change in shock pressure and
  large transverse pressure gradient
- Boundary layer flow ▸ $D_n(\kappa)$
  Not 1-D detonation along streamline
  Lead shock supported by interior
  Low burn rate compared to axis

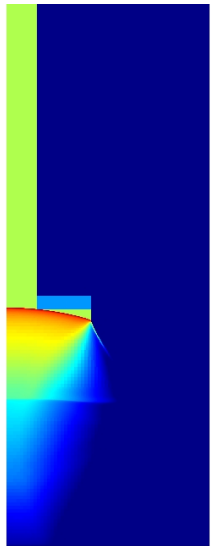

shock front & streamlines

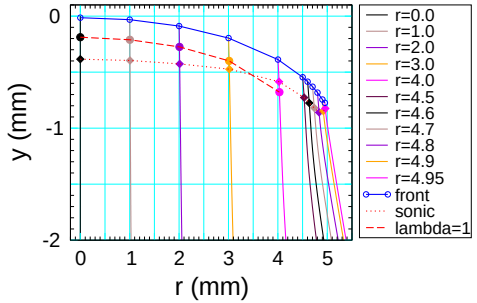

shock pressure along front

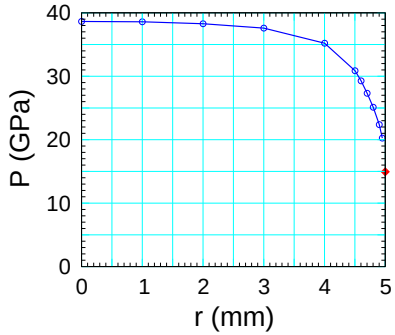

pressure along streamlines

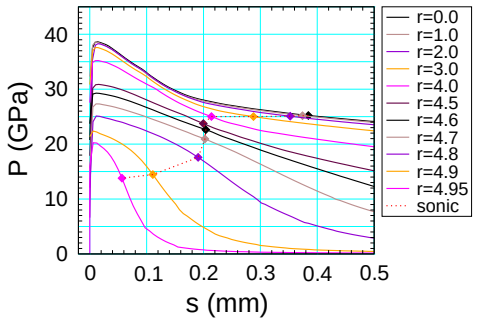

Weak confinement

Surround HE with PMMA instead of air

Independent of weak confiner

- Part of reaction zone
  Shock front to sonic locus
- Shape of detonation front
- Axial detonation speed
- Failure diameter

Affected by weak confiner

- Behind sonic locus
  Radial expansion
  Pressure along streamline

shock front & streamlines

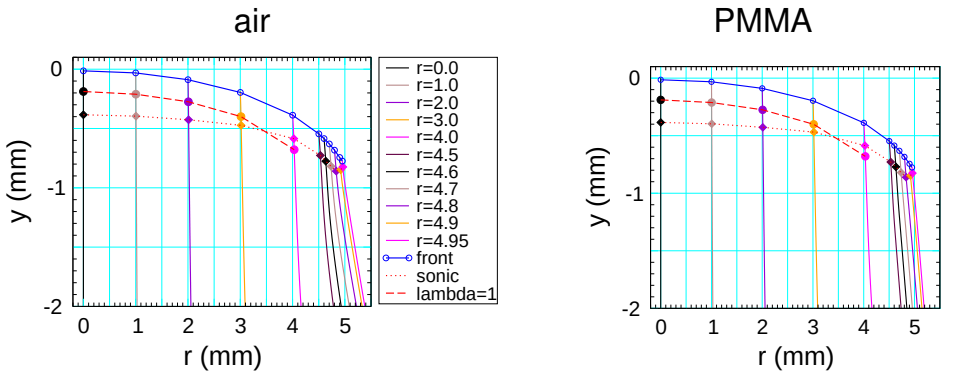

pressure along streamlines

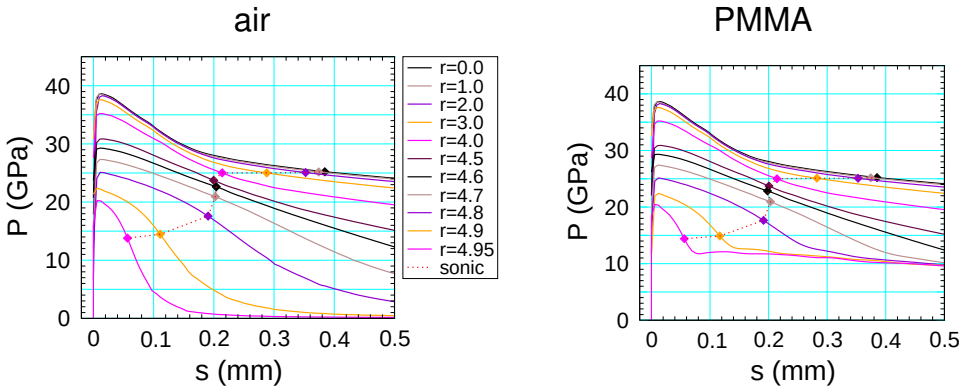

Simulation below failure diameter (PBX 9502)

Failure mechanism

- Transverse pressure gradient
  Transverse energy flow supports only
  Weak lead shock in boundary layer
  very low burn rate behind weak shock
- Failure wave
  Weak shock drains energy from detonation
  Weak shock grows radially inward
  Larger energy drain on detonation
- Weak shock after failure

shock pressure

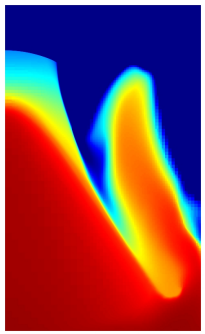

burn fraction

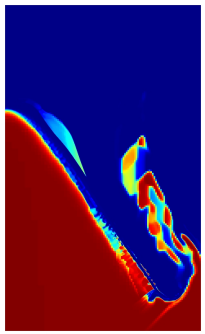

4 mm radius failing

5 mm radius propagates

density

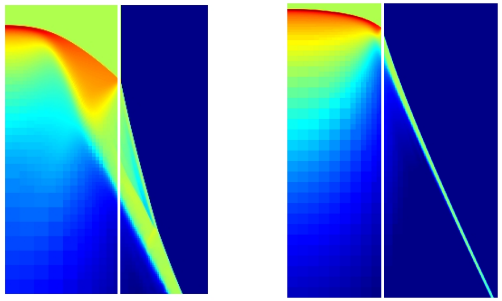

pressure

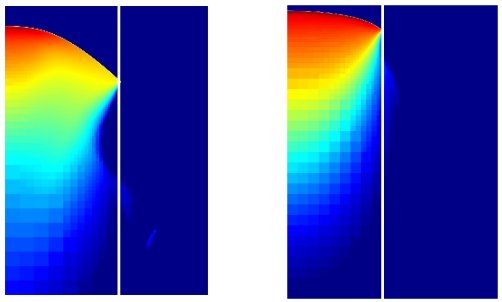

burn fraction

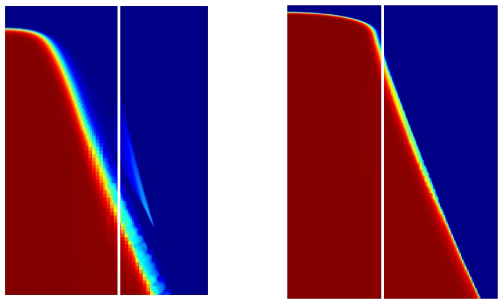

Additional comments on failure

Detonation wave failure

- Depends on geometry
  Unconfined rectangular slab of HE
  failure thickness $<$ failure diameter
- Depends on confinement
  Strong confinement, such as by steel
  Shock polar analysis at boundary
    Lead HE shock is subsonic
    Higher boundary pressure and smaller failure diameter
    Issue with boundary layer reduced or eliminated
  Caveat: To apply shock polar analysis at boundary
    No gap between HE and confiner

Corner turning – experiment

setup

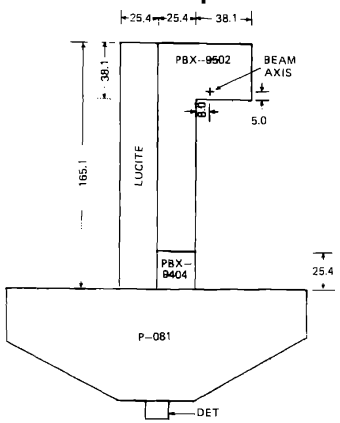

Shot 1941

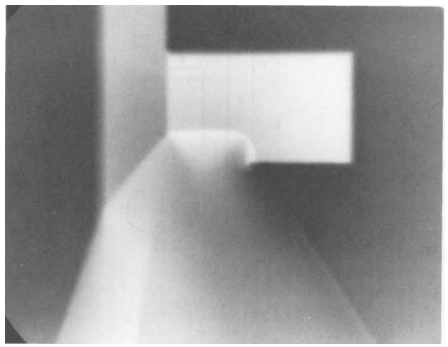

Shot 1796

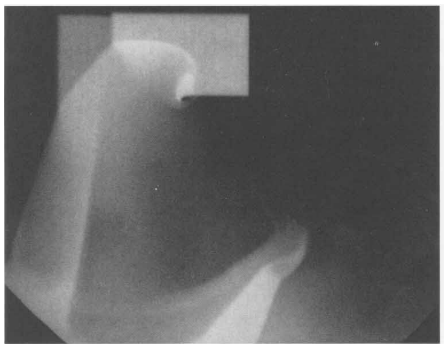

Shot 1943

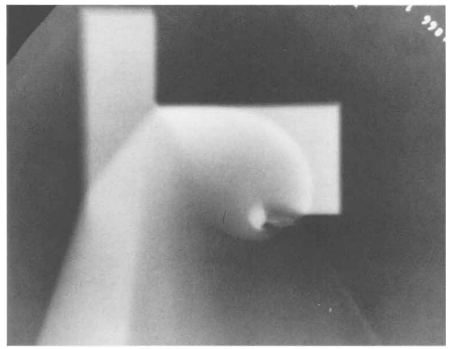

Phermex shots (1975, 1976)

- Time evolution
  Three experiment with 1 radiograph per shot
  Diffraction of lead shock lowers pressure
  Detonation spreads out laterally
- Dead zone
  Region of low rate or shock desensitized

Corner turning – simulation

- Setup similar to experiment

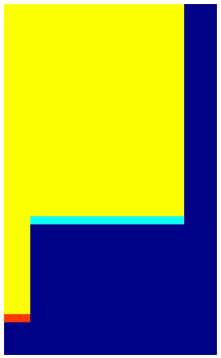

- Small HE cylinder width
  Affects corner turning
  and extent of dead zone
- Applications
  Detonator-booster
  Fragment impact

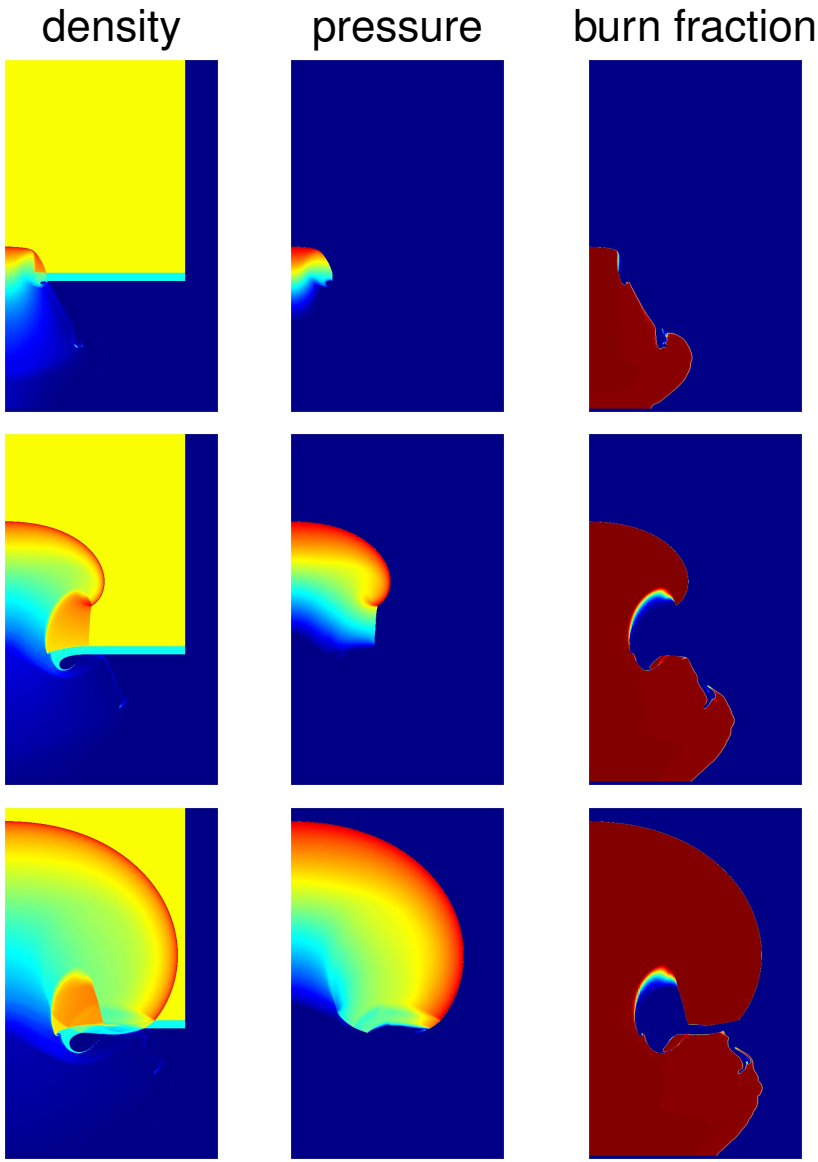

10. EOS models and calibration data

Mei-Gruneisen EOS

Most model EOS for HE based on Mei-Grüneisen form for pressure

$$\boxed{P(V,e) = P_{ref}(V) + \frac{\Gamma(V)}{V}\Big[e - e_{ref}(V)\Big]}$$

and constant specific heat

$$T(V,e) = T_{ref}(V) + \Big[e - e_{ref}(V)\Big]/C_V$$

Reference curve

- Reactants
  Principal shock locus
  or isentrope through ambient state
- Products
  Isentrope through CJ state

Mei-Gruneisen EOS – reference curve

Many fitting forms for $P_{ref}(V)$ to choose from
Thermodynamically consistent EOS
with reference curve for e and T determined by $P_{ref}(V)$ and $\Gamma(V)$

- Isentrope

$$e_{ref}(V) = -\int_{V_0}^{V} \mathrm{d}V\, P_{ref(V)}$$

$$T_{ref}(V) = T_0 \exp\left[-\int_{V_0}^{V} \mathrm{d}V\, \Gamma(V)/V\right]$$

- Principal Hugoniot locus

$$e_{ref}(V) = \tfrac{1}{2}(P_{ref}(V) + P_0)(V_0 - V)$$

$$\frac{\mathrm{d}T_{ref}}{\mathrm{d}V} + \frac{\Gamma(V)}{V} T_{ref} = \left(P_{ref} + \frac{\mathrm{d}e_{ref}}{\mathrm{d}V}\right) C_V^{-1}$$

Domain limited by maximum shock compression ratio

Mei-Gruneisen EOS – issues

Issues with Mei-Grüneisen EOS

1. Difficult to determine $\Gamma(V) = \frac{1}{V}\left(\frac{\partial P}{\partial e}\right)_V$ experimentally
   Typically, $\Gamma(V) = \Gamma_0 + (V/V_0)\Gamma'$
2. Limited data for calibration HE
   Can not achieve high temperature and high pressure statically
   For reactants, extrapolate outside range of data
3. Limited domain for thermodynamic stability
   Van der Waal loops at low temperature
   since C_V not 0 as $T \to 0$
   $K_T < 0$ for solids in expansion ($V > V_0$)
4. Constant specific heat is not good approximation for HE
   Thermodynamic consistent extension with non-constant C_V

Reactants EOS

Available data to calibrate EOS model

1. Principal shock Hugoniot
   Limited pressure range due to reaction
   Possibly take advantage of shock desensitization
2. Diamond anvil cell for isothermal compression
   Powder diffraction on small HE crystals not PBX
   Density measurement not accurate at high pressures
3. Isentropic compression experiment
   Compress sample with pressure ramp at Sandia Z-machine
   Experiments with PBX 9501
4. Specific heat from phonon frequencies (measured or DFT)
   C_V varies by factor of 2 between ambient and VN spike
   Shock temperature measurements based on Raman scattering

Reactants EOS – porosity

Temperature range for HE ($-55 < T_0 < 75\,\mathrm{C}$)

- Thermal expansion
  Initial density affects CJ state
  Hence detonation speed and release isentrope
- Thermodynamic identity for coefficient of thermal expansion

$$\beta = \frac{1}{V}\left(\frac{\partial V}{\partial T}\right)_P = \frac{\Gamma}{V}\frac{C_P}{K_S}$$

  Constraint on Γ, K_S and C_P at ambient state

- Porosity of PBX is extra degree of freedom
  Depends on how molding powder pressed into PBX
  Use porosity model to account for initial density at initial temperature
  Squeeze out pores at low pressure implies not sensitive to model

Products EOS

CJ state and release isentrope discussed in lecture 8

- Detonation wave to get in high pressure regime
  Allow for initiation
  Account for curvature effect
- Overdrive detonation ($P > P_{CJ}$)
  Planar detonation can use jump conditions
- 'Release Isentrope' ($P < P_{CJ}$)
  1-D release isentrope, Cylinder test and DAX
  In contrast to Hugoniot point need simulation to interpret data
- C_V not measured
  Solid like at CJ state (above solid density)
  Decreases with expansion
    Rotation of molecules rather than vibrations

Products EOS – carbon clustering

Explosives that produce excess of carbon have fast and slow reactions

- Slow reaction from carbon clustering
  Releases substantial amount of chemical energy
- Products EOS has extra degree of freedom $\boxed{P_{prod}(V, e, \lambda_{cc})}$
  where $\lambda_{cc} = 0$ is for products without carbon clustering
  $\lambda_{cc} = 1$ is for equilibrium products
- Detonation phenomena affected by carbon clustering
  Shock initiation determined by fast reaction, $P_{prod}(V, e, 0)$
  Curvature effect, sonic point for $0 < \lambda_{cc}^{sonic} < 1$
  Corner turning, λ_{cc} varies along sonic locus of detonation wave

Products EOS needs to account for carbon clustering

Example EOS model loci

EOS model shock and detonation loci for PBX 9502

Example 1
thermicity > 0

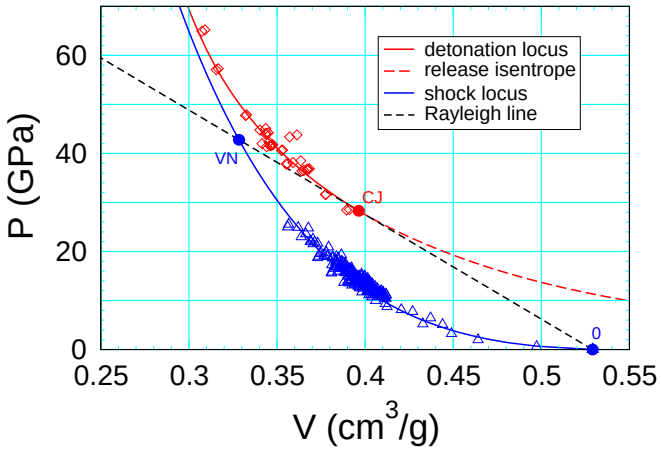

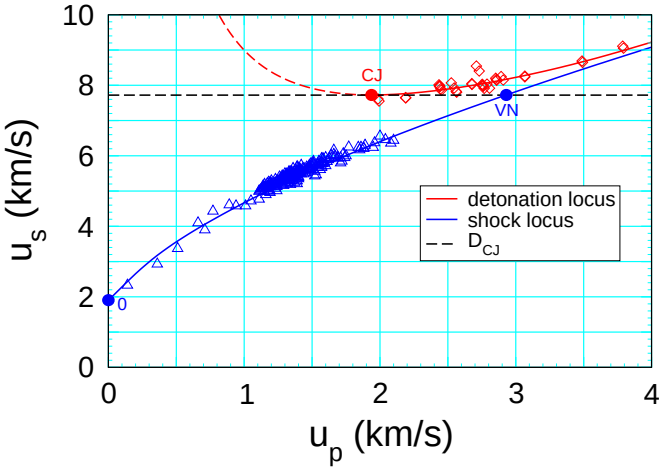

Example 2
thermicity
changes sign

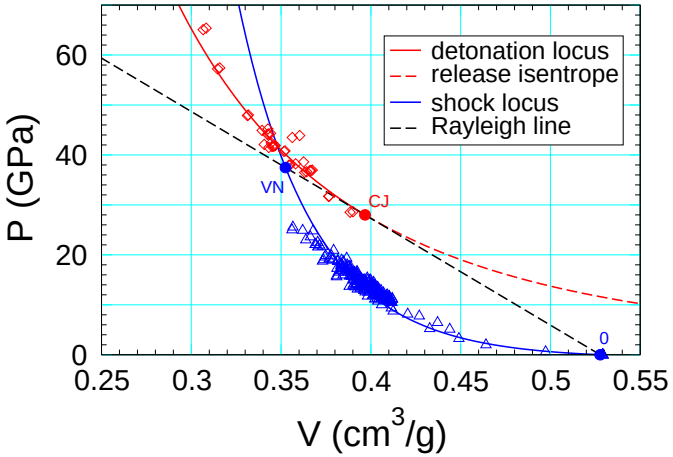

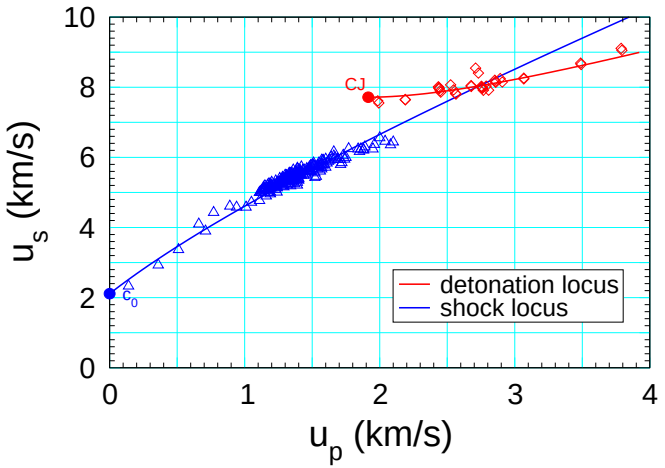

thermicity $= \frac{(\partial_\lambda P)_{V,e}}{K_s} = \frac{\Delta V}{V} - \Gamma \frac{\Delta H}{V K_s}$, expect $\Delta H < 0$ and $\Delta V > 0$

Does VN spike pressure matter ?

- Curvature effect
  Slope of $D_n(\kappa)$ strongly affected by reaction zone width
  Reaction zone width largely determined by rate at VN spike
  To fit shock initiation many models use $\mathcal{R} \propto P^n$
  Hence VN spike pressure strongly affects reaction zone width
  Caveat: limited numerical resolution
  can clipped VN spike pressure
- Sonic pressure boundary condition for weak confinement
  Low VN spike pressure due to stiff EOS
  Also would give low sonic pressure
  Can affect failure diameter and corner turning

Need accurate reactants EOS up to VN spike pressure
to model wide range of detonation phenomena

Example EOS model isotherms

PBX 9502 EOS model isotherms at low T and $V > V_0$

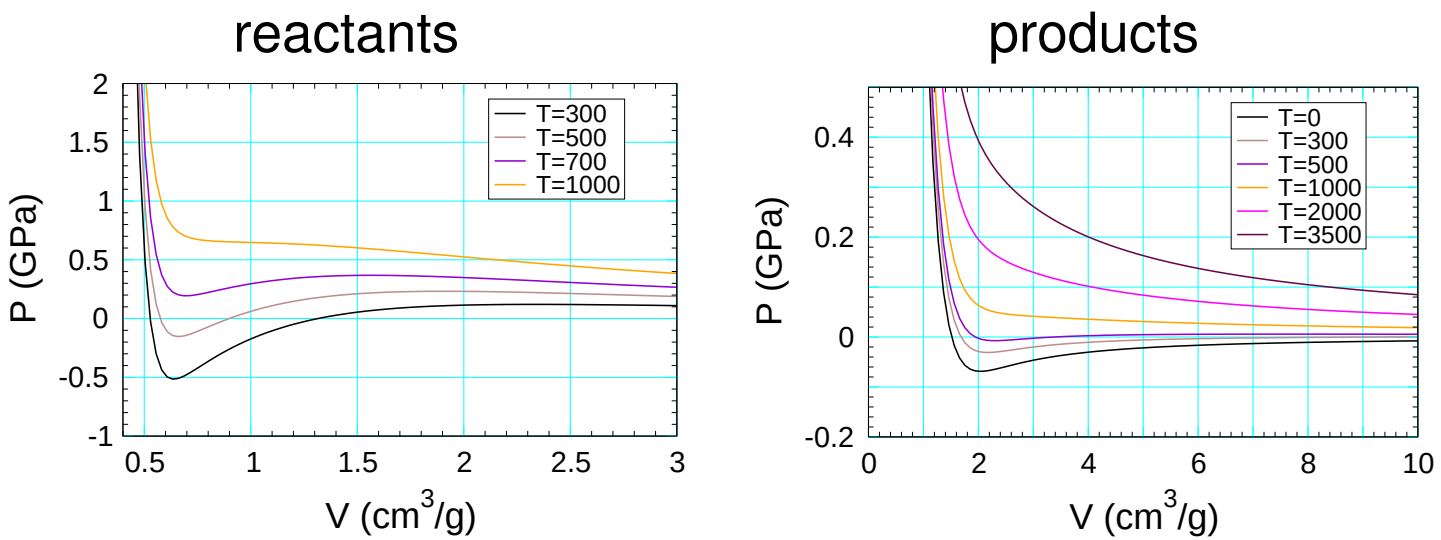

Limit on domain from negative isothermal bulk modulus

- Single phase reactants EOS
  Can not account for sublimation and phase separation
- Products
  Constant specific heat violates $C_V \to 0$ as $T \to 0$

Thermo-chemical codes I

Derive equilibrium EOS for products

BKW (Mader), CHEETAH (LLNL), MAGPIE (PEM-LANL)

Key step is to derive products composition

Example HMX: $\mathrm{C_4H_8N_8O_8} \rightarrow 4\mathrm{N_2} + 4\mathrm{H_2O} + 4\mathrm{CO}$

but also $\mathrm{CO_2}$, solid carbon clusters, NO, $\mathrm{NO_2}$, $\mathrm{H_2}$, $\mathrm{O_2}$ + *etc.*

Starting point is complete EOS of product species

Gibbs free energy $\boxed{G_i(P,T) = e + PV - TS}$

and approximation for EOS of mixture

$$G(P,T,\vec{\lambda}) = \sum_i \lambda_i G_i(P,T) + (RT/M) \sum_i c_i(\vec{\lambda}) \ln c_i(\vec{\lambda})$$

where λ_i is mass fraction, $c_i = \left[\lambda_i/m_i\right] / \left[\sum_i \lambda_i/m_i\right]$ is molar concentration

m_i is molecular weight of species i and M is molecular weight of HE

Last term is entropy of mixing

Thermo-chemical codes II

Determine $\lambda_i(P, T)$ that minimizes Gibbs free energy

subject to stoichiometric constraint

Equilibrium products EOS

$$G_{eq}(P,T) = \sum_i \lambda_i(P,T) G_i(P,T) + (RT/M) \sum_i (c_i \ln c_i)\left(\vec{\lambda}(P,T)\right)$$

Complication with solid carbon clusters (TATB, TNT)

Phase of carbon (graphite or diamond)

Size of carbon cluster and species bonding to surface

May depend on reaction dynamics (non-equilibrium)

Generate sesame table

EOS evaluation, $P(V, e)$ or $T(V, e)$, independent of model complexity

Or fit to Mie-Grüneisen form with CJ release isentrope

BKW EOS (Mader), JWL EOS fit to CHEETAH

Thermo-chemical codes III

Species EOS

- Fit to available data
  Limited data in regime of interest
    P up to 50 GPa and T up to 5000 K
- Molecular dynamics simulations
  Need potentials between atoms
    In principle, from quantum chemistry calculations
  Issue with temperature when vibrational modes not saturated
    Classical MD obeys equipartition for vibrational modes rather than quantum oscillators

References

References I

J. B. Bdzil and D. S. Stewart. The dynamics of detonation in explosive systems. *Annual Rev. Fluid Mech.*, 39:263–292, 2007. URL https://doi.org/10.1146/annurev.fluid.38.050304.092049.

F. P. Bowden and Y. D. Yoffe. *Initiation and growth of explosion in liquids and solids*. Cambridge University Press, 1952.

A. W. Campbell. Diameter effect and failure diameter of a TATB based explosive. *Propellants, Explosives, Pyrotechnics*, 9:183–187, 1984. URL http://dx.doi.org/10.1002/prep.19840090602.

A. W. Campbell and R. Engelke. The diameter effect in high-density heterogeneous explosives. In *Proceeding of the Sixth International Symposium on Detonation*, pages 642–652, 1976.

A. W. Campbell and J. R. Travis. The shock desensitization of PBX-9404 and composition B-3. In *Eighth Symposium (International) on Detonation*, pages 1057–1068, 1986.

References II

A. W. Campbell, W. C. Davis, J. B. Ramsay, and J. R. Travis. Shock initiation of solid explosives. *Physics of Fluids*, 4:511–521, 1961a. URL https://doi.org/10.1063/1.1706354.

A. W. Campbell, W. C. Davis, and J. R. Travis. Shock initiation of detonation in liquid explosives. *Physics of Fluids*, 4:498–510, 1961b. URL https://doi.org/10.1063/1.1706353.

W. C. Davis and J. B. Ramsay. Detonation pressures of PBX 9404, Composition B, PBX 9502, and Nitromethane. In *Seventh Symposium (International) on Detonation*, pages 531–539, 1982.

J. J. Dick, A. R. Martinez, and R. S. Hixson. Plane impact and response of PBX 9501 and its components below 2 GPa. Technical Report LA-13426-MS, Los Alamos National Lab., 1998. URL http://permalink.lanl.gov/object/tr?what=info:lanl-repo/lareport/LA-13426-MS.

W. Fickett and W. C. Davis. *Detonation*. Univ. of Calif. Press, 1979.

References III

T. R. Gibbs and A. Popolato, editors. *LASL Explosive Property Data*. Univ. of Calif. Press, 1980. URL http://lib-www.lanl.gov/ladcdmp/epro.pdf.

R. L. Gustavsen, S. A. Sheffield, and R. R. Alcon. Progress in measuring detonation wave profiles in PBX 9501. In *Eleventh (International) Symposium on Detonation*, pages 821–827, 1998.

R. L. Gustavsen, S. A. Sheffield, R. R. Alcon, and L. G. Hill. Shock initiation of new and aged PBX 9501 measured with embedded electromagnetic particle velocity gauges. Technical Report LA-13634-MS, Los Alamos National Lab., 1999. URL http://dx.doi.org/10.2172/10722.

R. L. Gustavsen, S. A. Sheffield, and R. R. Alcon. Measurements of shock initiation in the tri-amino-tri-nitro-benzene based explosive PBX 9502: Wave forms from embedded gauges and comparison of four different material lots. *J. Appl. Phys.*, 99:114907, 2006. URL http://dx.doi.org/10.1063/1.2195191.

References IV

R. L. Gustavsen, B. D. Bartram, and N. J. Sanchez. Detonation wave profiles measured in plastic bonded explosives using 1550 nm photon doppler velocimetry. In *Shock Compression of Condensed Matter*, pages 253–256, 2009. URL http://dx.doi.org/10.1063/1.3295117.

R. L. Gustavsen, T. D. Aslam, B. D. Bartram, and B. C. Hollowell. Plate impact experiments on the TATB based explosive PBX 9502 at pressures near the Chapman-Jouguet state. *Journal of Physics: Conference Series 500*, art. 052015, 2014. URL http://dx.doi.org/10.1088/1742-6596/500/5/052015.

B. F. Henson, B. W. Asay, L. B. Smilowitz, and P. M. Dickson. Ignition chemistry in HMX from thermal explosion to detonation. In *Shock Compression of Condensed Matter – 2001*, pages 1069–1072, 2002.

References V

L. G. Hill and T. D. Aslam. Detonation shock dynamics calibration for PBX 9502 with temperature, density and material lot variation. In *Proceeding of the Fourteenth International Symposium on Detonation*, pages 779–788, 2010.

L. G. Hill, J. B. Bdzil, and T. D. Aslam. Front curvature rate stick measurements and detonation shock dynamics calibration for PBX 9502 over a wide temperature range. In *Proceeding of the Eleventh International Symposium on Detonation*, pages 1029–1037, 1998.

E. L. Lee and C. M. Tarver. Phenomenological model of shock initiation in heterogeneous explosives. *Phys. Fluids*, 23:2362–272, 1980.

J. T. Mang, R. P. Hjelm, and E. G. Francois. Measurement of porosity in a composite high explosive as a function of pressing conditions by ultra-small-angle neutron scattering with contrast variations. *Propellants, Explosives, Pyrotechnics*, 35:7–14, 2010.

References VI

R. Menikoff. Complete Mie-Grüneisen Equation of State. Technical Report LA-UR-11-06921, Los Alamos National Lab., 2011. URL https://doi.org/10.2172/1045381.

R. Menikoff. Detonation wave profile. Technical Report LA-UR-15-29498, Los Alamos National Lab., 2015. URL https://doi.org/10.2172/1229720.

S. Pemberton, T. Sandoval, T. Herrera, and J. Echave. Test report for equation of state measurements of PBX 9502. Technical Report LA-UR-11-04998, Los Alamos National Lab., 2011a. URL http://permalink.lanl.gov/object/tr?what=info:lanl-repo/lareport/LA-UR-11-04998.

S. Pemberton, T. Sandoval, T. Herrera, J. Echave, and G. Maskaly. Test report for equation of state measurements of PBX 9501. Technical Report LA-UR-11-04999, Los Alamos National Lab., 2011b. URL http://permalink.lanl.gov/object/tr?what=info:lanl-repo/lareport/LA-UR-11-04999.

References VII

C. B. Skidmore, T. A. Butler, and C. W. Sandoval. The elusive coefficient of thermal expansion in PBX 9502. Technical report, Los Alamos National Lab., January 2003. LA-14003, https://www.osti.gov/scitech/servlets/purl/809945.

K. S. Vandersall, C. M. Tarver, F. Garcia, and S. K. Chidester. On the low pressure shock initiation of octahydro-1,3,5,7-tetranito-1,3,5,7-tetrazocine based plastic bonded explosives. *J. Appl. Phys.*, 107:094906, 2010. URL http://dx.doi.org/10.1063/1.3407570.

Zoomed figures

Shock initiation – wedge experiment

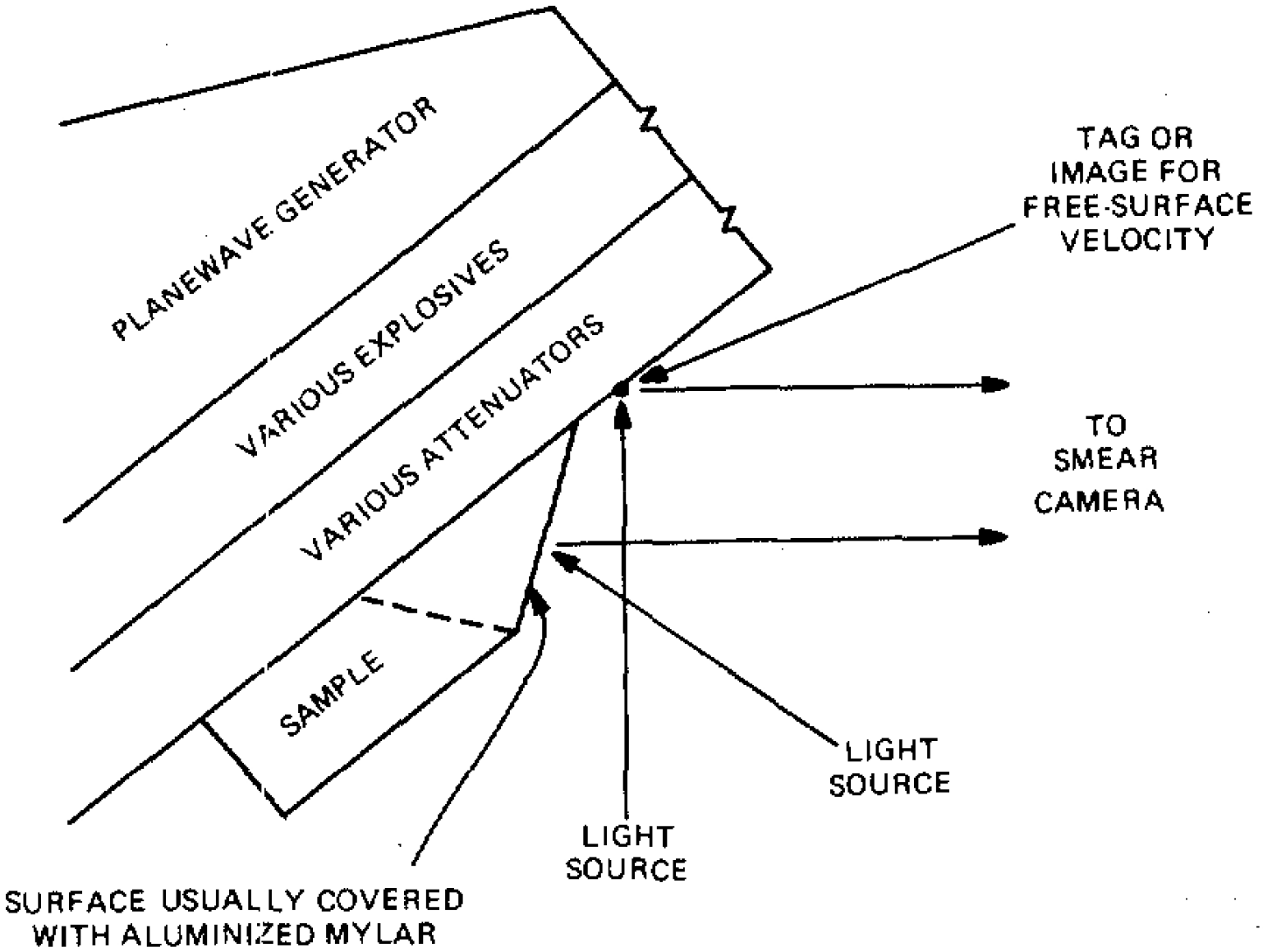

Shock initiation – embedded gauges

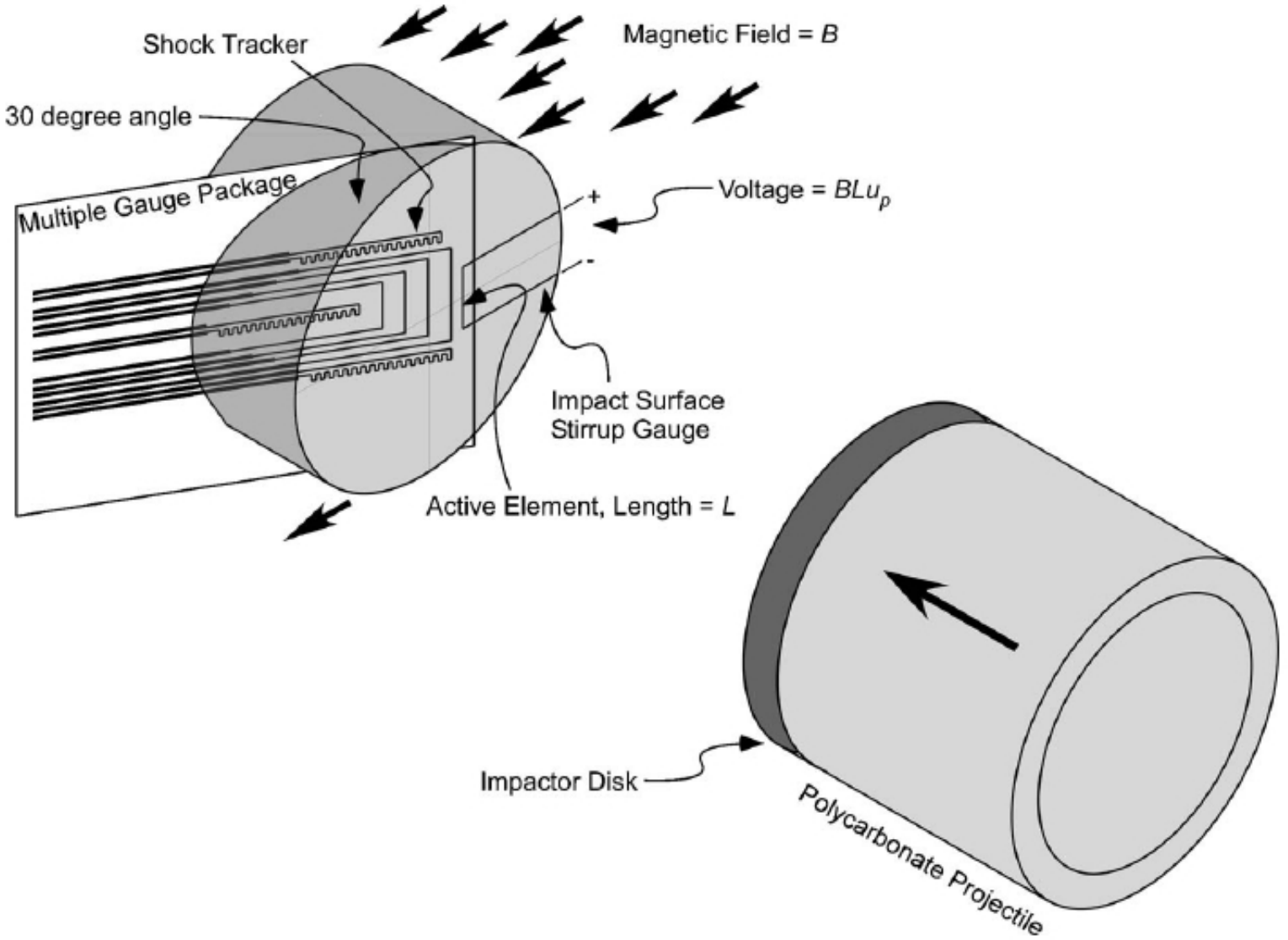

Pop plot data – shock trajectory

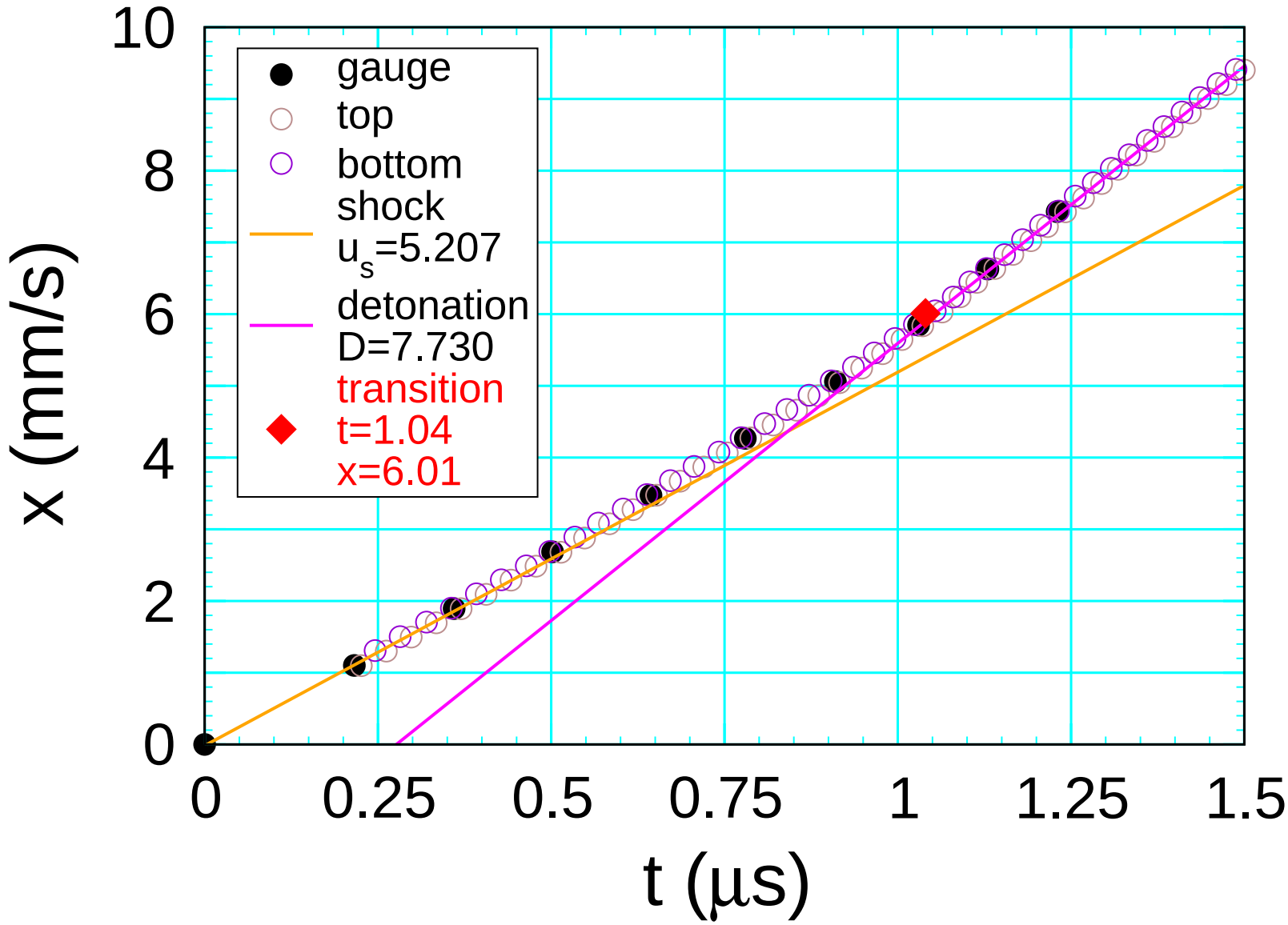

Pop plot data – velocity profiles

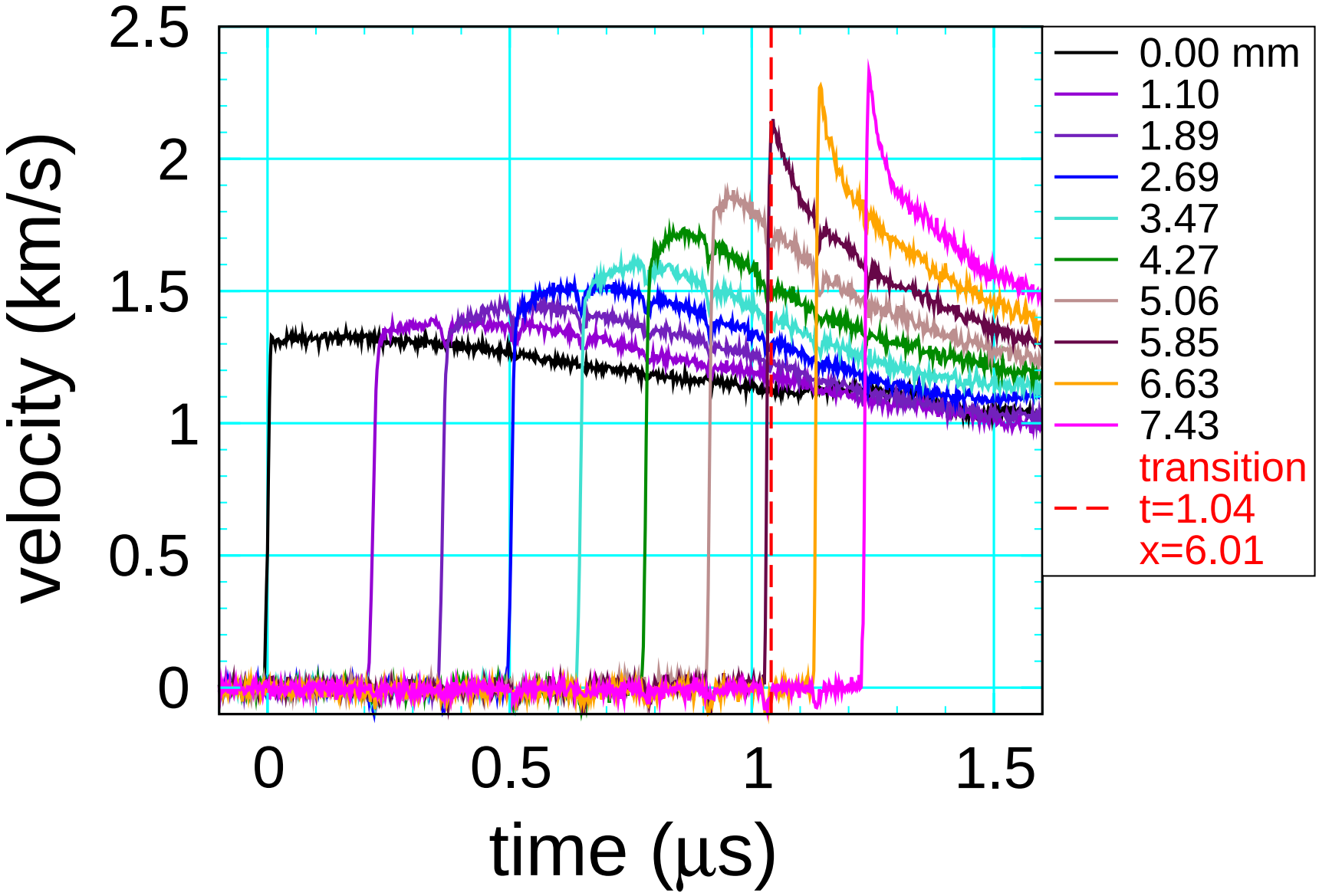

PBX 9501 – global rate (Henson & Smilowitz)

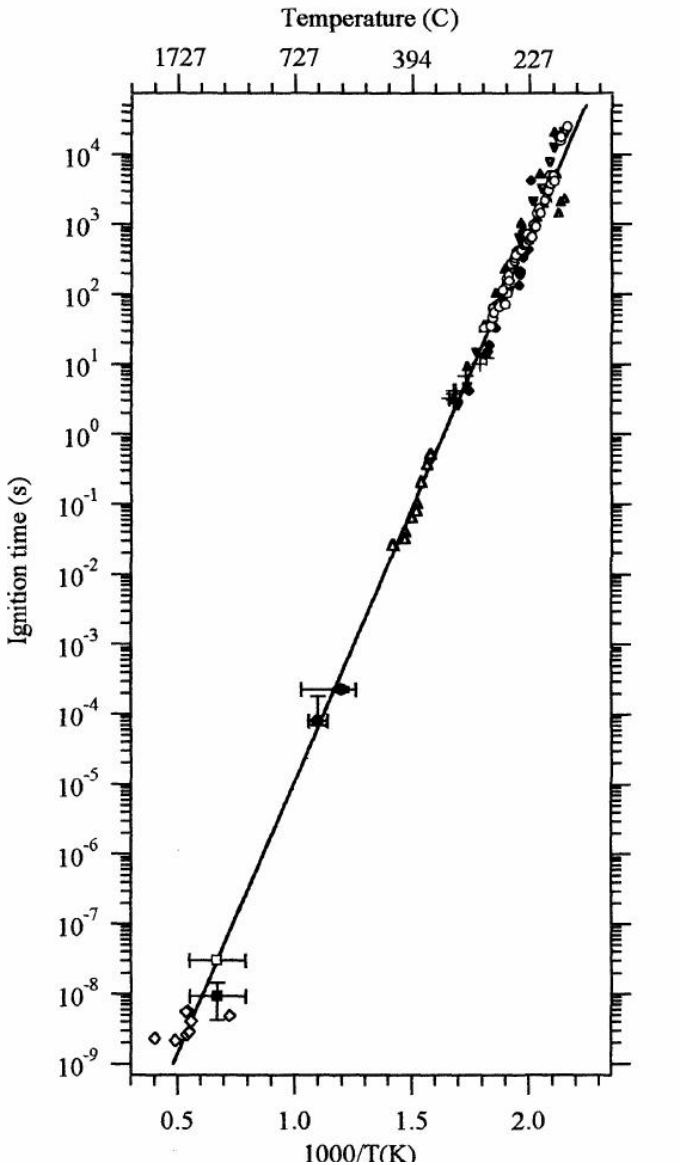

Super-detonation – nitromethane

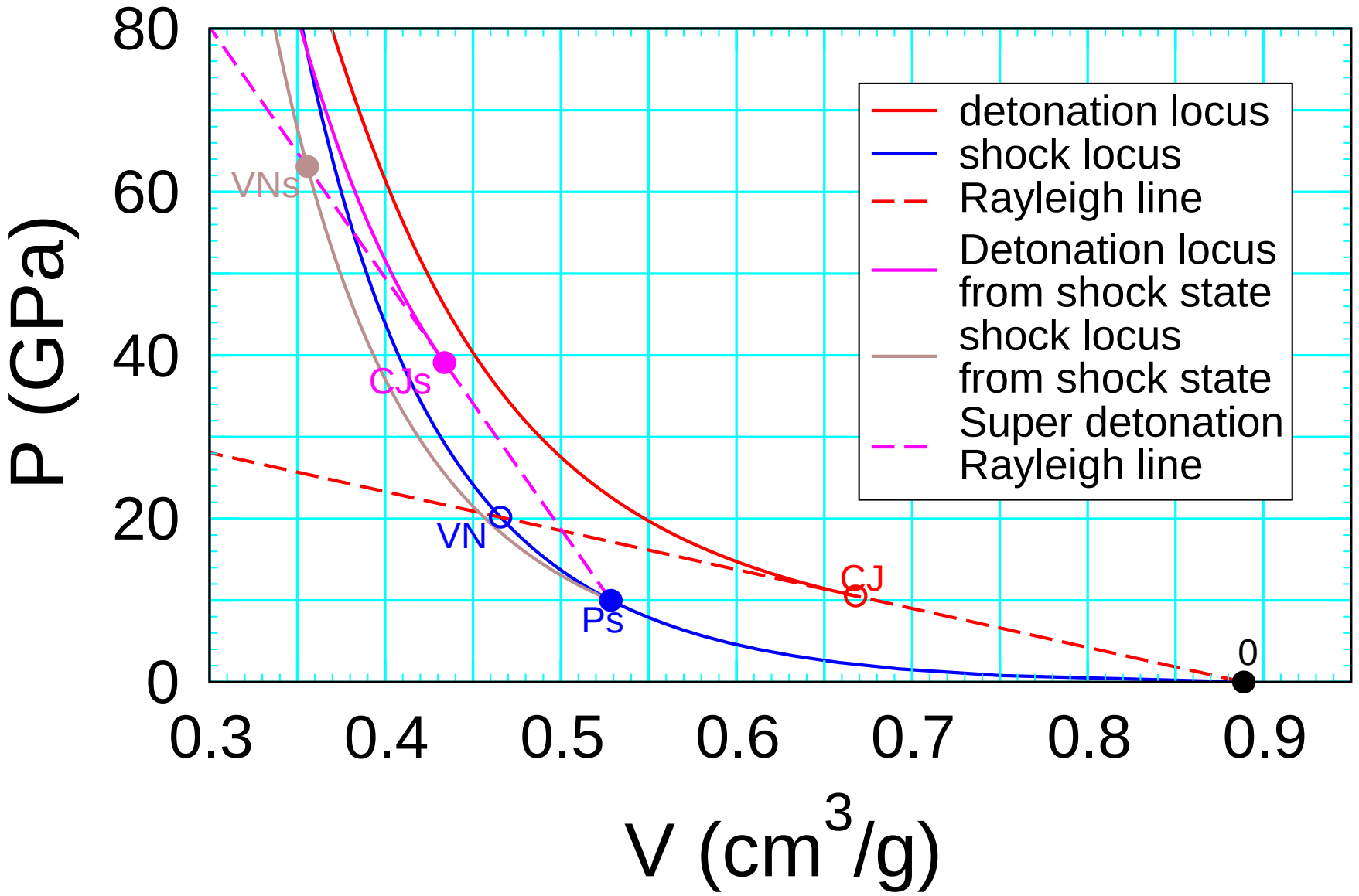

Diameter effect

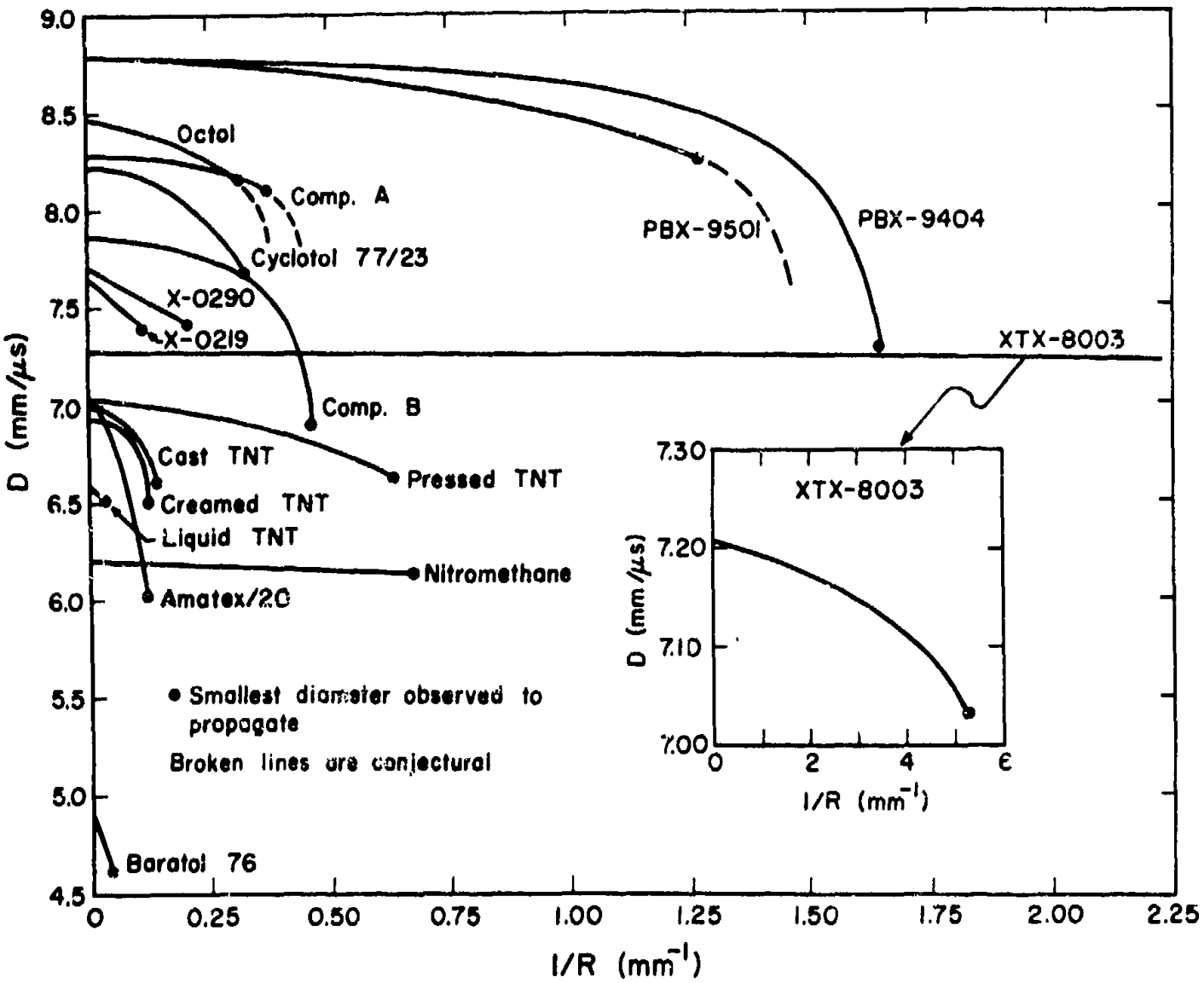

Detonation
Campbell &
6th Detonat

Detonation wave with curvature

Quasi-steady profile ODEs with front curvature κ

$$-\left[c^2-(D-u)^2\right]\frac{\mathrm{d}}{\mathrm{d}x}\begin{pmatrix} V \\ D-u \\ \lambda \end{pmatrix} = \begin{pmatrix} \left[\sigma\,\mathcal{R}\,c^2 - u\,\kappa\,(D-u)^2\right] V/(D-u) \\ (\sigma\mathcal{R}-u\,\kappa)\,c^2 \\ \left[c^2-(D-u)^2\right]\mathcal{R}/(D-u) \end{pmatrix}$$

and Bernoulli equation $e + P\,V + \frac{1}{2}(D-u)^2 = \text{constant}$

$$\kappa \begin{cases} > 0, & \text{diverging front, unsupported detonation} \\ = 0, & \text{planar front, reduces to ZND profile} \\ < 0, & \text{converging front, overdriven detonation} \end{cases}$$

- Diverging detonation wave
  Sonic point within reaction zone
  Critical point of ODEs, factor $[c^2-(D-u)^2]$
- $D_n(\kappa)$ determined by "eigenvalue" like problem
  ODE trajectory such that $\sigma\mathcal{R}-u\kappa=0$ at critical point

Shock polar

1-D shock interaction
P and u continuous
across contact
particle trajectory $\sim$ time direction

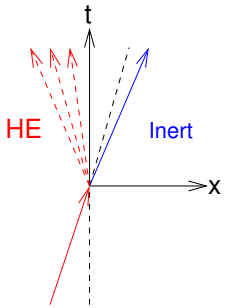

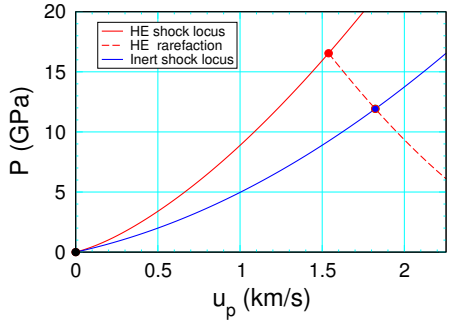

Oblique shock
& turning angle

$$\tan\theta = \frac{u_p u_s}{q_0^2 - u_p u_s} \cdot \frac{q_{||}}{u_s}$$

$$q_{||}^2 = q_0^2 - u_s^2$$

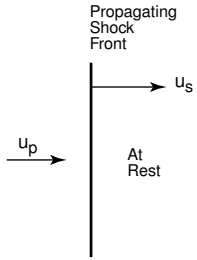

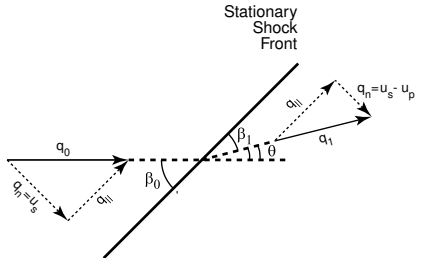

Steady 2-D wave pattern
P and $u_\perp$ continuous
$u_{||}$ discontinuous (slip line)
across contact
streamline || contact
streamline $\sim$ time direction

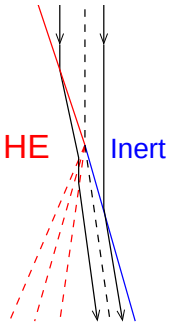

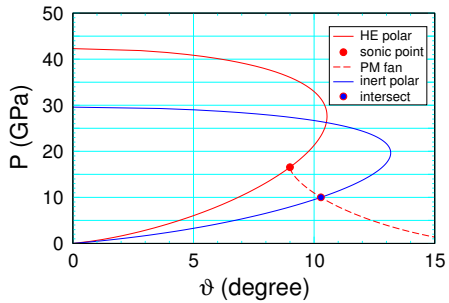

1-D interaction

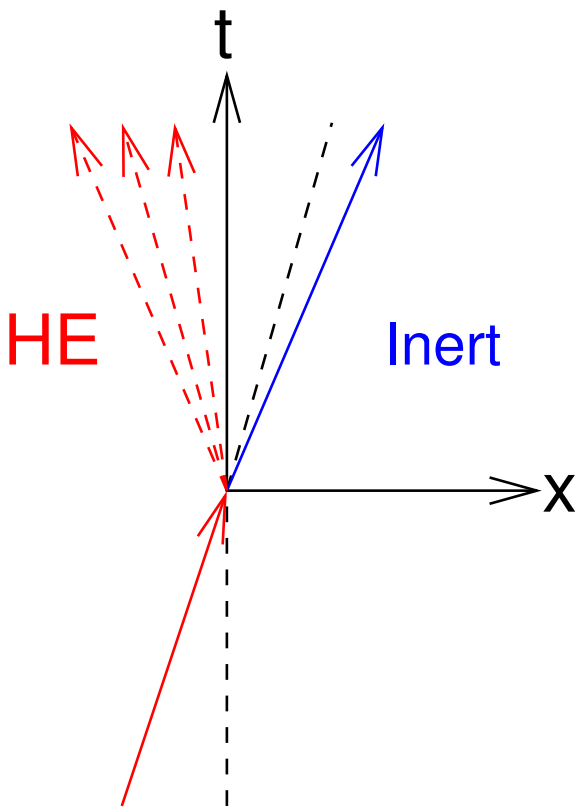

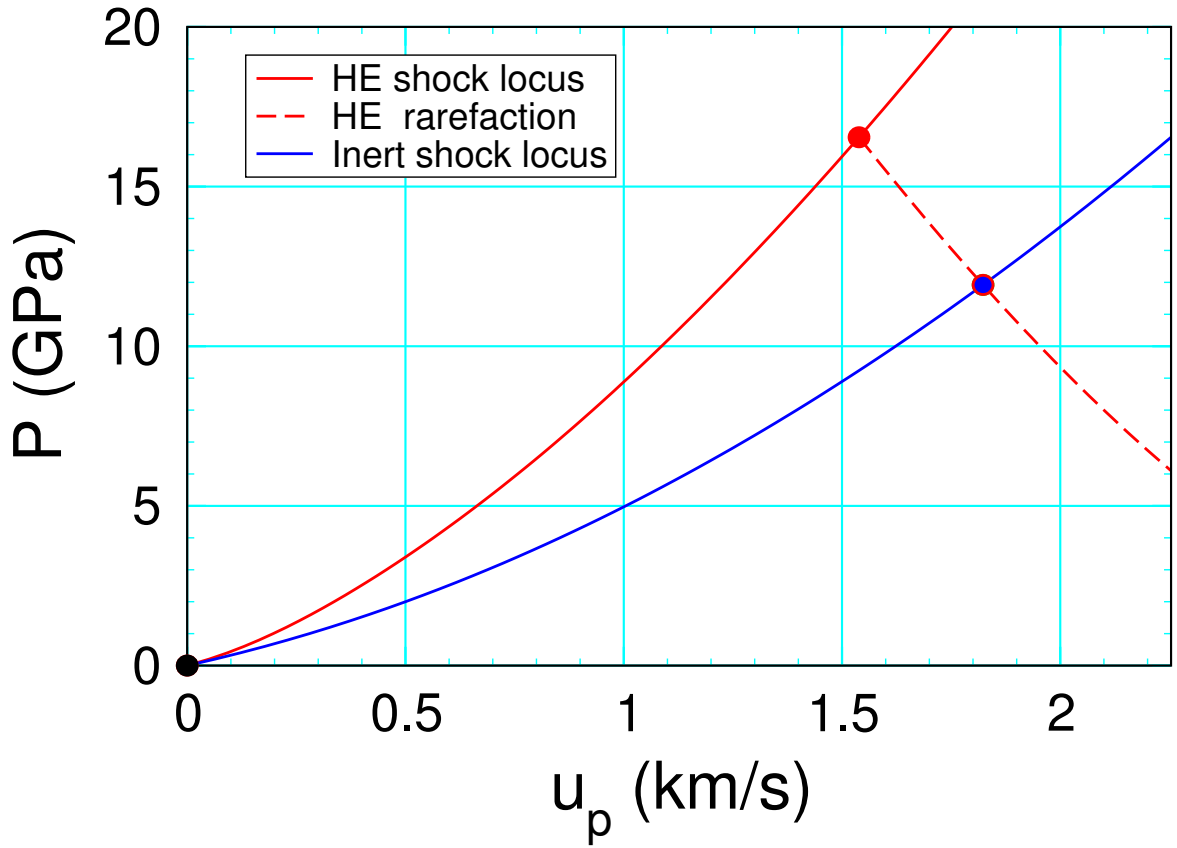

Oblique shock

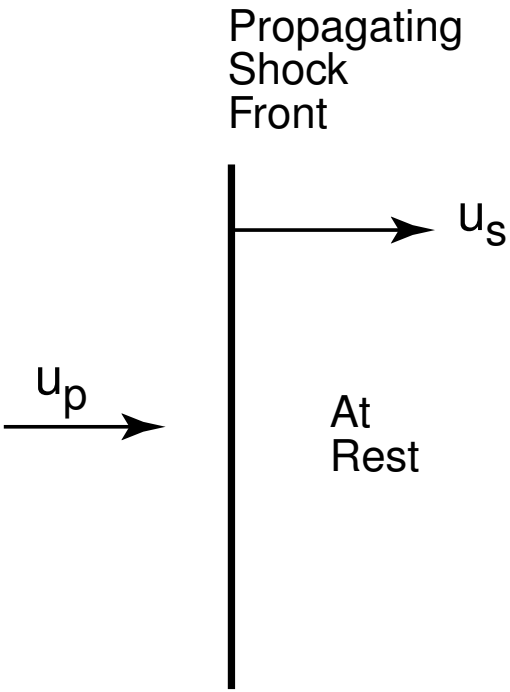

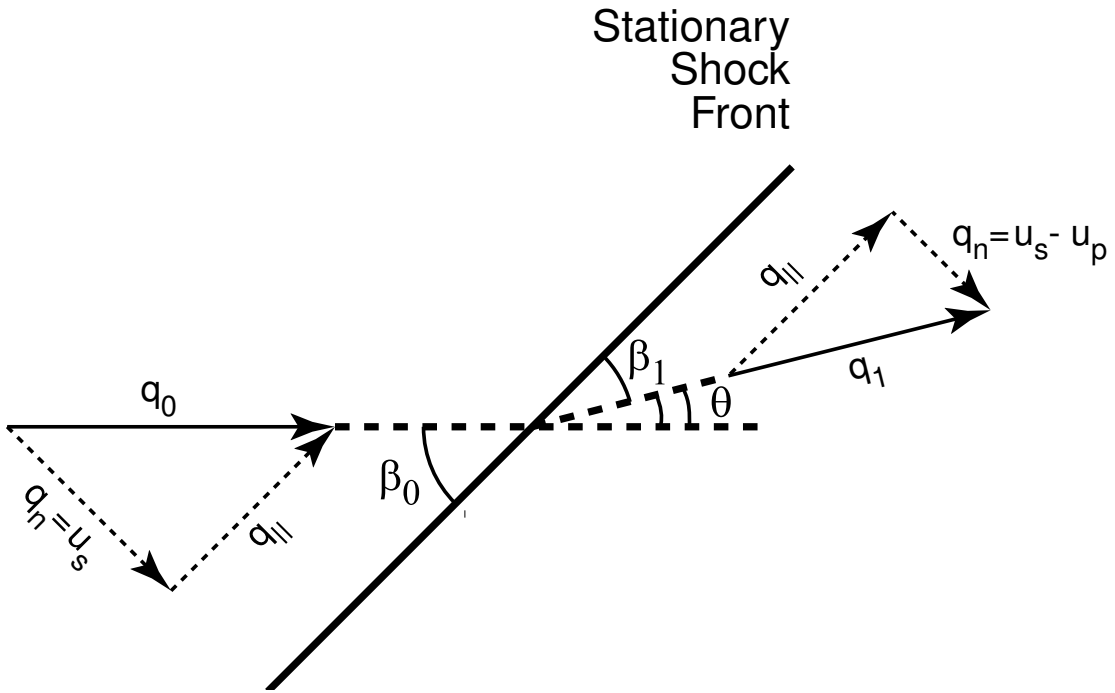

2-D wave pattern

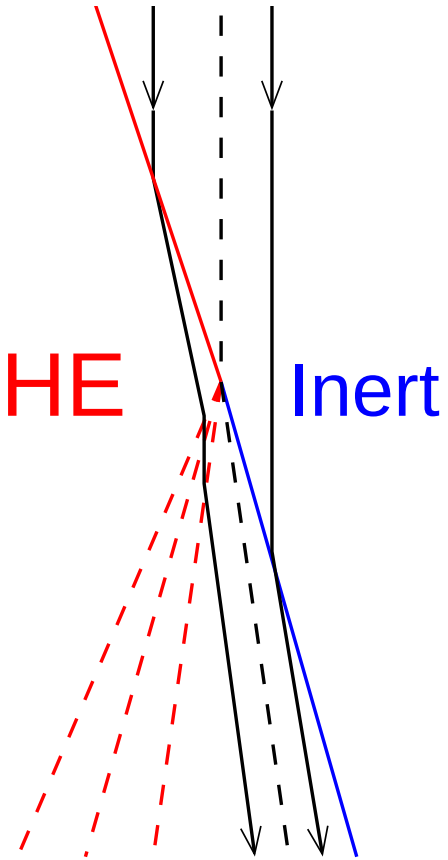

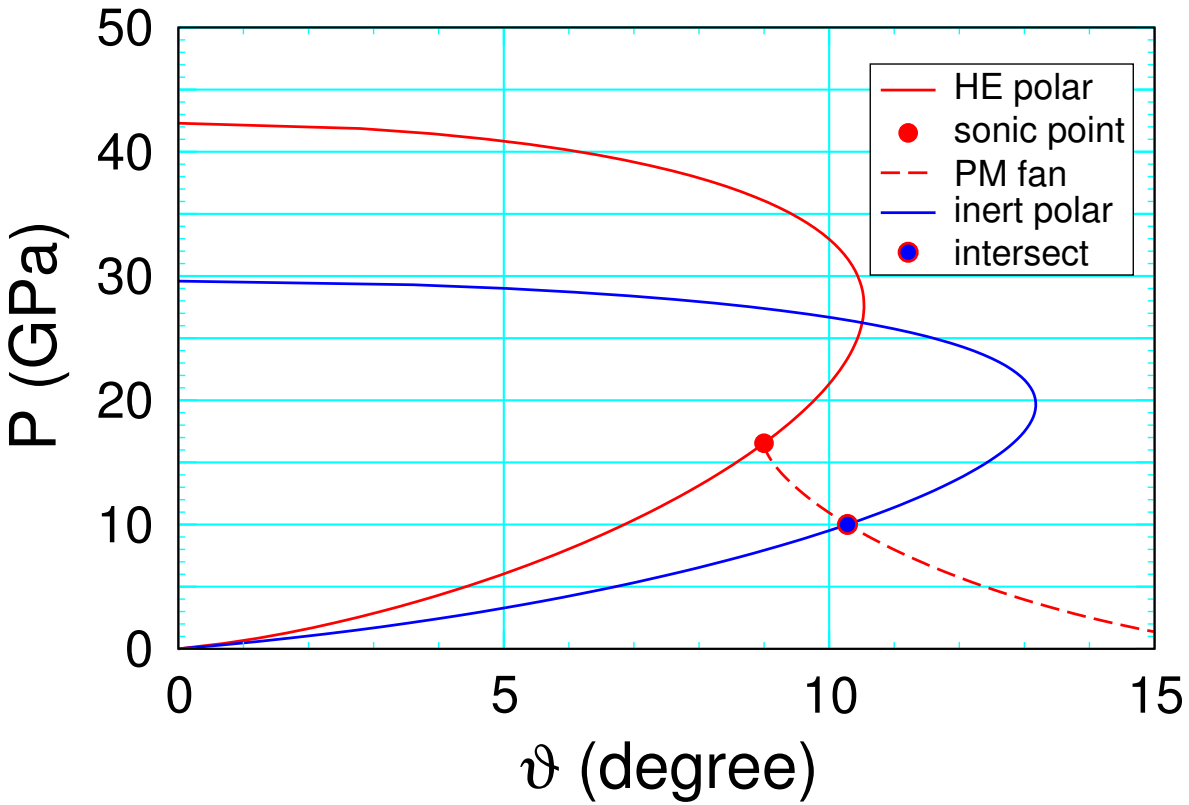

Intersecting detonation wave fronts

Phermex shot 1037

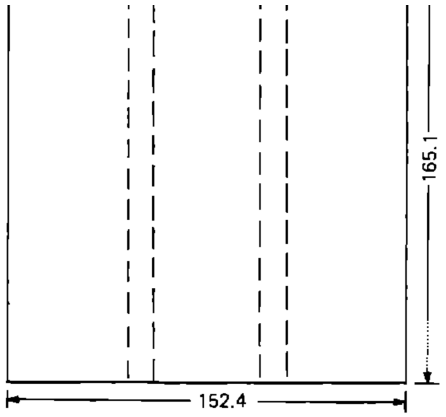

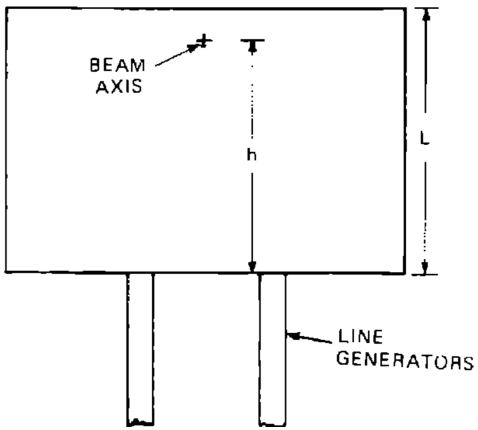

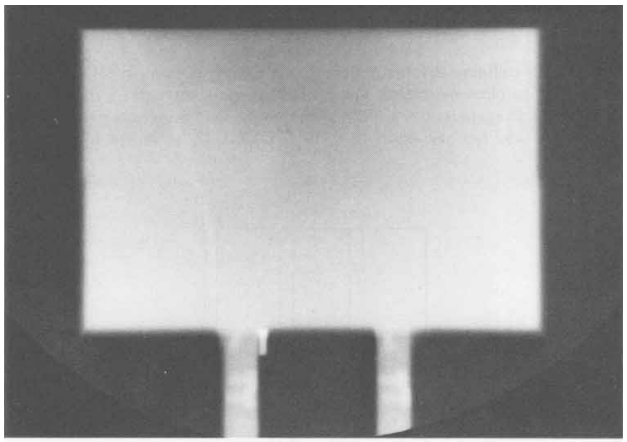

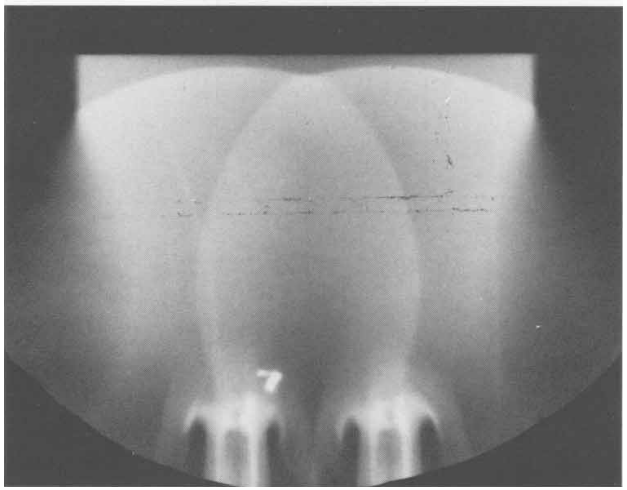

Simulation above failure diameter

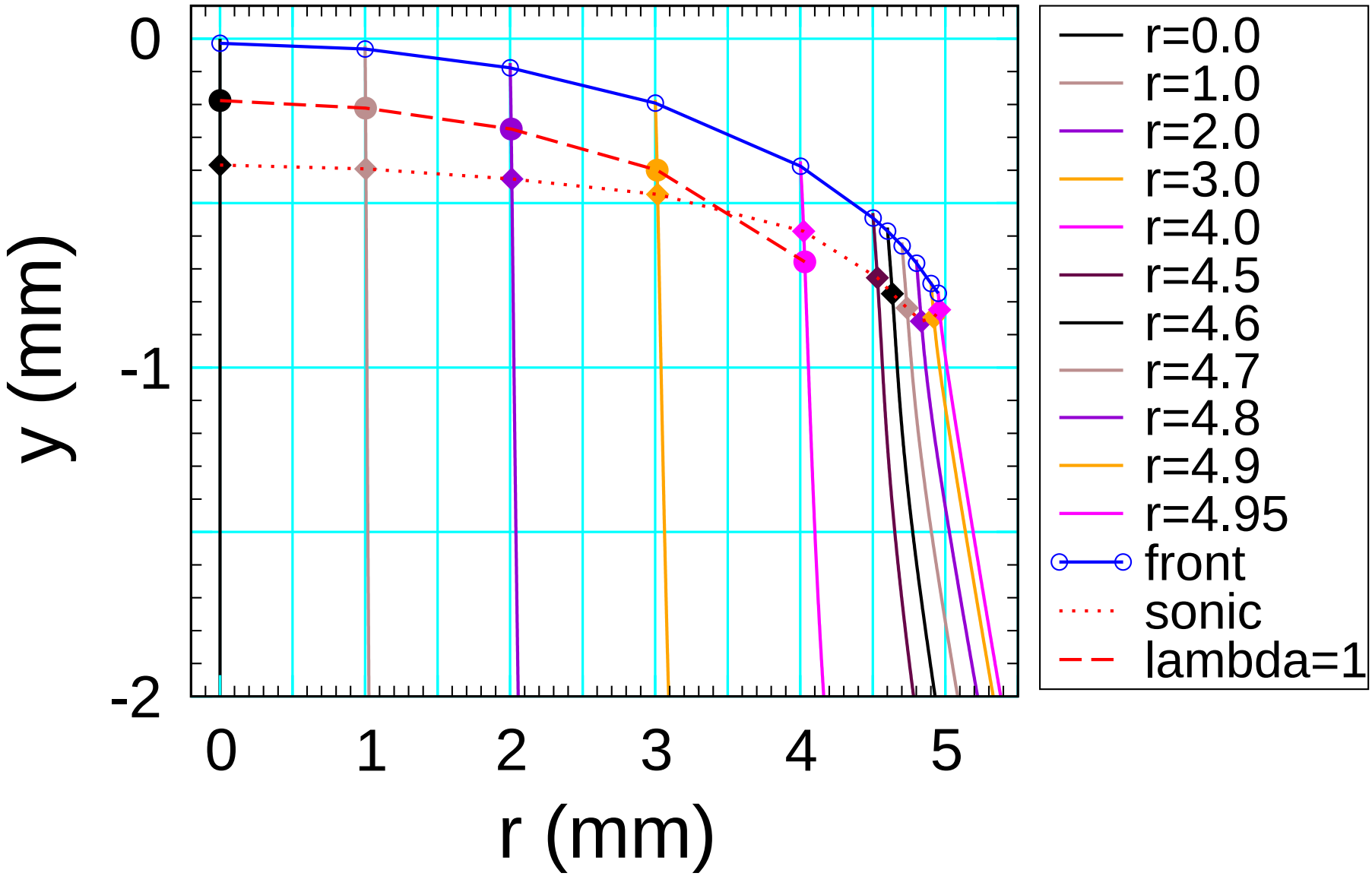

Simulation above failure diameter

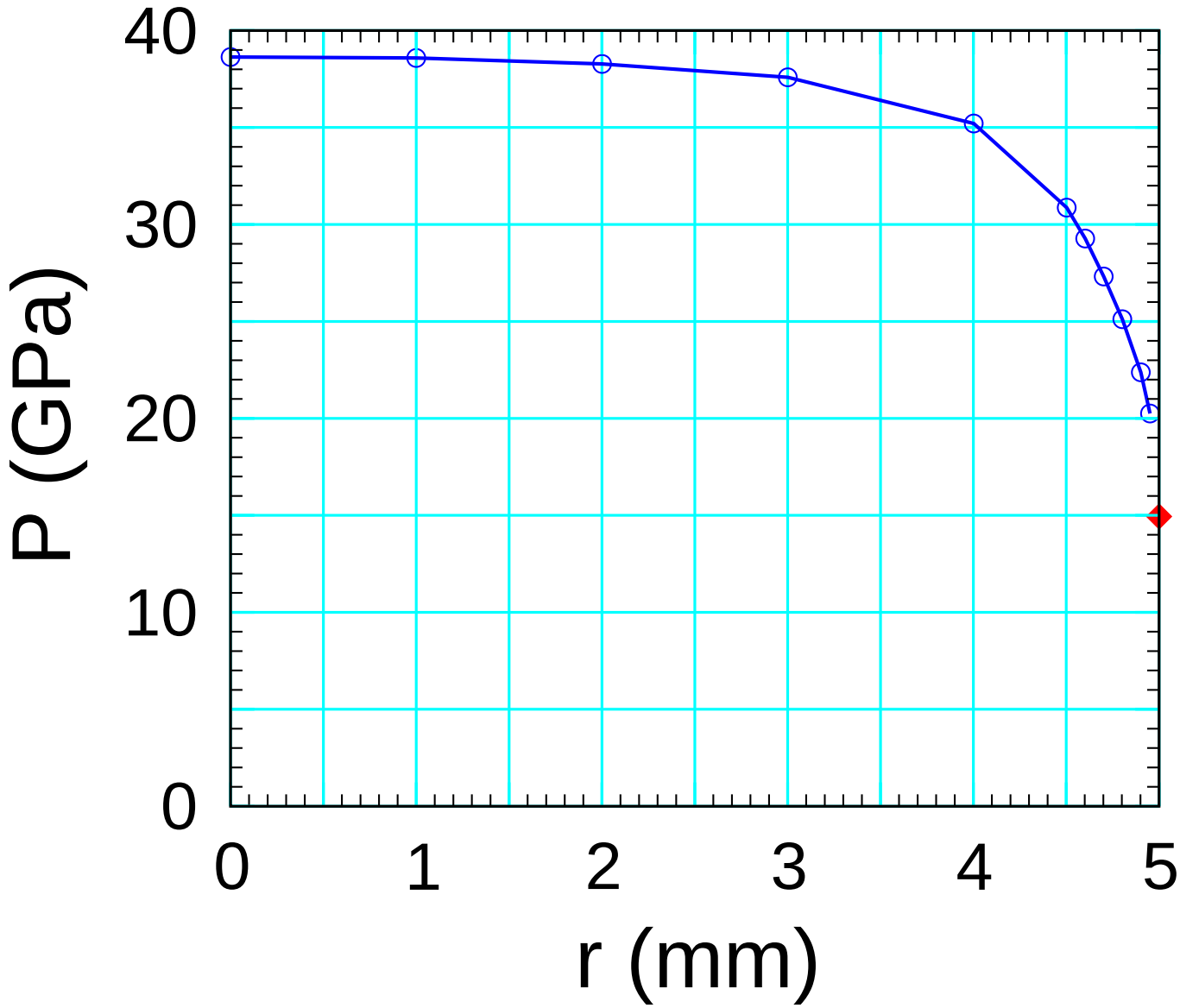

Simulation above failure diameter